Anti-plasmodial activity of fatty acids and macrophage immune modulation during robust erythrophagocytosis

Thesis submitted for the award of the degree of

DOCTOR OF PHILOSOPHY

By

Naidu Babu Ommi

(Enrolment No: 13LTPH07)



Department of Biotechnology & Bioinformatics, School of Life Sciences University of Hyderabad Hyderabad-500 046, INDIA

October-2020



(A Central University established in 1974 by an Act of Parliament)

CERTIFICATE

This is to certify that the thesis entitled "Anti-plasmodial activity of fatty acids and macrophage immune modulation during robust erythrophagocytosis" submitted by NAIDU BABU OMMI, bearing registration number 13LTPH07 in partial fulfilment of the requirements for award of Doctor of Philosophy in the Department of Biotechnology & Bioinformatics, School of Life Sciences is a bonafide work carried out by him under my supervision and guidance.

This thesis is free from plagiarism and has not been submitted previously in part or in full to this or any other University or Institution for the award of any degree or diploma.

Parts of the work performed in relation to this thesis have been:

A. Published in the following publication.

- 1. Archiv der Pharmazzie; https://doi.org/10.1002/ardp.201900079
- 2. ChemistrySelect; https://doi.org/10.1002/slct.201700242

B. Presented in the following conferences.

- 1. **International symposium** on malaria biology and 29th congress of parasitology and applied aspects held at University of Hyderabad, Hyderabad on Nov 1-3, 2018.
- 2. **BIO-QUEST 2017 Symposium** held at School of Life Sciences, University of Hyderabad on 12-13th Oct 2017.
- 31st Annual Conference of Society for Neurochemistry, India held at Banaras Hindu University, Varanasi 20-22nd Sep 2017.
- 4. **GIAN workshop** on Lipid signaling in Heath and Diseases in Plants and Animals held at University of Hyderabad on 5 to 15th Dec 2016.

Further, the student has passed the following courses towards the fulfilment of the coursework requirement for PhD.

	S. No.	Course Code	Name	Credits	Pass/Fail
	1	BT 801	Seminar	1	Pass
	2	BT 802	Research Ethics & Management	2	Pass
	3	BT 803	Biostatistics	2	Pass
	4	BT 804	Analytical Techniques	3	Pass
	5	BT 805	Lab Work	4	Pass
		22/10/2020		1/1	Moule
		Supervisor	Head of the Department	Theam o	of the School
rt	Prof. P. ment of Bio School	Prakash Babu htechnology & Bioinforma of Life Sciences	tics 中EAD Dept. of Biolecchnology & Bioinformatics	School	DEAN of Life Sciences ity of Hyderabad

epartment of Biotechnology & Bioinformatics
School of Life Sciences
University of Hyderabad
Hyderabad-500 046. (T.S.)

Pept. of Biolechnology & Bioinformatics
University of Hyderabad
Hyderabad.

Hyderabad - 500 046.



(A Central University established in 1974 by an Act of Parliament)
Department of Biotechnology & Bioinformatics
School of Life Sciences
University of Hyderabad-500046
India

DECLARATION

I hereby declare that the work presented in this thesis entitled "Anti-plasmodial activity of fatty acids and macrophage immune modulation during robust erythrophagocytosis" has been carried out by me under the supervision of Prof. P. Prakash Babu in the Dept. of Biotechnology & Bioinformatics, School of Life Sciences, University of Hyderabad. This work has not been submitted for any degree or diploma of any other University or Institute.

Naidu Babu Ommi (Candidate)

Enrol. No. 13LTPH07

Prof. P. Prakash Babu (Supervisor)

Prof. P. Prakash Babu

Department of Biotechnology & Bioinformatics
School of Life Sciences
University of Hyderabad
Hyderabad-500 046. (T.S.)

22/10/2020



University of Hyderabad Hyderabad- 500 046, India

PLAGIARISM FREE CERTIFICATE

This is to certify that the similarity index of this thesis as checked by the Library, University of Hyderabad excluding bibliographic content 17%. Out of this 9% similarity has been found to be identified from the candidate's own publication as second author (Naidu Babu Ommi) which forms the part of the thesis. The details of student's publication are as follows:

- a. Sujatha K, Ommi NB, Mudiraj A, Babu PP, Vedula RR. Synthesis of thiazolyl hydrazonothiazolamines and 1,3,4-thiadiazinyl hydrazonothiazolamines as a class of antimalarial agents. Arch Pharm (Weinheim). 2019 Dec;352(12):e1900079. doi: 10.1002/ardp.201900079. Epub 2019 Oct 11. PMID: 31602690. Similarity Index: 7%
- b. Naveen, Naidu Babu Ommi, Anwita Mudiraj, T. Mallikarjuna, P. Babu and R. Nagarajan, Total Synthesis of Penicinoline E, Marinamide, Methyl Marinamide and their Antimalarial Activity ChemistrySelect 2017, 2, 3256–3261. Similarity Index: 2%

About 8% similarity was identified from external sources in the present thesis which is according to prescribed regulations of the University. Publications related to this thesis have been appended at the end of the thesis. Hence the present thesis may be considered to be plagiarism free.

Prof. P. Prakash Babu

Supervisor

Prof. P. Prakash Babu

Department of Biotechnology & Bioinformatics

School of Life Sciences

University of Hyderabad

Hyderabad-500 046. (T.S.)

Dedicated to

MY FATHER

"Behind every young boy who believes in himself is a father who believed in him first."

Table of contents

1. Introduction	1
1.1 History of malaria	2
1.2 Life cycle	4
1.3 Erythrocytic stage	5
1.4 Pathogenicity of malaria	7
1.4.1 Fever	7
1.4.2 Anaemia	8
1.4.3 Cerebral malaria.	8
1.4.4 Experimental cerebral malaria	9
1.4.5 Metabolic acidosis.	
1.4.6 Placental malaria	.10
1.5 Choroid plexus and blood-cerebrospinal fluid barrier	11
1.6 Subventricular zone.	
1.7 Lipid droplets	
1.8 Cell death in the host response t.o infection	
1.8.1 Apoptosis	
1.8.2 Autophagy.	
1.8.3 Autophagy and apoptosis cross talk	
1.9 The rationale of the study.	
2. Anti-plasmodial activity and mechanism of action of fatty acids against P.	
falciparumfalciparum	17
2.1 Introduction.	
2.2 Materials and methods.	20
2.2.1 Parasite culture.	.20
2.2.2 Plasmodium growth inhibition assay	.20
2.2.3 Stage specific growth assessment	
2.2.4 NP-40 mediated β-hematin polymerization assay	
2.2.5 Fatty acid- hemin interaction.	
2.2.6 Docking analysis of heme-fatty acid interaction	
2.2.7 Neutral lipid bodies (NLB) staining	
2.2.8 JC-1 staining to measure the mitochondrial membrane depolarization	.23
2.2.9 Semi-quantitative PCR	.23
2.3 Result	.24
2.3.1 Polyunsaturated fatty acids inhibits the growth of <i>P. falciparum</i>	.24
2.3.2 DHA inhibits the growth of <i>P. falciparum</i> trophozoite stage irreversibly	
2.3.3 Polyunsaturated fatty acids inhibit β- hematin polymerization	
2.3.4 Polyunsaturated fatty acids shown interaction with heme and alters Soret band	.29
2.3.5 <i>In silico</i> analysis of heme (ferriprotoporphyrin)-fatty acid interaction	.30
2.3.6 DHA abrogates neutral lipid bodies (NLBs) of <i>P. falciparum</i>	.31
2.3.7 DHA effect on diglyceride acyltransferase enzyme gene expression	
2.3.8 Antiplasmodial activity of DGAT1 inhibitor T-863	
2.3.9 DHA depolarizes <i>P. falciparum</i> mitochondrial membrane potential	.35
2.4 Discussion.	
3. Robust erythrophagocytosis induced cell death and immune modulation in Raw 26-	
macrophage cell line	
3.1 Introduction	
3.2 Methods and materials.	
3.2.1 Infection of and blood recovery.	.45

3.2.2 Raw 264.7 cell culture and treatment	.45
3.2.3 CFSE staining of RBC	.46
3.2.4 Quantification of erythrophagocytosis in DHA treated macrophage	46
3.2.5 Western blot analysis	.46
3.2.6 Immunofluorescence	.47
3.2.7 Bodipy 493/503 staining	.47
3.2.8 Semi-quantitative PCR	.48
3.3 Results.	
3.3.1 Lipid droplets biogenesis and cell adhesion molecule induction in iRBC engulfe	
macrophages	
3.3.2 Robust erythrophagocytosis induced apoptosis in Raw 264.7 macrophage	
3.3.3 Robust erythrophagocytosis inhibits autophagy in Raw 264.7 macrophages	
3.3.4 Enhanced iRBC phagocytosis activates macrophage M1 polarization	
3.3.5 Cerebral malaria induces infiltration of circulatory leukocytes into brain	
3.3.6 DHA enhances the erythrophagocytic activity of Raw 264.7 macrophage	
3.3.7 Lipid droplet induction in cerebral malaria infected brain.	
3.3.8 Lateral ventricle enlargement and choroid plexus degeneration in CM brain	
3.4 Discussion.	.59
4A. Anti-parasitic activity of penicinoline alkaloids and their mechanism of action	
against Plasmodium falciparum6	
4A.1 Introductio	
4A.2 Material and methods.	
4A.2.1 Parasite culture	
4A.2.2 Compound preparation	
4A.2.3 Giemsa staining.	
4A.2.4 Flow cytometry	
4A.2.5 Cytotoxicity assay (MTT).	
4A.2.6 β-hematin polymerization assay	
4A.2.7 Stage specific growth assessment.	
4A.3 1 <i>P. falciparum</i> growth inhibition effect of penicinoline alkaloids	
4A.3.2 Cytotoxicity of penicinoline alkaloids against Raw 264.7 macrophages	
4A.3.3 β-hematin synthesis inhibition of penicinoline alkaloids	
4A.3.4 <i>P. falciparum</i> stage specific growth inhibition of penicinoline alkaloids	
4A.4 Discussion.	
4B. Thiazolyl derivatives as a class of antimalarial agents	
4B.1 Introduction.	
4B.2 Material and methods	
4B.2.1 SYBR green fluorescence-based antiplasmodial assay	
4B.2.2 Cytotoxicity assay (MTT)	
4B.2.3 Stage-specific growth assessment.	
4B.2.4 Lactate dehydrogenase (LDH) assay	
4B.3 Results	
4B.3.1 <i>In vitro</i> antimalarial activity and cytotoxicity of compounds	
4B.3.2 <i>P. falciparum</i> stage specific growth inhibition	
4B.4 Discussion	
5. References	

List of Figures

- Figure 1.1: Plasmodium life cycle
- Figure 1.2: Cerebral malaria induced blood brain barrier disruption
- **Figure 1.3:** Path from choroid plexus to sub-ventricular zone
- **Figure 2.1:** Fatty acid-induced death of *P. falciparum*
- Figure 2.2: Effect of partial treatment of DHA at various *Plasmodium* stages
- **Figure 2.3:** Effect of fatty acids on β -hematin formation
- **Figure 2.4:** Effect of fatty acids on interaction with ferriprotoporphyrin (FP)
- Figure 2.5: In silico interaction of ferriprotoporphyrin to docosahexaenoic acid
- Figure 2.6: Effect of DHA and chloroquine on neutral lipid bodi
- Figure 2.7: Effect of pyrimethamine and oleic acid on neutral lipid bodies synthesis
- **Figure 2.8:** Stage specific expression of pfDGAT and effect of DHA on trophozoite stage pfDGAT gene expression
- **Figure 2.9:** Anti-plasmodial effect of T-863 against *P. falciparum*
- **Figure 3.1:** Lipid droplet accumulation and induced ICAM-1 expression in enhanced iRBC phagocytosed Raw 264.7 macrophages
- **Figure 3.2:** Cell death and Caspase-3, p53 expression in robust iRBC phagocytosed Raw 264.7 macrophages
- **Figure 3.3:** mTORC1/p70S6K mediated autophagy inhibition in robust iRBC phagocytosed Raw 264.7 macrophages
- **Figure 3.4:** Robust iRBC incubation induces proinflammatory cytokine gene expression in Raw 264.7 macrophages
- **Figure 3.5:** FACS analysis of peripheral leukocyte infiltration into *P. berghei ANKA* infected mice brain tissue
- **Figure 3.6:** Docosahexaenoic acid (DHA) induced iRBC phagocytosis in Raw 264.7 macrophages
- Figure 3.7: Cerebral malaria induced lipid droplets accumulation in brain tissue

Figure 3.8: Cerebral malaria infection induced the choroid plexus structure deformation and active astrocytosis at subventricular zone of lateral ventricle

Figure 4A.1: Penicinoline E inhibits the *P. falciparum* growth

Figure 4A.2: Marinamide inhibits the *P. falciparum* growth

Figure 4A.3: Methyl marinamide inhibits the *P. falciparum* growth

Figure 4A.4: Cytotoxicity assay for the compounds against RAW 264.7 macrophages

Figure 4A.5: β-hematin polymerization inhibition effect of penicinoline alkaloids

Figure 4A.6: Effect of transient treatment of penicinoline E at various plasmodial stages

Figure 4A.7: Effect of transient treatment of marinamide at various plasmodial stages

Figure 4A.8: Effect of transient treatment of methyl marinamide at various plasmodial stages

Figure 4B.1: Effect of compound 4h transient treatment at various plasmodial stages

Figure 4B.2: Effect of compound 4k transient treatment at various plasmodial stages

Figure 4B.3: Effect of compound 4l transient treatment at various plasmodial stages

List of Tables

- **Table 1:** C-Docker score of fatty acid- ferriprotoporphyrin interaction
- **Table 2:** DHA induced mitochondrial membrane depolarization of *P. falciparum*
- **Table 3:** Compounds (4a–l, 6a–k) half-maximal inhibitory concentration (IC50) values with 3D7 strain and Dd2 strain
- **Table 4:** Antimalarial activities of active compounds against blood-stage parasites and in vitro cytotoxicity

List of Abbreviation

AA arachidonic acid

BCSFB blood cerebrospinal fluid brain barrier

BSA bovine serum albumin

CM cerebral malaria

CP choroid plexus

CFSE carboxyfluorescein Succinimidyl ester

DDT Dichlor- diphenyl trichloroethane

DHA docosahexaenoic acid

DGAT diglyceride acyltransferase

EPA eicosapentaenoic acid

FP ferriprotophopyrin

GFAP Glial fibrillary acidic protein

GPI glycophosphatidylinositol

HRP2 Plasmodium histidine-rich protein 2

IL interleukin

ICAM intercellular adhesion molecule

IC50 half-maximal inhibitory concentration

NLB neutral lipid bodies

PVM parasitophorus vacuole membrane

PUFA polyunsaturated fatty acid

iRBC plasmodium infected mice erythrocytes

cRBC control mice erythrocytes

SDS sodium dodecyl sulphate

SVZ subventricular zone

TAG triacylglycerol

TNF tumor necrosis factor

VCAM vascular cell adhesion molecule

Acknowledgements

I would like to express my profound gratitude to my supervisor **Prof. P. Prakash Babu** for freedom, guidance, constant encouragement and suggestions throughout my PhD.

I thank my DC members **Prof. K. P. M. S. V. Padmasree** and **Prof. G. Ravi kumar** for their critical comments and valuable suggestions.

I thank Prof. **K. P. M. S. V. Padmasree**, Head Dept. of Biotechnology and former Head Prof. J. S. S. Prakash, Prof. Anand Kondapi and Prof. P. Prakash Babu for providing the necessary facilities in the department to carry out my research work.

I am grateful to **Prof. S. Dayananda** Dean, School of Life Sciences, and former Deans Prof. K. Ramaiah, Prof. P. Reddanna, Prof. Aparna Dutta Gupta, Prof. A. S. Raghavendra, Prof. M. Ramanadham, and Prof. R. P. Sharma for providing all the facilities in the school.

I thank **Dr. Anwita Mudiraj** for her suggestions and moral support

I am thankful to my lab members **Dr. Prabhakar**, **Dr. Ramu**, **Dr. Apoorv Suresh**, **Dr. Kamusha Valli**, **Dr. Nobel Kumar**, **Mr. Sireesh Kumar**, **Mr. Karthik**, **Dr. Ravindra**, **Dr. Deepak babu Dr.Praveen**, **Dr. Parimala**, **Dr. Ranjana**, **Dr. Vimal**, **Mr. Kishore**, **Mr. Nikhil**, **Ms. Neera**, **Ms. Shubhangee**, **Mr. Rahul**, **Ms. Shailaja** for their encouragement and support during this time.

I thank office staff of Dept. of Biotechnology, **Ms. Nalini** for Confocal, **Mr. Ramesh** for FACS assistance.

We thank our collaborators **Prof. Nagarajan** and **Prof. Lalitha Guruprasad**, School of Chemistry, University of Hyderabad.

I thank **Prof. Anand Kondapi, Dr. Suresh Yenugu, Prof. Naresh Babu, Prof. Brahmanandam** and their **students** for allowing me to use their facilities.

I thank **Dr. Gangadhar** and **Dr. Usha** for their support

I thank all the **Life science research scholars**

I thank my **family members** and **friends** for their moral support

1. Introduction

1.1 History of malaria

Malaria is an ancient disease. The dating of Egyptian remains shows that it has existed from 3200 and 1304 BC (1). Vedic period of Indian writings called malaria "the king of diseases" in 270 BC. Before the human genesis, malaria-infected our ancestors and had an intense effect on the evolutionary process (2) by inducing human genetic polymorphisms. The Mediterranean Sea's malaria-endemic region possesses thalassemia (3), sickle cell trait, and Glucose-6-Phosphate Dehydrogenase deficiency are significant changes. Formerly malaria was called by different names like ague or marsh fever, intermittent fever, tertian fever. The word malaria is coined from the Italian mala aria-"bad air" because of its association with swamps and marshes(4). A late-nineteenth-century Louis Alphonse observed parasites inside the infected person and proposed that malaria is caused by protist organisms making the first significant breakthrough in malaria research. After that, Ronald Ross proved that mosquito was the vector to transmit malaria to the birds and discovered the complete life cycle of malaria in culicine mosquito. Grassi and Giesuppe's work confirmed the transmission of malaria in humans experimentally (5). Among the *Plasmodium* species, *falciparum* is lethal to humans and transmitted through female Anopheles mosquito. Malaria is prevalent in tropical and subtropical regions where the temperature is critical for the multiplication and survival of these Anopheles mosquitos and to complete growth cycle of parasite in the mosquito (6). The tropical regions sub-Saharan Africa and Papua New Guinea are more prevalent in malaria transmission year around. At the same time P. vivax is tolerant to lower temperatures transmits in colder areas seasonally (7). Shortt and Garnham found mosquito inoculated sporozoites in liver biopsy samples of human patients infected with P. vivax and P. falciparum. In the 19th century, the first antimalarial drug quinine was isolated from cinchona bark, and used against intermittent fever. However, the drawbacks were short half life span, drug resistance to P. falciparum, a debate about the administration route, and

hypoglycaemia (8, 9). During World War I, anti- German forces created the shortage of quinine. At this time, the Germans developed dye-based antimalarial prototype methylene blue and atabrine. Side effects like yellowing of the skin and Japanese propaganda caused impotence in treating service members searching for new compounds (10). During World War II, the Japanese occupied Java and interrupted the supply of cinchona trees, led to the discovery of synthetic antimalarial drugs. At this time, chloroquine, a 4- aminoquinoline, was discovered by German chemist Andersag. Even though chloroquine was available late to the malaria prevalent region likes Pacific theater or Silicy, it became potent molecule against Plasmodium parasite. Dichlor- diphenyl trichloroethane (DDT), an insecticide, kills the vector Analphelous mosquito. Chloroquine and DDT became potent weapons to eradicate malaria. However, chloroquine resistance falciparum evolved primarily at Tahi Combodia in 1957 (11). By the 1970s, the resistance started spreading throughout the world. Another antimalarial compound in the pipeline during World War II was pyrimethamine but within a year of its introduction it developed resistance. These quinine based drugs act mostly on the hemoglobin digestion pathway. From the request of North Vietnam in the impending conflict, China initiated a project 523 on 23rd May 1967, and isolated organic extracts from Artemesia annua leaves which are potent against malaria parasite. The plant's leaves active moiety, artemisinin is now front line chemotherapy against uncomplicated and cerebral malaria (12).

Climate is the primary driving force in the transmission of malaria. A short rise in temperature and rainfall associated with El-Nino caused a malaria epidemic in Kenya, northeast Punjab, India, and Sri Lanka about four folds(13).

1.2 Life cycle

Plasmodium falciparum caused human malaria is more lethal and accounts for a significant number of deaths. P. vivax, P. oval, are less severe, but they remain dormant in the liver of

infected patients for liver for months and reoccur again. Recently in South Africa the macaque monkey parasite P. knowlesi was also found to infect humans. P. falciparum has a complex life cycle with an exogenous sexual phase in vector mosquito midgut where male and female gametes combine. This is followed by an exogenous asexual phase (sporogony) where parasite multiplies in mosquito's gut and releases sporozoites into the mosquito's salivary glands. The mosquito bites and releases the sporozoites into the vertebrate host multiplying through an endogenous asexual phase called schizogony. High motile sporozoites traverse through the skin cells and enter into the bloodstream to reach the liver. In liver blood capillaries, the parasite traverse through sinusoidal endothelial cells (14) and liver-derived kupffer macrophages (15) to reach the parenchyma and infect hepatocytes. Vacuolar membrane surrounded sporozoites observed in kupffer macrophages infected with P. berghei suggest the immune evasion of the parasite (16). Sporozoite surface protein circumsporozoite (CS) binds to the microvilli of hepatocytes and invades the cell and develop to produce merozoites through pre-erythrocytic schizogony. Hepatocytes rupture and release merozoites which contain membrane proteins that bind to erythrocyte glycophosphatidylinositols (GPI) and invade into erythrocytes and forms ring-like structures (17). Ring stage parasites grow into a trophozoite stage by utilizing the host cell hemoglobin. Trophozoite develops into schizont stage, egress, and releases 8-24 merozoites into the blood circulation. Each merozoite infects fresh erythrocyte and multiplies its number. Egress of these merozoites from the infected erythrocyte display intermittent fever, which is a characteristic feature of malaria. Some of these blood-stage parasites transform into male and female gametocytes, which are further taken up by mosquitoes in their blood meal. These zygotes undergo sexual reproduction in mosquito midgut and release the sporozoites, which also migrate into salivary glands. When mosquito bites, another individual inoculates these sporozoites and, the cycle continues.

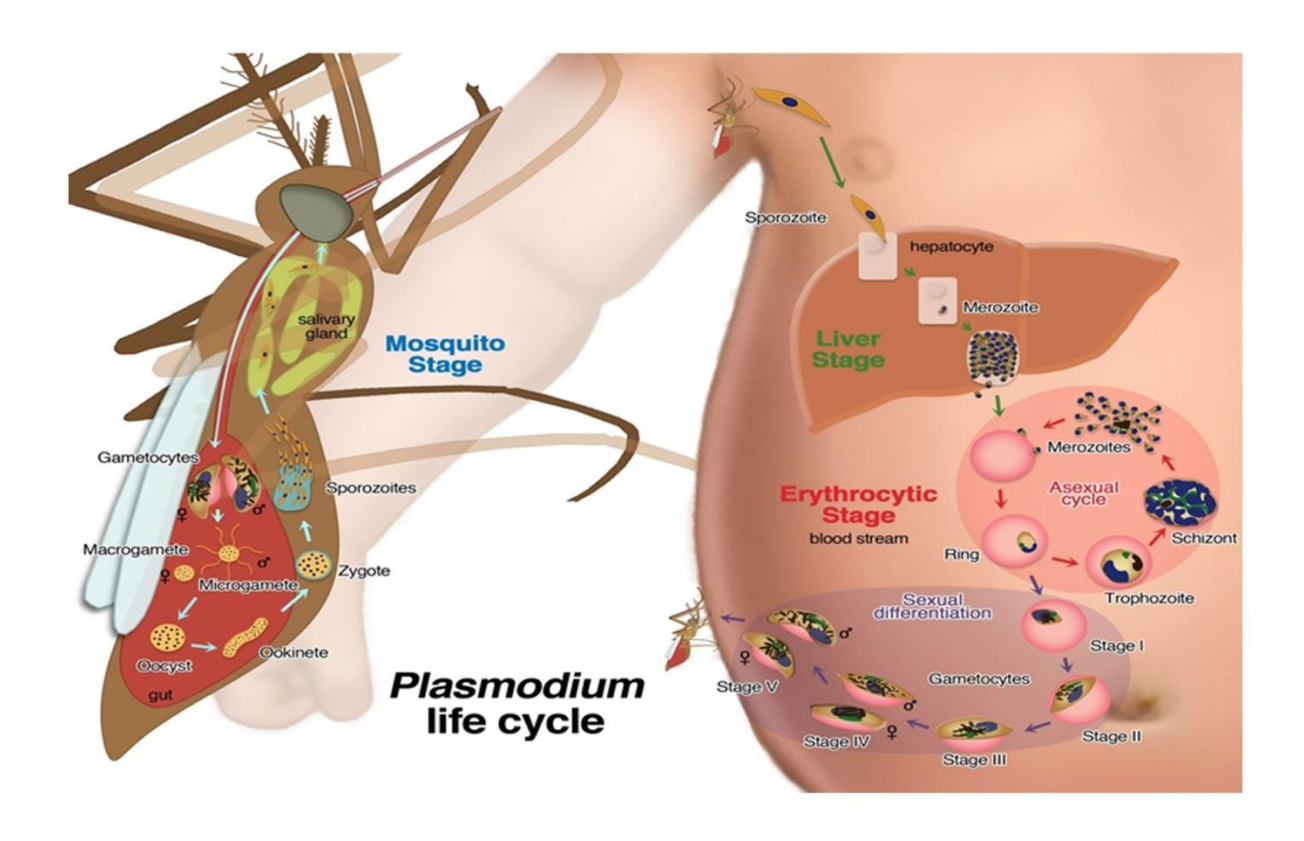


Figure 1.1 Plasmodium life cycle. Credit: Le Roch Lab, UC Riverside

1.3 Erythrocytic stage

The invasion of merozoites into erythrocyte is almost similar in all *Plasmodium* species. The binding of merozoite to the host erythrocyte is the crucial step in the invasion procedure because the parasite should distinguish the erythrocytes with other cell types. The initial adherence is a low affinity with long-distance and reversible until the merozoite apical end juxtaposes with the erythrocyte membrane, which allows a closer interaction and formation of tight junctions (18). The apical end of the merozoite contains three organelles called rhoptries, micronemes, and dense granules that are the characteristic features of phylum Apicomplexa. The apical end micronemes contain the Duffy receptor family that mediates the erythrocyte invasion (19). As the parasite enters into erythrocyte, it forms a parasitophorus vacuole contains parasitophorus vacuole membrane (PVM), which separates it

from the host cell cytoplasm. As the merozoite pushes the erythrocyte to enter into host, the PVM contains the lipids similar to the host erythrocytes (20, 21), which signifies that the PVM is derived from the host RBC membrane. Unlike lipids, erythrocyte membrane proteins are not detected in the PVM (20, 22). Whereas PVM contains rhoptry proteins of the parasite (23) shows the formation of PVM is complex. *Plasmodium* undergoes a 48 h life cycle in host erythrocyte with three major morphological stages. The first is a ring stage, which appears like a ring or headphone structure with Giemsa staining, but the actual structure is a cup or biconcave shape. The export of parasite synthesized proteins to the host cell's surface occurs mainly at this stage (24). The ring stage lasts for 24 h. During this stage, the parasite engulfs erythrocyte hemoglobin in a vesicle form into the parasite's digestive vacuole (25). Parasite degrades the hemoglobin in the acidic digestive vacuole, and utilizes the amino acids for its growth and, crystallizes the free heme into nontoxic hemozoin substance during the trophozoite stage. Plasmepesin I and II an aspartic and falcipain cysteine proteases are crucial in the digestion of hemoglobin in a digestive vacuole. These proteases are active at acidic pH (26). The ferrous form of Iron in haemoglobin is converted into a ferric form in free heme, which damages the membrane by its per-oxidative nature. Digestive vacuole neutral lipids and Plasmodium histidine-rich protein 2 (HRP2) act as catalysts to crystallize the free heme (27, 28). The neutral lipid droplets contain diacylglycerol which polymerizes the hemozoin at low activation energy compared with monoacylglycerol. The phospholipid content of the parasite increases six-fold to synthesize the vacuole membranes during its development in host erythrocyte(27). Host erythrocytes do not possess lipid biosynthesis metabolism. To some extent, it has phospholipid remodelling capacity. Parasite synthesizes phospholipids using fatty acid synthase II enzyme. It scavenges from the host to modify the membrane composition with enriched phosphatidylcholine, phosphatidylethanolamine, and reduced cholesterol and sphingomyelin compared with the host membrane. Parasite modifies the host erythrocyte membrane by decreasing polyunsaturated phospholipids (29). Parasite engulfs the erythrocyte hemoglobin in small cytostome like structures. These structures fuse to form the large digestive vacuole where hemozoin crystallization occurs. Digestive vacuole occupies a large space of the cell. The mitochondria, apicoplast form, branched like structures and segregate into the merozoite (30). Trophozoite stage lasts 32-34 h post-infection. It develops into schizont stage where parasite undergoes asynchronous DNA replication and produces 32 nuclei distributed to merozoite. After 48 h of a life cycle, infected erythrocyte egress and releases the merozoite and digestive vacuole.

1.4 Pathogenicity of malaria

1.4.1 Fever

After completing schizogony in infected erythrocyte, which lasts for 24-72 h depending on the *Plasmodium* species, erythrocytes egress and releases merozoite and some toxic substances like GPI and hemozoin into blood circulation. The fever is believed to be induced after every cycle because these toxic products released after each cycle will activate macrophages and release the cytokines like IL-2, IFN- γ which stimulate the fever. Malaria symptoms like fever, headache, nausea, and central nervous system manifestations are linked to the various cytokines released from the macrophages in response to the parasite toxins (31). plasmodial DNA binding to hemozoin activates the Toll-like receptor 9 and releases the cytokine that causes fever (32). Hemozoin impairs the monocyte function and differentiation (33).

1.4.2 Anemia

Anemia is defined as a decrease in hemoglobin or hematocrit levels according to age, gender, physiological state, and geographic location of the person (34). Parasite releases several

ligands to invade the host cell. During this time, some ligands may attach to the uninfected erythrocytes, which get opsonized, undergo clearance and cause anemia (35, 36). Ring stage infected erythrocyte and uninfected erythrocyte membrane contain the parasite protein RSP on the surface, which promotes complement-mediated lysis and macrophage engulfment of the uninfected erythrocytes (37). Malaria toxins induce macrophage innate immune system, which reduces the erythropoiesis and causes anemia condition. In severe malaria condition, parasite reduces the erythrocyte deformability, which is correlating with a reduction in haemoglobin levels.

1.4.3 Cerebral malaria

Cerebral malaria (CM) is a neurological complication that occurs with *P. falciparum* infection, which leads to the coma and death of the patient. *Plasmodium*-infected erythrocytes express erythrocyte membrane proteins (PfEMP) cytoadhere to the vascular endothelial cell adhesion molecules like ICAM and VCAM which, hinders the blood flow and, cause the hypoxic condition (38). The binding of infected erythrocytes to the uninfected erythrocytes is called rosetting, which forms the blood microvessels' clumps. Human brain parenchyma is separated from the blood circulation by the endothelial cell layer with tight junctions. Trophozoite and schizont stage parasites sequester to the microvasculature endothelial cells and induce the permeabilization and break down of the blood-brain barrier. Parasite antigens stimulate the innate immune cell macrophages and produce pro-inflammatory cytokines. TNF- α , IL-1 and, IFN- γ pro-inflammatory cytokines induce cell adhesion molecules on vascular endothelial cells, facilitate the sequestration of infected erythrocytes. Cell to cell interaction induces signal transduction, which activates the endothelial cells and produces endothelial microparticles (EMPs) and apoptosis of the host cell (39). Increased nitric oxide (NO) levels induce vasodilation of microvessels and permeabilization of endothelial cells.

NO diffuse into the brain and interfere with neurotransmission which might be the responsible factor for reversible coma (40).

1.4.4 Experimental Cerebral Malaria (ECM)

Post-mortem samples and CM patient blood sample analysis highlight the pathophysiology of human cerebral malaria. A rodent model where c57BL/6 mice infected P. berghei ANKA induces ECM within 7-10 days of post-infection is a potent model to study the mechanism responsible for the occurrence disease. Mice display the neurological symptoms of ataxia, convulsions, and coma leading to death. Similar to human cerebral malaria, infected erythrocyte sequestration and increased proinflammatory cytokine levels are observed in ECM. CXCL10 is a chemoattractant for leukocytes and lymphocytes. CXCL10 and CXCR3 expression play a crucial role in ECM pathogenesis (41). The cell adhesion molecules on endothelial cells ICAM-1 and VCAM capture the leukocytes and lymphocytes and increase the cytokine and chemokine production at the site of infection. Blocking of this interaction prevents the CM in infected mice (42). In addition to the blood-brain barrier, the cerebrospinal fluid brain barrier (CSFBB) is the vulnerable site for the invading of foreign particles. P. yoelii yoelii infected mice exhibited ependymal cell morphological changes like thickening of cilia, absence of microvilli, and cell layer detachment during the severe neurological complications. These changes induce the permeability of CSFBB and facilitate the diffusion of toxic substances, and inflammatory cytokines through the barrier into the brain tissue and result in its damage (43).

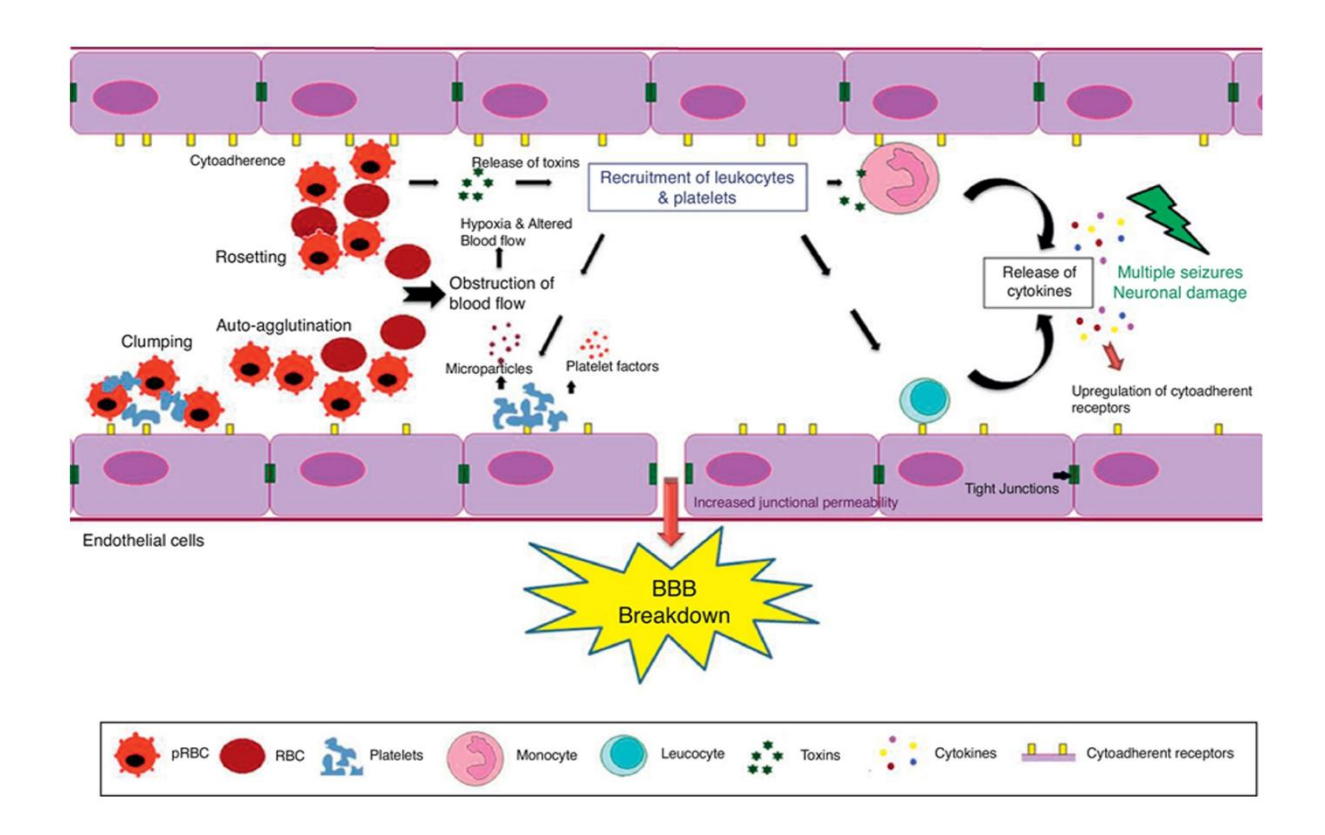


Figure 1.2 Cerebral malaria induced blood brain barrier disruption. Braz J Infect Dis. 2013;17:579-91

1.4.5 Metabolic acidosis

In severe malaria, metabolic acidosis is the strongest predictor for survival. Metabolic acidosis associated with lactic academia is a significant reason to cause respiratory distress in African children with malaria (44). Sequestration in microvasculature elevates the plasma lactate levels and further causes impaired renal failure and hepatic function (45). Hypovolemia caused by Septic shock- like response is also a contributor to metabolic acidosis (46).

1.4.6 Placental malaria

Sequestration of *Plasmodium* infected erythrocytes and immune cells to the placenta's intervillous space are the characteristic feature of placental malaria (47). First time pregnant

women are more susceptible to the infection compared to the second and third time. The resistance is because of the development of placental specific immunity in second and third-time pregnancy (48, 49). Placental malaria-associated parasites utilize chondroitin sulfate A as a receptor protein instead of CD36 used by other malaria parasites (50, 51).

1.5 Choroid plexus and blood-cerebrospinal fluid barrier

Choroid plexus (CP) forms the blood-cerebrospinal fluid barrier (BCSFB) at lateral ventricles. CP comprises of epithelial cells, highly vascularized stroma with fenestrated blood capillaries. CP cells produce cerebrospinal fluid by filtrating the blood. The CP's epithelial cells are interconnected with tight junctions and function as barriers to restrict toxins and foreign bodies' infiltration into the CSF. CP barrier maintains the homeostasis of its composition by regulating the ion and molecule transport in and out of the CSF (52). CP epithelial cells are continuous with lateral ventricle ependymal cells.

1.6 Subventricular zone (SVZ)

SVZ situates immediately beneath the lateral ventricle ependymal layer. It is a niche region present near the nutrient-rich cerebrospinal fluid of the ventricles. It can differentiate into 3 layers where the initial layer is composed of neuroblast cells that lay beneath the ependymal layer of lateral ventricle. Second layer is rich in astrocytes that are positive for Glial fibrillary acidic protein (GFAP) that act as primary progenitor cells for the newly synthesized neurons. The last layer comprises of myelinated fibers (53). In response to neurodegeneration, the progenitor cell production increase at SVZ, migrates to the site of damage, and is differentiated into neurons and glial cells.

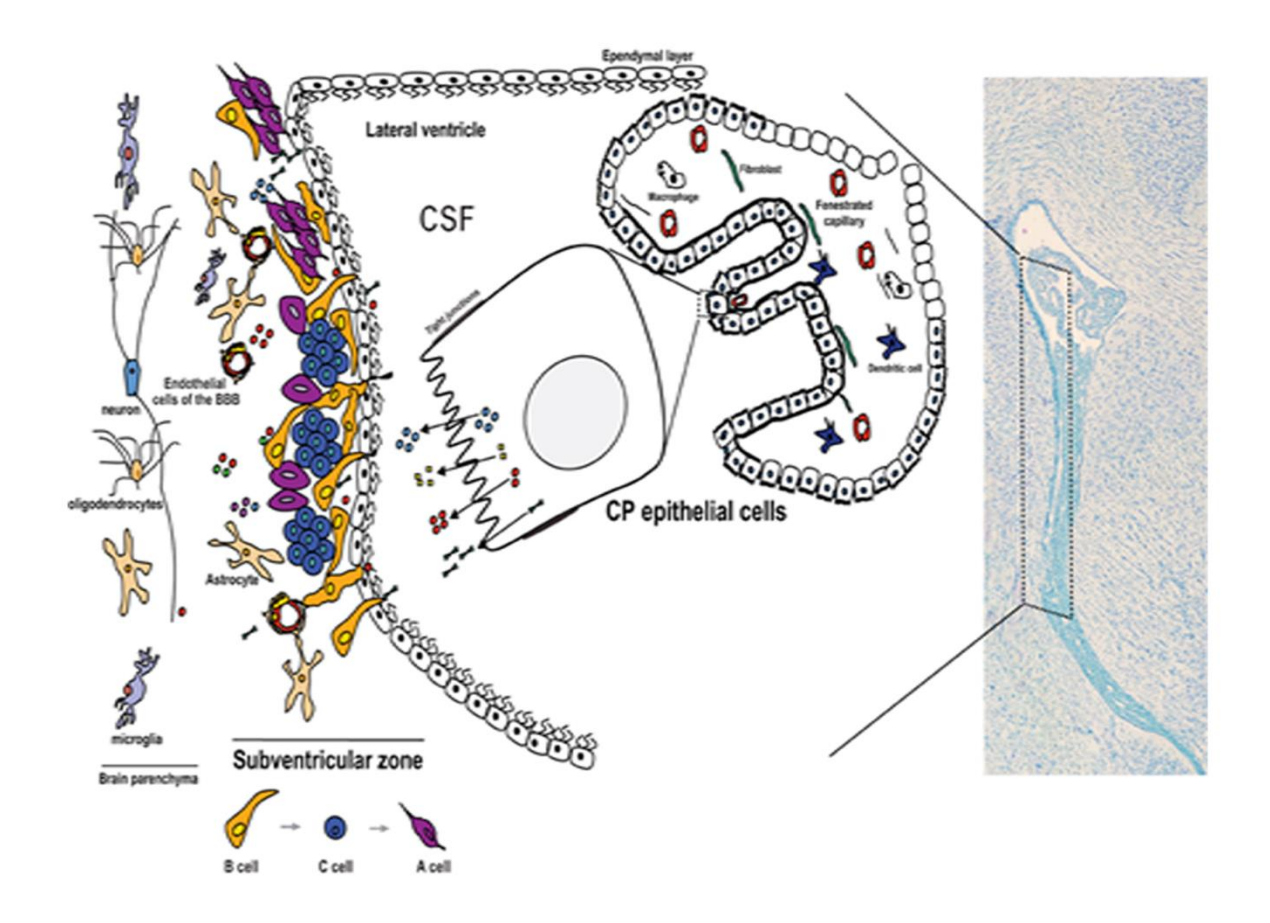


Figure 1.3 Path from choroid plexus to sub-ventricular zone. *Front. Cell. Neurosci.* 6:34. doi: 10.3389/fncel.2012.00034

1.7 Lipid droplets

Lipid droplets are spherical organelles rich in triacylglycerol and cholesteryl esters. They are synthesized by the blabbing off from the inner leaflet of the ER membrane (54). Stress and starvation induce the lipid droplets filled with cellular debris that may protect the cell from cytotoxicity. Interaction of perilipin proteins with lipids forms the dynamic structures of lipid droplets that maintain lipid homeostasis necessary for neuronal function and synaptic plasticity. Lipid droplets co-localized with a microglia surface protein ion calcium-binding adaptor protein (Iba1) indicate the brain's pro-inflammatory condition (55). Lipid metabolism is crucial in brain development and function. During Alzheimer's disease, neutral lipid droplets accumulate at SVZ ependymal cells and impair the neural stem cell function. These

lipid droplets are composed of triglycerides rich in oleic acid (56). CNS tissue damage also induces lipid droplets in neurons, and astrocytes which indicate different cell types in the brain can cause lipid droplets according to the condition. Age is also another factor that accumulates the lipid droplets in ependymal cells at the SVZ region.

1.8 Cell death in the host response to infection

The infection causes various host responses that include activation of innate immune system, inflammation, and cell death. The innate immune system is the host's primary immune response to kill the pathogen by several mechanisms. These include the activation of complement system, immune cell chemo-attraction to the site of infection, antigen presentation and, activation of the inflammatory pathway to kill the pathogen. Host-pathogen interaction mediates cell death. The mode of cell death depends on the nature of the pathogen, pathogen burden, and site of infection. The three major cell death modes include apoptosis, autophagy, and necrosis (57). *Plasmodium falciparum* virulence is linked to immune evasion ability. In the human host, the parasite evades the immune response by antigenic variation, polymorphism, and sequestration. Sporozoites of *Plasmodium* infection reduce the antigen-presenting cell function and induce the apoptosis of kupffer cell in exoerythrocytic stage (58, 59). Malaria pigment hemozoin phagocytosis inhibits MHC class II antigen expression in human monocytes and impairs their function (60, 61). Robust erythrophagocytosis induces the ferroptosis in mouse red pulp macrophages, and the apoptosis is mainly mediated by hemin induced redox imbalance (62-64).

1.8.1Apoptosis

Apoptosis morphologically is defined as nuclear fragmentation, chromatin condensation, and formation of apoptotic bodies. Caspases cysteine aspartase enzymes activation induces the apoptosis (65). Caspases are activated by two essential pathways, including extrinsic and

intrinsic pathways. The extrinsic pathway, also called a receptor-mediated pathway, triggers apoptosis through TNF-α, Fas, or tumor necrosis factor-related apoptosis-inducing ligand (TRAIL) binding the receptor (66). The binding of a ligand to the death receptor activates the upstream caspase-8 or caspase-10, further activating the downstream functional caspases, caspase-3, caspase-6, and caspase-7. Functional caspases degrade the DNA into small fragments, a hallmark of apoptosis. The intrinsic pathway has mediated by the activation of Bcl2 family proteins. Bcl2 family proteins include anti-apoptotic proteins like Bcl-2, Bcl-XL, Bcl-W, pro-apoptotic proteins like Bak, Bax, Bad, Bid, and PUMA. Sequestration of pro-apoptotic proteins inhibits the apoptosis. Stress stimulates the transport of pro-apoptotic proteins from the cytosol into the mitochondrial membrane and induces the mitochondrial depolarization and increase in permeability. Mitochondria depolarization causes the release of cytochrome-c into the cytosol, cytochrome-c which promotes APAF-1/caspase-9 complex and activates functional caspases inducing cell death (67).

1.8.2 Autophagy

Autophagy is an evolutionarily conserved degradation process that occurs under basal condition, and cellular stress condition activating the autophagy. Cytoplasmic proteins and damaged organelles engulfed by double or multi-membrane vesicles form the autophagosomes. Later, the lysosome fusion with the autophagosome's outer membrane activates the lysosomal enzymes to digest and recycle the autophagosome's inner membrane and cargo (68, 69). Autophagy related genes (ATG) regulate autophagy by modulating autophagosome biogenesis and maturation (70). Cellular stress or nutrient deprivation initiates autophagy nucleation by dephosphorylating rapamycin's mammalian target or by activation of Beclin-1/phosphatidylinositol-3 kinase (PI3K) complex. After nucleation, the auto-phagosome formation is regulated by two essential ubiquitin-like conjugation systems. The first system includes the conjugation of ATG12-ATG5, and the second is LC3 protein conjugated to a

lipid molecule phosphatidylethanolamine (PE). E1-(ATG7) and E2 (ATG3 and ATG10) like enzyme required to complete the above conjugation system. ATG12-ATG5 complex further conjugates with ATG16 and forms E3- like enzyme complex, which catalyses the conjugation of LC3 to PE (71). LC-PE conjugates to the auto-phagosome membrane and transports them to bind to the lysosome. After auto-phagolysosome formation, the LC3-PE will degrade or be removed by de-conjugation(72).

1.8.3 Autophagy and apoptosis cross-talk

Autophagy and apoptosis both are strongly regulated biological mechanisms. Many studies indicated the crosstalk between the components of these two pathways that promote cell survival and cell death. mTOR influences the apoptosis through the downstream targets such as p53, BAD and Bcl2 proteins (73). AKT phosphorylates the Forkhead box O (FOXO) family of transcription factors, and tumor suppressor p53 which results in the downregulation of several pro-apoptotic genes and upregulates several autophagy genes like LC3, BNIP3(74). The anti-apoptotic Bcl-2 and Bcl-XL bind to pro-apoptotic Bax, inhibits their translocation into the mitochondrial membrane, and regulates the cytochrome-c release into the cytoplasm, activating caspase-3. Bcl-2/Bcl-XL complex to beclin-1 inhibits autophagy. Once the complex disrupts beclin-1 releases and activates autophagy (75, 76). N-terminal cleavage of ATG-5 by calpain induces the ATG5 translocation into the mitochondria and promotes the cytochrome-c release by binding to anti-apoptotic Bcl-2/Bcl/XL causing apoptosis (77).

1.9 The rationale of the study

Pathogen infection modulates the host cell environment to favor their survival and growth. In malaria infection, *Plasmodium falciparum* synthesizes fatty acids through fatty acid synthase II enzyme and transports them to the infected host erythrocyte plasma membrane and alters the phospholipid and fatty acids composition to support their growth. Fatty acid synthesis metabolism is absent in mature erythrocyte. Polyunsaturated fatty acids displayed antiparasitic effect against *Plasmodium* parasite. Anti-parasitic compound artemisinin derived from plant Artemisia annua leaves contain up to 10% of fatty acids in their dry matter, which infers the importance of fatty acids against *Plasmodium* growth. Hence in this thesis, we studied the mechanism of action of saturated and unsaturated fatty acids against *P. falciparum* growth *in vitro* condition.

P. falciparum evades the innate immune system by inducing cell death in macrophages upon phagocytosis. *Plasmodium* infection modulates macrophages and promotes migration into the targeted tissue and causes inflammation and damage to the tissue. Hence, we studied the possible pathways mediating cell death in *Plasmodium* engulfed macrophages and macrophage infiltration in the malaria-infected mouse brain.

P. falciparum drug resistance is the major challenge in malaria control. There is an urgent need for new compounds in the market. Hence we evaluated the anti-parasitic effects of naturally occurring alkaloids and some synthetic derivatives against *P. falciparum in vitro*.

2. Anti-plasmodial activity and mechanism of action of fatty	acids
in vitro	

2.1 Introduction

Malaria is a tropical parasitic disease and according to WHO estimates, 228 million malaria cases with 405000 deaths occurred globally in 2018. Malaria is caused in humans by four species of Plasmodium, amongst which Plasmodium falciparum, is the most virulent. Plasmodium replicates asexually in host erythrocytes by developing a parasitophorous vacuole. The parasite requires phospholipids, for cell membrane formation, as an energy source, for signal transduction, electron transport, initiation of DNA replication, and cell division (78). Plasmodium synthesizes fatty acids by utilizing type II fatty acid synthase, while the higher eukaryotes use type I fatty acid synthase (79). As, lipid metabolism is absent in mature normal erythrocytes, it could be a potential target to inhibit *Plasmodium* growth. Plasmodium synthesizes fatty acids de novo and alters the phospholipid composition of the infected erythrocyte plasma membrane, which is characterized by high phosphatidylcholine, phosphatidylinositol, and less sphingomyelin content with reduced unsaturation index than normal uninfected erythrocytes. Infection alters the phospholipid and fatty acid composition of the host erythrocyte plasma membrane similar to that of the parasite to favor its growth in host erythrocyte. Infection also increases saturated palmitic acid and monounsaturated oleic acid and reduces polyunsaturated fatty acids (PUFAs) viz., Docosahexaenoic acid (DHA) and Arachidonic acid (AA) of the parasite (80).

Fatty acids are essential in host defense against potential pathogens by inhibiting their growth or killing the pathogen. They act as antimalarial, antifungal, and antibacterial components. Previous reports indicate that PUFAs with a high degree of unsaturation are potent in inhibiting the growth of the *Plasmodium*. However they are non-toxic to both normal erythrocytes, and *Plasmodium*-infected erythrocytes and do not induce hemolysis (81). C18 fatty acids, oleic acid, and linoleic acid are active against *Plasmodium* growth (82). A natural C18 fatty acid scleropyric acid isolated from *Scleropyrum wallichianum* was shown

to exhibit antiplasmodial effect (83). Similarly marine sponge isolated cis C23–C26D5, 9 fatty acids displayed antiparasitic activity by inhibiting the FabI enzyme of *P. falciparum* (*Pf*FabI) (84). Saturated fatty acids are inactive against mycobacterium except for capric acid (C_{10:0}) and lauric acid (C12:0). Unsaturated fatty acids forbid topoisomerase I and FabI enzymes of mycobacterium and displayed an inhibitory effect proportional to their degree of unsaturation (28, 85-88). The 2-hexadecynoic acid inhibits *Plasmodium* and fungal growth by inhibiting fatty acid acylation and triacylglycerol (TAG) synthesis (89, 90).

Transport of parasite proteins to erythrocyte membrane and alterations of infected erythrocyte membrane composition occur maximum at the mature trophozoite stage of the *Plasmodium*. During the trophozoite stage, parasite consumes 80% of host hemoglobin and utilizes the globin protein for its progression to the next stage and releases α -haematin dimers, which are toxic to the parasite(91). Hence parasite further polymerizes these α -haematin dimers into a non-toxic β -hematin (hemozoin) product inside the digestive vacuole(90). Chloroquine accumulates in digestive vacuole through the ion trapping mechanism and inhibits hemozoin polymerization by forming π - π interaction with heme (92, 93). Xanthone family compounds form heme-xanthone complexes that inhibit the bio mineralization of β -Hematin (94). The iron molecule of heme activates the endoperoxide bridge of artemisinin derivatives. These endoperoxide compounds inhibit hemozoin synthesis by accumulating in lipid droplets of digestive vacuole (95). Neutral lipids promote β -Hematin polymerization in close association with hemozoin in the digestive vacuole (96). Mass spectrometry analysis showed the abundance of saturated monoacylglycerol in these digestive vacuole neutral lipids and hemozoin.

Treatment of malaria is of high preference and there is an immediate need for multiple approaches to handle this disease. Presently available compounds include aryl amino alcohol compounds such as quinine and chloroquine, pyrimethamine, an antifolate compound, and artemisinin derivatives(97). Currently, three primary therapeutics efforts are in existence, which includes vaccine development, drug development, and pathogenesis. The need for developing new drugs that target the specific biochemical pathways of the parasite is continuous because of the resistance towards existing drugs. Single drug treatment is not sufficient; hence adjunctive therapy has been recommended. Presently the artemisinin–amodiaquine and the artemether-lumefantrine combination are being used against the *Plasmodium* parasite (98). *Plasmodium* infection modulates infected erythrocyte lipid composition, and those lipids have a pivotal role in hemozoin polymerization. Hence in our study, we elucidated the effect of saturated and unsaturated fatty acids on *P. falciparum* growth inhibition, β-hematin polymerization and neutral lipid bodies synthesis of the parasite.

2.2 Material and methods

Fatty acids and JC-1 dye were purchased from Cayman chemicals. Synthetic hemin, Giemsa stain, BODIPY 493/503 stain from Sigma-Aldrich, USA. SYBR green from Molecular Probes, Inc.

2.2.1 Parasite culture

P. falciparum 3d7 culture was maintained by the bell jar candle method at 37° C (99). Parasite was cultured in RPMI 1640 medium supplemented with HEPES 25 mM, 0.5% AlbuMAX I (Invitrogen), hypoxanthine 100 μ M, gentamicin 12.5 μ g/ ml, sodium bicarbonate 1.77 mM) containing 5% hematocrit of RBC and 0.5-0.8% parasitemia.

2.2.2 Plasmodium growth inhibition assay

Fatty acids half-maximal inhibitory concentration (IC $_{50}$) against the *P. falciparum* 3d7 strain was determined using the SYBR Green fluorescence-based method. Briefly, parasite culture was synchronized with 5% sorbitol at the ring stage and further allowed to grow in complete

media until it attains the mature trophozoite. In a 96 well plate, fatty acids were incubated with mature trophozoite culture in a proportion of 1% parasitemia and 2% hematocrit in a total volume of 200 μl for 48 h. After incubation 100 μl of resuspending, culture transferred to 96 well flat-bottom plates which contain 100μl of SYBR Green I lysis buffer (2XSYBR Green, 20 mM Tris base pH 7.5, 20 mM EDTA, 0.008% w/v saponin, 0.08% w/v Triton X-100) (100). Plates were incubated for 1h at 37°C. Fluorescence associated with SYBR Green I- intercalated parasitic DNA was measured at 490 nm excitation and 530 nm emission (TECAN Infinite F-200 spectrophotometer, Switzerland). Half-maximal inhibitory concentration (IC50) of compounds was calculated from three independent experiments using Prism 6.0 software (Graph Pad Inc., US).

2.2.3 Stage-specific growth assessment

The tightly synchronized culture has aliquoted into ring, trophozoite, and schizont stages. Each stage was incubated with Docosahexaenoic acid of 100µM concentration for 12 h. Afterwards, the compound was removed by several washes and culture was allowed to grow in complete media for 84 h. Culture without compound (untreated) and a culture grown in a compound without removing until the experiment (continuous) were used as the controls (101). During the experiment, the smear was prepared for every 12 h, stained with Giemsa, and examined under a microscope to assess the stage specific growth morphology of parasite upon treatment.

2.2.4 NP-40 mediated β-hematin polymerization assay

Fatty acids were incubated with $100\mu M$ hematin, 1 M acetate buffer of pH- 4.8 and $30.55\mu M$ NP-40 in a 96 well plate at $37^{\circ}C$ and shaken at 55rpm for 4 h. The incubation plate was centrifuged at $1100 \times g$ for 1 h at $25^{\circ}C$. After discarding the supernatant, $200\mu l$ of 0.15M sodium bicarbonate containing 2% SDS was added to each well. The centrifugation repeated,

and the supernatant containing free heme was discarded. Then $200\mu l$ 0.36M sodium hydroxide and 2% SDS was added to dissolve the synthesized β -hematin (102). The absorbance was then measured at 400nm using a multi-plate reader (Tecan infinite F-200, Switzerland). The graph was plotted with absorbance against fatty acid concentration. The IC50 value was measured using Prism 6.0 software (Graph Pad Inc., US).

2.2.5 Fatty acid- hemin interaction

To find the interaction of fatty acids and heme, 15µM final concentration of hemin or ferriprotophopyrin (FP) was dissolved in 40% DMSO containing 10mM sodium phosphate buffer, pH- 5.9, and incubated alone or with increasing concentration of saturated and unsaturated fatty acids. After 2 min of incubation (103), the absorption spectrum of hemin was recorded at 400nm and the graph was plotted using Prism 6.0 software (Graph Pad Inc., US).

2.2.6 Docking analysis of heme-fatty acid interaction

Molecular docking is a method that can be used to find the nature of relative conformations between two or molecules that are capable of interacting with each other. We extracted the structure of protoporphyrin ring from PDB_id: 3P5Q (104), converted the Fe⁺² into Fe⁺³ and used minimization protocol for geometry optimization by applying CHARMM force field [Brooks et al., 1983] The structures of chloroquine and unsaturated fatty acids used in the experimental work were drawn using ChemDraw Pro 8.0 and optimized the structures by minimization using CHARMM force field. The entire structure of ferriprotoporphyrin was defined as a receptor target and CDOCKER docking method (105) that is integrated into Discovery Studio 2.5 (Accelerys Inc.) was used to dock chloroquine and unsaturated fatty acids into ferriprotophopyrin and the number of docking conformations was set to 30. The

docking results were analysed graphically and the docking poses were ranked based on their scoring functions PLP1, PLP2 (106, 107), PMF and PMF04 (108, 109).

2.2.7 Neutral lipid bodies (NLB) staining

To study the effect of DHA on inhibition of stage-specific synthesis neutral lipid bodies (NLBs), trophozoite and schizont stage cultures were incubated with DHA for 10 h. Further cultures were stained with BODIPY 493/503, stains the NLB of *P. falciparum*. Micro images were taken with confocal microscopy (Carl-Zeiss, Germany) at 100x magnification.

2.2.8 JC-1 staining to measure the mitochondrial membrane depolarization

JC-1, a membrane-permeable stain was used to study the status of the mitochondria membrane during the apoptotic condition. DHA was incubated with the trophozoite stage of *Plasmodium* for 10 h and stained with JC-1 for 30 min at 37°C. The fluorescence shifts of JC-1 in treated cultures were measured using a spectrofluorometer (Tecan infinite F-200, Switzerland) and compared with untreated culture. Change in mitochondrial polarization was detected by alteration in red (590nm)/green (529) fluorescence ratio.

2.2.9 Semi-quantitative PCR

RNA was isolated from the parasite infected RBC using TRI Reagent® (Sigma-Aldrich, US) and measured the quantity using NanoDropTM spectrophotometer. cDNA was synthesized from the 1 μg of RNA of each sample using BluePrintTM 1st strand cDNA synthesis kit 6115A (Takara) following manufacturer instructions. For pfDGAT quantification 1 μl of cDNA of the sample was subjected to semi-quantitative PCR using DreamTaqTMGreen PCR Master Mix K1081 (Thermo Scientific, US) as per the manufacturer's protocol.

2.3 Results

2.3.1 Polyunsaturated fatty acids (PUFAs) inhibit the growth of P. falciparum

A reduction of SYBR green I fluorescence for PUFAs treated culture indicates reduction in P. falciparum parasitemia. PUFAs viz., DHA, EPA, and AA inhibited Plasmodium growth in a concentration-dependent manner with IC50 values of 38.4 µM, 46.2 µM, 50.8 µM, respectively, after 48 h of treatment. Linoleic and linolenic acid with lower unsaturation index had less parasite growth inhibitory effect compared to the above PUFAs with an inhibitory effect >250µM concentration. Saturated fatty acids viz., stearic acid, palmitic acid, myristic acid had no inhibitory effect on the growth of *P. falciparum* as the treated cultures exhibited fluorescence similar to untreated control culture, as shown in Figure 2.1A. These results indicate that *Plasmodium* growth inhibitory effect of fatty acids is proportional to their degree of unsaturation. Giemsa stained P. falciparum in Figure 2.1B represents the accumulation of trophozoite stage, and pyknotic forms in DHA IC₅₀ (40µM) and IC₉₀ (100µM) concentration incubated cultures correspondingly. At the same time, untreated culture had schizont stage parasites. Figure 2.1C represents changes in developmental morphology of *P. falciparum* in the presence of DHA, vehicle (BSA), and untreated culture. Vehicle-treated culture was similar to untreated culture and could complete the trophozoite stage followed by schizont and ring stages in its 48 h life cycle. At the same time, DHAtreated culture was arrested in the trophozoite stage at 48 h of post-infection. Subsequently, few parasites could attain the schizont stage with increasing time and, after 48 h post-DHA treatment, parasites were noticeably pyknotic.

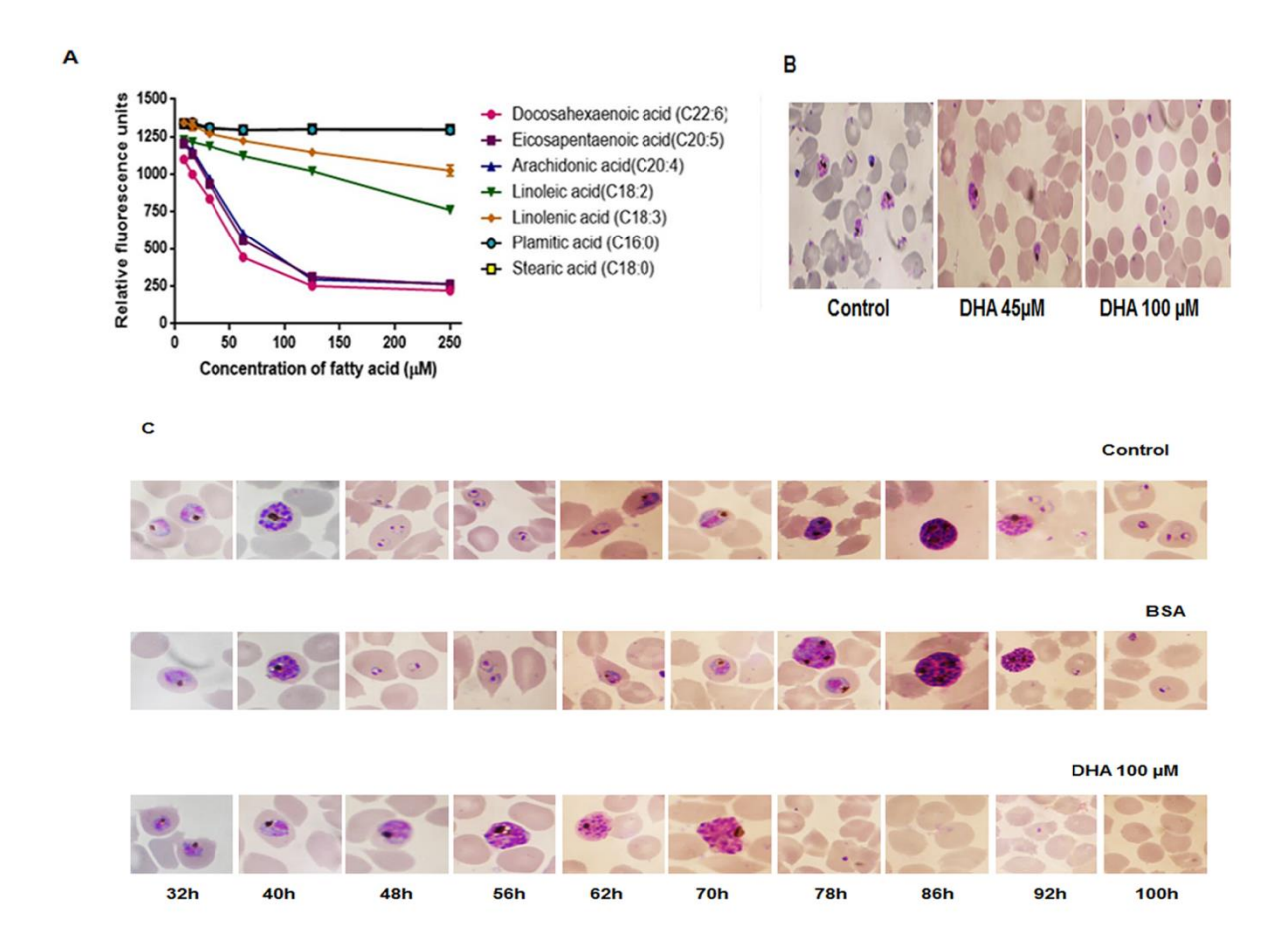
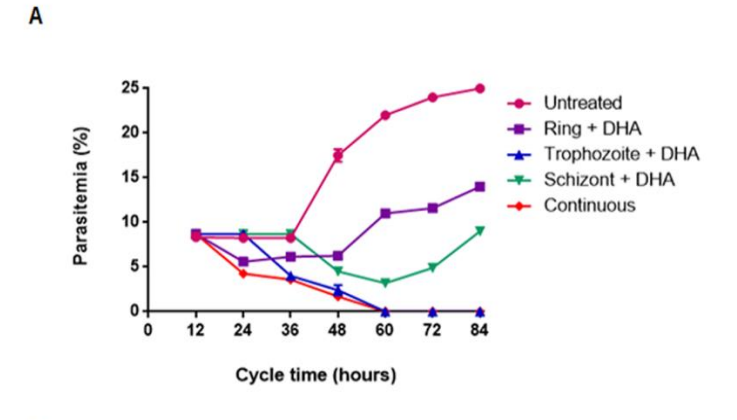


Figure 2.1 Fatty acid-induced death of *P. falciparum*. (A) The synchronized schizont-stage culture was incubated with increasing concentrations of different fatty acids for 48 h. Parasitemia was estimated using SYBR green I fluorescent dye and optical density measured by a spectrofluorometer. The graph was plotted between absorbance values and concentration of fatty acids. (B) Giemsa stained microscopic images of control and parasite culture treated with DHA IC_{50} and IC_{90} concentrations for 48 h. (C) microscopic images of control, vehicle (BSA), and DHA IC_{90} concentration treated *Plasmodium* culture for every 8 h up to 100 h of post-infection.

2.3.2 DHA inhibit the growth of *P. falciparum* trophozoite stage irreversibly

DHA delays the growth of *P. falciparum* and promotes accumulation of trophozoite and pyknotic forms of the parasite in a concentration-dependent manner. To determine if this impact was reversible and if the parasite survives after removing the DHA, the ring, trophozoite, and schizont stages were transiently treated with DHA. After 12 h of treatment, DHA was removed and, parasitemia was estimated for every 12 h up to 84 h. As shown in Figure 2.2A, all DHA treated cultures did not infect erythrocytes. Further there was no

increase in parasitemia at 48 h when compared to the untreated culture. The ring stage treated culture could recover in growth, exhibiting an increase in parasitemia at 60 h. At the same time, the schizont specific incubation of DHA further delays the growth and an expansion in parasitemia was observed at 84 h of post-infection. Decreased parasitemia was seen with trophozoite-specific treated culture even after removing the DHA and was similar to continuous treated culture. These results infer the parasitostatic effect of DHA against ring and schizont stages and parasiticidal effect of DHA against the trophozoite stage. Thin blood smear prepared for every 12 h and Giemsa stained to examine the DHA effect on parasite development morphology. As shown in Figure 2.2B, DHA treatment leads to the analogous delay in the appearance of the successive parasite stages. It was confirmed in the 48 h samples, which exhibited freshly infected ring stage erythrocytes in untreated culture. At the same time, the DHA treated culture accumulated previous cycle trophozoite and schizont stage parasites at 48 h of post-infection. Ring stage-specific DHA incubated culture exhibited trophozoite stages at the end of treatment, i.e., at 24 h and successively developed to mature trophozoite and schizont stages. Ring stage-treated culture displayed a 12 h delay in showing freshly infected ring stage erythrocytes of the next cycle as compared to untreated culture. Trophozoite stage-specific DHA treated parasite was unable to progress to the subsequent schizont stage which induces death after 36 h of treatment. It forms pyknotic structures in 60 h samples, similar to the continuous treated DHA culture. Schizont stage-specific DHA treated culture arrests the parasite progression, showing 36 h delay to attain the consecutive ring-stage parasite as compared to control culture, which appeared at 84 h post-infection. These results indicate that DHA incubation slows down the recovery rate in the schizont stage compared to the ring stage, and recovery is absent in the trophozoite stage.



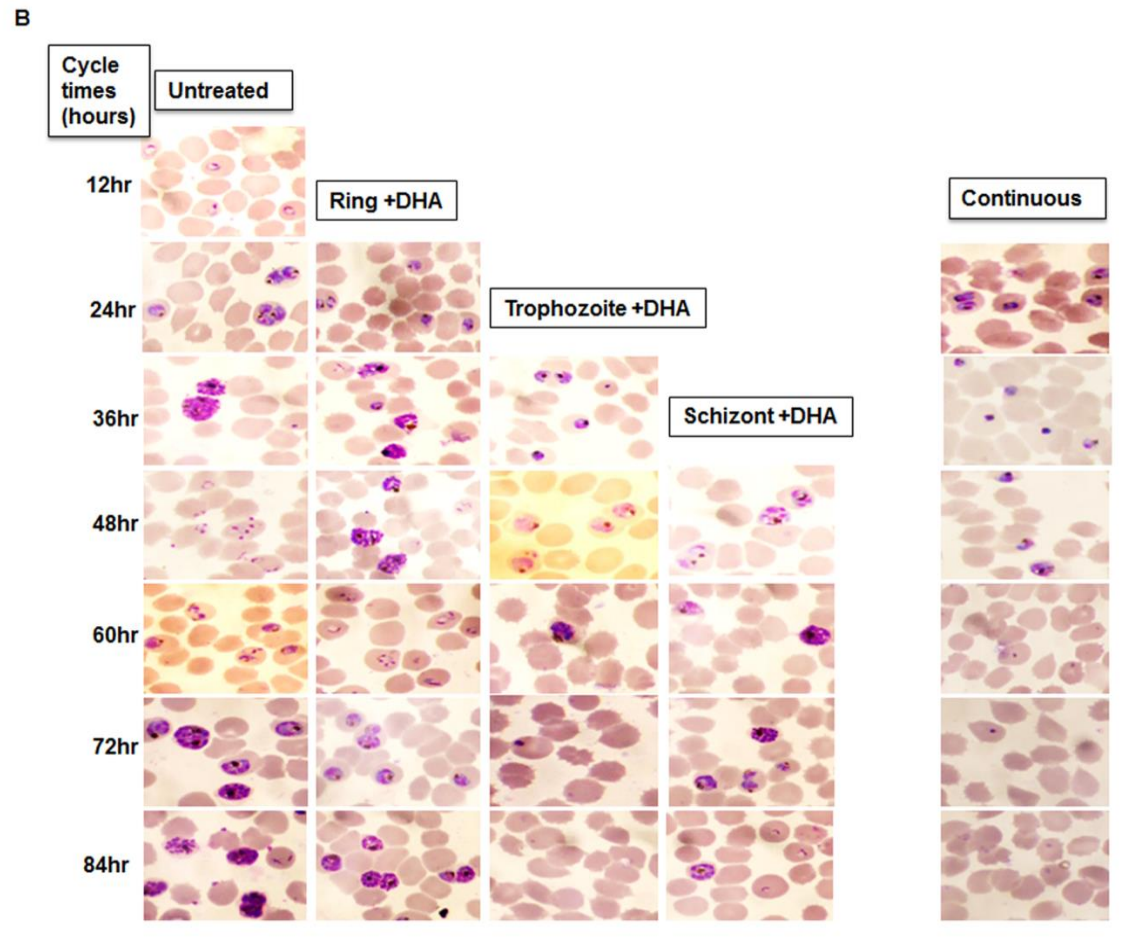


Figure 2.2 Effect of partial treatment of DHA at various *Plasmodium* stages. (A) Growth of parasitemia after treatment with DHA at different stages of P. falciparum infection. 12 h post-infection cultures were treated with DHA at various stages corresponding to ring (Ring + DHA), trophozoite (Trophozoite + DHA), and schizont (Schizont + DHA) stages. After the withdrawal of the compound, parasitemia was assessed every 12 h up to 84 h post-infection. The corresponding graph was plotted for parasitemia against time interval. Results are represented as the mean and error of three individual experiments \pm SEM. (B) Giemsa stained images represent the changes in the morphology of the parasite at the corresponding stages.

2.3.3 Polyunsaturated fatty acids inhibit β- hematin polymerization

The concentration of fatty acid that inhibits half of the β - hematin formation was considered as half-maximal inhibition concentration (IC50). Figure 2.3A shows the graph of PUFAs DHA and AA treatment reduced the relative absorbance of β - hematin in a concentration-dependent manner with IC50 concentration of 35 μ M and 48 μ M, respectively. The positive control chloroquine was found to inhibit β - hematin synthesis with IC50 of 38 μ M. Linoleic acid exhibited a low unsaturation index as indicated by an IC50 of 118 μ M. Monounsaturated fatty acids such as oleic, palmitoleic acid had a less inhibitory effect on β - hematin synthesis compared with PUFA. No alteration in relative absorbance of β - hematin was observed in saturated fatty acid incubation samples even at higher concentrations which were similar to a negative control pyrimethamine and vehicle control. Figure 2.3B I show representative images showing the presence of free hemin in the wells corresponding to DHA, AA, and Chl (chloroquine) of a 96 well plate, where free hemin binds with NaHCO3 and develops color in proportion with the concentration of fatty acids. In Figure 2.3B II, the above wells failed to produce color after adding NaOH due to the absence of β - hematin.

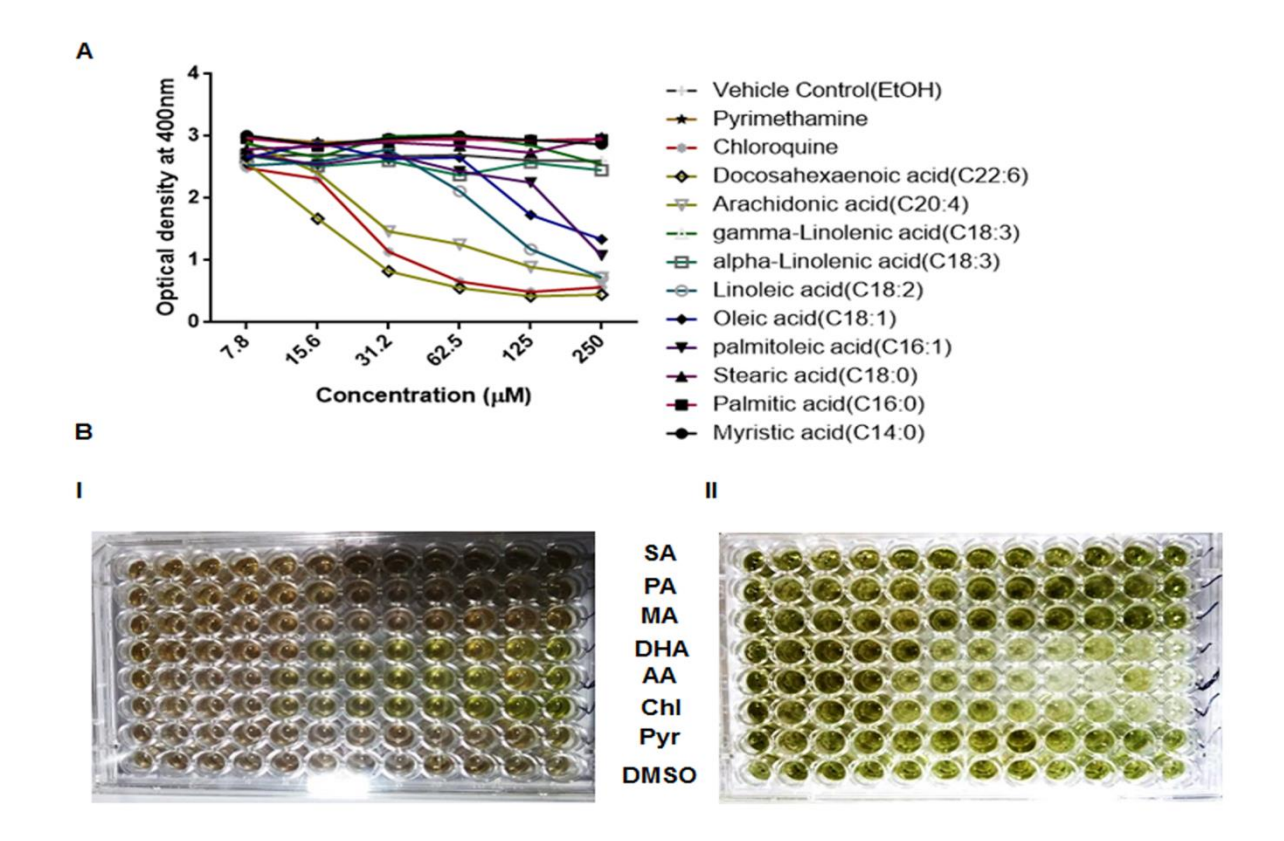


Figure 2.3 Effect of fatty acids on β-hematin formation. (A) Graph showing the decreasing optical density values (corresponding to β-hematin) against increasing fatty acid concentrations. (B) Images showing the 96 well plate containing free hemin is dissolved in 0.15M sodium bicarbonate containing 2% SDS and forms the colour (I). Image showing the 96 well plate containing β- hematin polymers dissolved in 0.36M sodium hydroxide and 2% SDS and develops the colour (II).

2.3.4 Polyunsaturated fatty acids shown interaction with heme and alters Soret band

As the PUFAs inhibit β -Hematin polymerization, we sought to determine the interaction of these fatty acids with synthetic hemin monomers. Synthetic hemin or ferriprotoporphyrin (FP) is monomeric in 40% DMSO solution and gives a sharp Soret band at 400nm. When any compound interacts with this, the spectrum of hemin changes and the Soret band absorption decreases. Fatty acid interaction with synthetic hemin was investigated by checking the alteration of the Soret band. As shown in Figure 2.4, the Soret band absorption spectrum declines with increasing concentration of PUFAs like DHA and AA starting at 1:7 ratio of hemin: fatty acid. With chloroquine as a positive control, Soret band absorption altered

starting from 1:3 ratio of hemin: chloroquine. Sharp Soret band was observed in saturated fatty acid incubated with synthetic hemin similar to vehicle control and pyrimethamine as a negative control, indicating the absence of the interaction of saturated fatty acids with hemin.

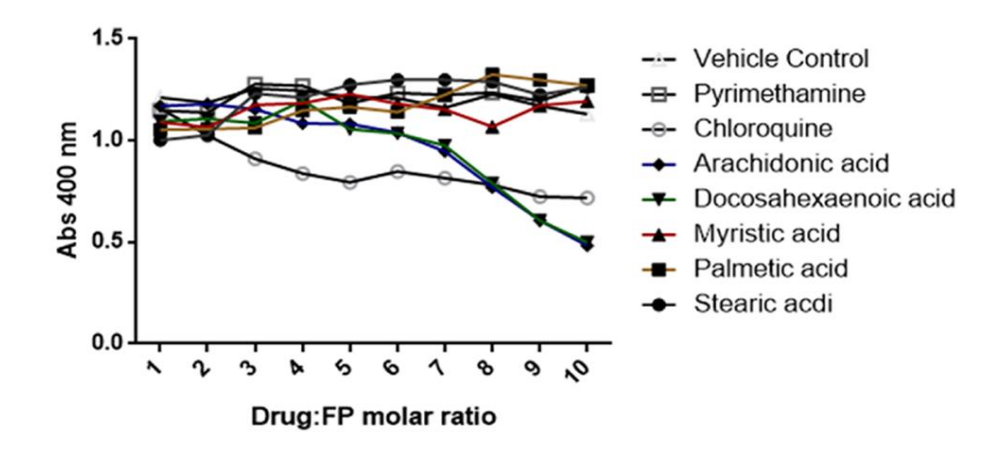


Figure 2.4 Effect of fatty acids on interaction with ferriprotoporphyrin (FP). Graph represents the alteration of the Soret band of $15\mu M$ FP with increasing concentration of chloroquine and PUFAs such as docosahexaenoic acid and arachidonic acid.

2.3.5 *In silico* analysis of heme (ferriprotoporphyrin)-fatty acid interaction

The structures of chloroquine and fatty acids were docked into the structure of ferriprotophopyrin using blind docking. Of the docking poses, the best pose was identified based on the scores, also these poses had maximal occurrences among all the poses. Chloroquine makes pi-pi stacking interactions with ferriprotoporphyrin. For the fatty acid docking, the carboxylic group approaches ferriprotoporphyrin perpendicular to Fe⁺³, and the aliphatic chain wraps around the bridged methylene units connecting the pyrrole rings in the receptor. The binding of docosahexaenoic acid to ferriprotophopyrin is shown in Figure 2.5. The docking scoring values of all the molecules are provided in the Table 1. Chloroquine and docosahexaenoic acid display high scores and myristic acids have the lowest score.

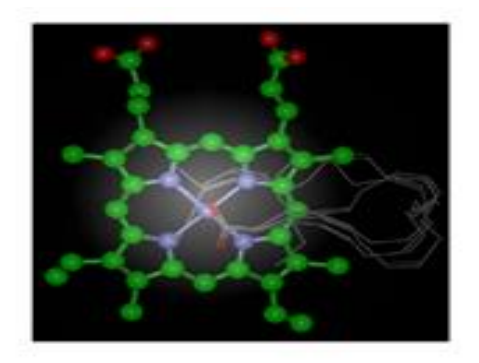


Figure 2.5 *In silico* **interaction of ferriprotoporphyrin to docosahexaenoic acid.** Image represents the binding pose of docosahexaenoic acid (stick representation, carbon-grey, and oxygen-red) to ferriprotoporphyrin (ball and stick representation, carbon-green, nitrogen-blue, oxygen-red).

S.NO.	Compound	PLP1	PLP2	PMF	PMF04
1	Chloroquine	-54.83	-50.87	-27.47	-36.65
2	Docosahexaenoic acid	-42.56	-37.39	-23.8	-23.26
3	Arachidonic acid	-34.9	-28.73	-23.36	-24.42
4	Eicosapentaenoic acid	-29.64	-23.81	-19.93	-16.69
5	Linoleic acid	-30.46	-23.56	-21.46	-15.25
6	Linolenic acid	-25.95	-21.16	-19.31	-15.78
7	Palmitoleic acid	-23.03	-17.68	-21.55	-25.06
8	Oleic acid	-12.88	-10.07	-27.7	-22.6
9	Stearic acid	-22.75	-18.38	-18.94	-25.76
10	Palmitic acid	-15.86	-11.26	-16.62	-21.95
11	Myristic acid	-6.87	-3.89	-13.36	-14.82

Table 1 C-Docker score of fatty acid-ferriprotoporphyrin interaction.

2.3.6 DHA abrogates neutral lipid bodies (NLBs) of P. falciparum

Neutral lipid bodies (NLBs) crystallize the heme degraded from haemoglobin in the digestive vacuole of *P. falciparum* mature stages. Previous results showed that PUFAs prevent hematin synthesis by binding to free hemin. Synchronized trophozoite and schizont-specific stages of *P. falciparum* were treated with DHA for 10 h, stained with BODIPY 493/503 and observed under the confocal microscope to estimate its effect on *Plasmodium* NLB synthesis. Figure 2.6A indicates that DHA reduces the NLB formation at a low concentration of 30 μM and disappears with increasing concentration in trophozoite stage-specific incubated culture. While Figure 2.6B represents more concentration of chloroquine required (60 μM) to reduce

Plasmodium NLB synthesis compare to DHA, it disappears NLBs at 100 μM. Interestingly, both DHA and chloroquine did not affect NLB synthesis of schizont stage-specific treated culture as shown in Figure 2.6C & 2.6D. Pyrimethamine (an anti-folate compound inhibits *Plasmodium* growth by inhibiting its DNA) and oleic acid (a monounsaturated fatty acid which has no antiparasitic effect) did not show any effect on NLB formation of trophozoite and schizont stage-incubated cultures as shown in Figure 2.7A &2.7B. These results infer that DHA specifically acts on trophozoite hemoglobin degradation metabolism by inhibiting digestive vacuole NLBs synthesis.

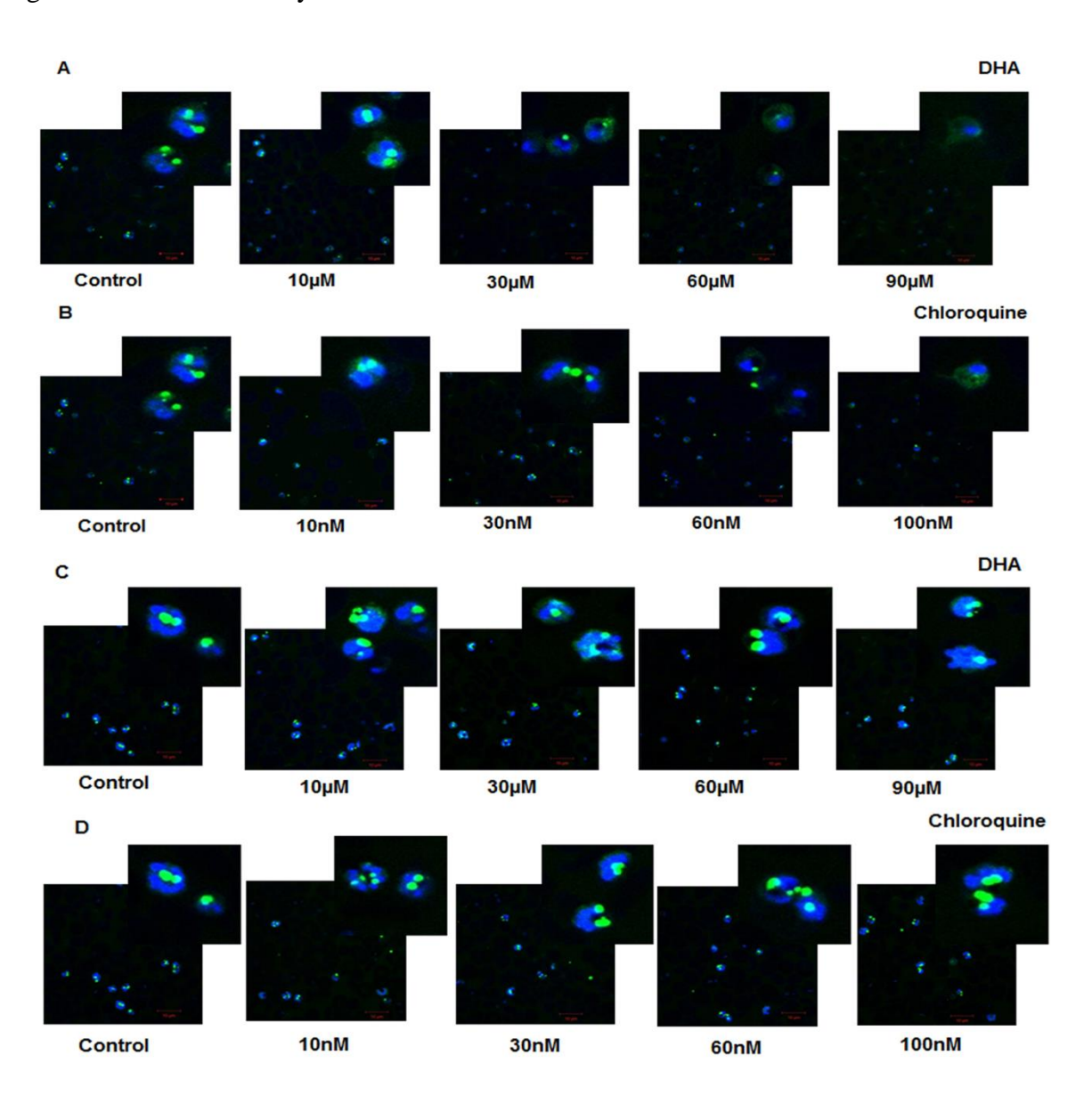


Figure 2.6 Effect of DHA and chloroquine on neutral lipid bodies synthesis. (A) Confocal microscopy images of BODIPY 493/503 stained neutral lipid bodies of trophozoite stage specific treated with increasing concentrations of (a) DHA and (b) chloroquine for 10 h. (B) Confocal microscopy images of BODIPY 493/503 stained neutral lipid bodies of schizont stage culture treated with increasing concentrations of (a) DHA and (b) chloroquine for 10 h. Green (neutral lipid bodies) - BODIPY 493/503; Blue (nucleus) – DAPI.

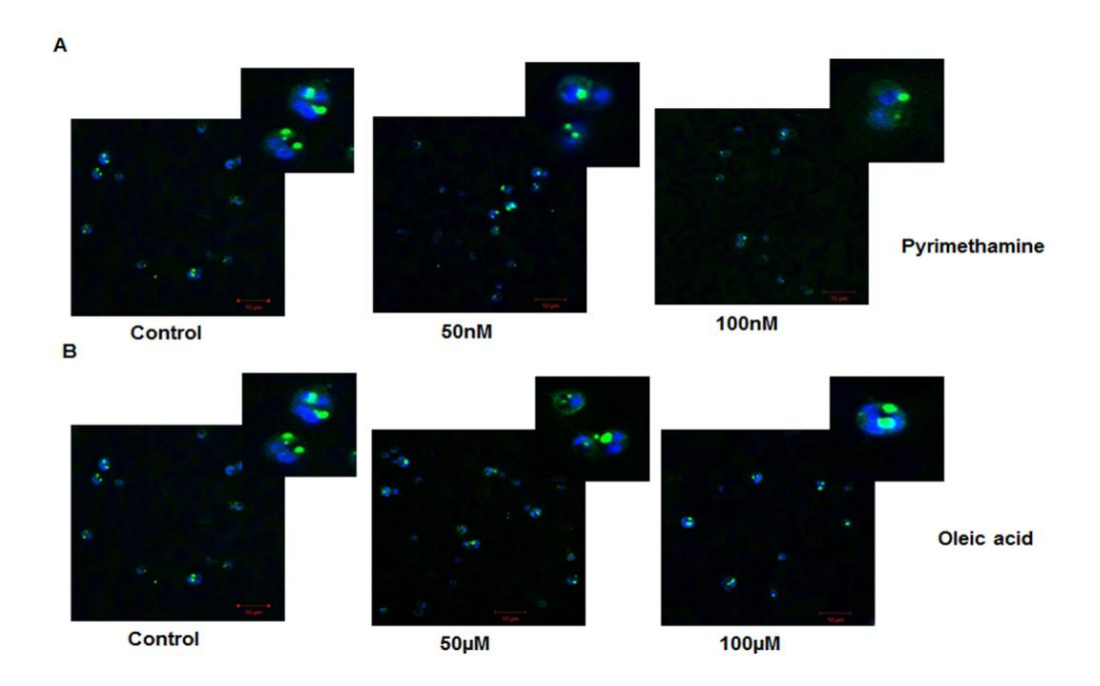


Figure 2.7 Effect of pyrimethamine and oleic acid on neutral lipid bodies synthesis. (A) Confocal microscopy images of BODIPY 493/503 stained neutral lipid bodies of trophozoite stage specific treated with increasing concentrations of pyrimethamine and (B) oleic acid for 10 h.

2.3.7 DHA effect on *P. falciparum* diglyceride acyltransferase (pfDGAT) enzyme gene expression.

DGAT1 is one of two known two DGAT enzymes that catalyse the final step in triglyceride synthesis. pfDGAT (CAB39042) is more closely related to the DGAT1 family of acyltransferases. Hence we estimated the pfDGAT gene expression in ring, trophozoite and schizont stage parasite culture i.e. at 12 h, 24 h, and 36 h post infection parasite cultures respectively by using semi-quantitative PCR analysis. As shown in Figure 2.8A we found increased expression of pfDGAT gene in mature stages i.e. trophozoite and schizont stages of parasite culture compared to ring stage culture. Further we estimated the DGAT expression in

DHA treated trophozoite stage culture we couldn't observe any alteration of gene expression compared to untreated or control culture even with increase in the DHA concentration as shown in Figure 2.8B.

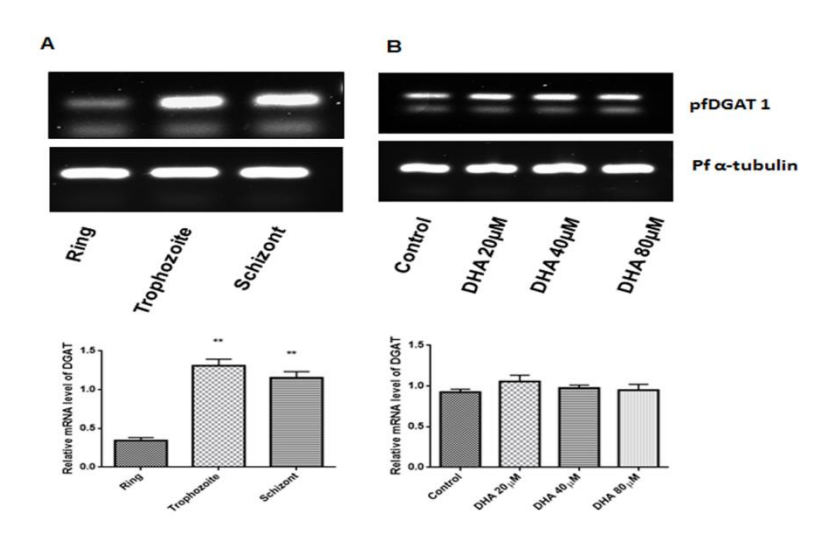


Figure 2.8 Stage specific expression of pfDGAT and effect of DHA on trophozoite stage pfDGAT gene expression. (A) Gene expression of pfDGAT in ring, trophozoite and schizont stage parasite culture and (B) DHA treated trophozoite stage parasite culture. Housekeeping gene pf α -tubulin used as loading control.*,p<0.05 for statistical significance.

2.3.8 Anti-plasmodial activity of DGAT1 inhibitor T-863

Synchronized P. falciparum 3d7 parasite culture was treated with T-863 for 48 h and estimated the parasitemia using SYBR green fluorescence assay. As shown in Figure 2.9 with increasing concentration of T-863 percentage of parasitemia was decreased and observed half maximal inhibition (IC50) at 200µM concentration.

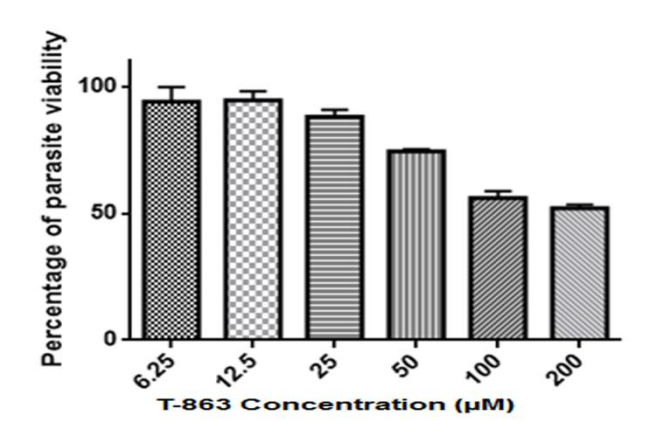


Figure 2.9 Anti-plasmodial effect of T-863 against *P. falciparum.* Graph represents the decrease in percentage of parasitemia with increasing concentration of T-863.

2.3.9 DHA depolarizes P. falciparum mitochondrial membrane potential

The pyknotic bodies formed in *Plasmodium*-infected erythrocytes at higher concentrations of DHA might be due to apoptosis-like cell death of the *Plasmodium*. To evaluate the effect of DHA on mitochondrial membrane polarization of *P. falciparum*, the culture incubated with increasing concentrations of DHA for 10 h and stained with JC-1 and fluorescence measured at 598nm (red) and 533nm green. As shown in Table 2, a low concentration DHA treated sample exhibited strong red fluorescence, which shows a healthy condition. While the high dose of DHA incubated samples displayed green fluorescence because of low membrane potential compared with control. Reduction in 598(red)/533 (green) ratios at a high concentration of DHA represents the depolarization of mitochondria.

S.NO.	Docosahexaenoic acid	Emission at	Emission at	Red/Green
	concentration (µM)	533nm (Green)	598nm (Red)	ratio
1	Control	72	90	1.25
2	15.6	91	91	1
3	31.25	91	89	0.97
4	62.5	102	108	1
5	125	103	80	0.77
6	250	107	65	0.60
7	500	86	37	0.43

Table 2 DHA induced mitochondrial membrane depolarization of *P. falciparum*.

2.4 Discussion

In the current study, we observed that polyunsaturated fatty acids (PUFAs) are potent against *P. falciparum* growth inhibition compared to monounsaturated and saturated fatty acids. This growth inhibition effect of fatty acids is proportional to their unsaturation index (presence of double bonds). Our observation is in agreement with the findings of Kumaratilake et al (81) who reported that among all fatty acids DHA with the highest unsaturation index was more potent against *P. falciparum* growth inhibition. DHA at higher concentrations might induced

apoptotic like cell death and formed the pyknotic structures in Plasmodium-infected erythrocytes. Under in-vitro conditions, these PUFAs might exhibit pyknotic structure formation machinery (81) or, the oxygen, nitrogen derived reactive species(110-112), oxidized polyamines(113) and lipid peroxides (110) might induce these degenerated pyknotic forms. Plasmodium-infected erythrocytes were less susceptible to lipid peroxidation than non-infected erythrocytes. In addition to the host cell membrane of the parasitized erythrocyte, the plasma membrane of the neighbouring cells also exhibits resistance to oxidative stress (114). In contrast, some reports confirmed lipid peroxidation and alteration in antioxidant enzymes, in P. vivax-mediated jaundice (115). Parasite synthesized hemozoin establishes a potential catalyst for this lipid peroxidation. Nonenzymatic heme catalysed peroxidation of lipids in parasite-infected erythrocytes, and hemozoin were found to contain large amounts of monohydroxy derivatives of polyenoic fatty acids (OH-PUFAs) like 9 HETE and 12 HETE in their ester lipids(116). These observations imparted ambiguity to the lipid peroxidation environment in the parasite-infected erythrocytes. In our study when we auto-oxidize DHA by exposing it to air overnight, the antiparasitic effect was doubled as compared to its non-oxidized form (data not shown). Hence further studies are required to confirm PUFAs peroxidation-mediated parasite death.

The stage-specific growth inhibition assay results indicate that DHA inhibits the growth of trophozoite stage of *P. falciparum* irreversibly. It delays the growth of the ring and schizont stage of the parasite. As per our results, the recovery capability of the schizont stage parasite is much slower than the ring stage of transiently DHA treated culture. The previous study stated that DHA induces 90% death of *P. falciparum* at a concentration of 20-40µg/ml (81). The survived parasites were in the ring form. AA caused 80% of the death. In the survived parasites along with ring form, some percentages of schizont were also observed

(81). These observations indeed support the specific inhibition effect of DHA on trophozoite stage of parasite.

Plasmodium utilizes the host erythrocyte haemoglobin and releases the free heme which is toxic to the parasite. Hence *Plasmodium* crystallizes free heme to nontoxic insoluble hemozoin polymers in the digestive vacuole (117). This makes inhibition of hemozoin synthesis a potent drug target. Chloroquine and quinoline are influential antimalarial compounds that act through inhibiting hemozoin synthesis. Fitch et al. reported that the unsaturated fatty acids like arachidonic, linoleic, oleic, palmitoleic acids, and mono- and dioleoylglycerol were active on β-hematin synthesis and, saturated fatty acids such as stearic and palmitic acids were inactive (118). In contrast to this our study indicates that among all fatty acids the PUFAs have antiplasmodial effect and are potent against inhibiting the βhematin synthesis. The β-hematin inhibition effect of PUFAs viz., DHA and AA is proportional to their unsaturation index. Linoleic acid with lesser unsaturation index and palmitoleic acid with single unsaturation required high concentration to inhibit β-hematin polymerization. While Oleic acid, a monounsaturated fatty acid, did not show any effect on the β-Hematin polymerization, similar to the saturated fatty acids. Bendrat et al. identified the presence of methyl esters of oleic, stearic, and palmitic acid in acetonitrile fractions of hemozoin by mass spectrometry analysis. This study further support that saturated and monounsaturated fatty acids are required in β -hematin synthesis(119).

Heme - drug complex inhibits the hematin polymerization. In line with this, chloroquine and other quinolones bind to the free heme derived from the hemozoin degradation in a digestive vacuole (120). Hematin polymer degradation was not observed with chloroquine and quinolone treatment indicates the importance of chloroquine- heme interaction in inhibition of β -hematin synthesis(121). As PUFAs inhibited the hemozoin synthesis we studied the heme- fatty acid interaction. Our results confirmed the binding of

free hemin with PUFAs DHA and AA by Soret band assay. Our observations suggested that more fatty acid concentration is required for interaction with hemin as compared to chloroquine. The previous study exhibited the interaction of LDL glycerophospholipids fatty acids oleic, linoleic, and arachidonic acid to myeloperoxidase (MPO) heme prosthetic group by alteration in the Soret region of the visible spectrum (122). It supports the fatty acid-heme interaction. The saturated and monounsaturated fatty acids did not show interaction even at higher concentrations similar to the pyrimethamine, a negative control in our study. The binding affinity of the fatty acids to MPO is proportional to their unsaturation index further confirms the PUFAs with high unsaturation inhibits β -hematin formation (122). Our *in silico* analysis of fatty acid – hemin interaction study elucidated that among all fatty acids DHA has exhibited highest C-Docker score with ferriprotoporphyrin perpendicular to Fe⁺³, which further supports the role of unsaturation in binding to hemin. Similarly unsaturated or cyclopropanated fatty acids binding to Escherichia coli flavohemoglobin and modifies the visible absorption spectrum of the ferric heme, strengthen our observations (123). These previous studies support the unsaturated fatty acid- heme complex-mediated inhibition of hematin polymerization shown in our study.

The literature illustrates three hypotheses for the hematin crystallization mechanism. Those include enzyme-catalysed heme polymerase (124), histidine-rich proteins (125, 126), and lipid mediated(118) or a combination of both(28). Acidic digestive vacuole, which mediates the hemozoin crystallization, contains neutral lipid bodies (NLBs). The synthesized hemozoin crystals surrounded by lipid nano spear further indicates the role of lipids in hemozoin polymerization (96). The neutral lipid nano spear protects hemozoin from peroxide degradation. A high concentration of H2O2 is required to degrade the neutral lipids enveloped hemozoin than the delipidated hemozoin(127). As PUFAs can promote lipid peroxidation from our study we observed a decrease of neutral lipid bodies size in DHA

treated Plasmodium trophozoite stage culture compared to the untreated culture. Further increase in DHA concentration abrogates the lipid bodies of *Plasmodium*. The presence of these NLBs and their localization in the digestive vacuole is stage-dependent (128, 129). Late trophozoite and early schizont stages of the Plasmodium digestive vacuole contains more number of lipid bodies (129, 130). In our study when we incubated DHA at the schizont stage of *Plasmodium* it did not show any alteration in NLBs size and number. Similarly chloroquine also decreases and at high concentration abrogates the *Plasmodium* trophozoite stage NLBs, while it did not show any effect on schizont stage NLBs. A previous study reported that the parasite treated with Brifeldin A for 26 or 30 h, i.e., when parasite develops into mature trophozoite stage, it reduced the numbers of lipid droplets significantly compare with untreated. After removing the BFA the parasites are viable, able to continue development and accumulate lipid droplets. At the same time Trifluoperazine (TFA) a compound that modulates fatty acid incorporation into TAG incubated with late trophozoite stage of *Plasmodium*, reduces the lipid droplets number probably through inhibiting the Diacylglycerol acyltransferase (DGAT) the principal enzyme in TAG synthesis. DGAT is more active at trophozoite and schizont stages of the *Plasmodium* parasite (131). We found increased expression of DGAT in trophozoite and schizont stage parasite culture compared to ring stage parasite culture. DHA inhibited the neutral lipid droplets in trophozoite stage treated culture hence we hypothesized the effect of DHA in regulation of DGAT expression but interestingly DHA treated trophozoite stage culture didn't show alteration in DGAT expression compared to untreated culture even we increase the DHA concentration. 80 µM T863 a DGAT1 inhibitor showed 95% growth reduction in Toxoplasma gondii after 24 h treatment and 5 µM concentration abrogates the neutral lipid bodies (132). Whereas T863 showed 50% growth inhibition at 200 µM against P. falciparum after 48 h treatment supports the T863 inability to inhibit the *Plasmodium* trophozoite DGAT gene expression. These

studies support the trophozoite specific NLBs alteration by DHA and chloroquine in our study.

Our results indicated that when we incubate *Plasmodium* with pyrimethamine, and oleic acid at trophozoite and schizont stage, they did not exhibit any alteration of NLBs at both stages of *Plasmodium*. This further supports that the trophozoite stage-specific NLBs inhibition is DHA and chloroquine dependent. The fatty acid methyl ester analysis of digestive vacuole and purified hemozoin identified prevailing saturated stearic and palmitic acids and also a lesser amount of unsaturated oleic and linoleic acid, and absence of PUFA arachidonic acid(124). Digestive vacuole and trophozoite are rich in oleic acids than stearic acid (124), which may be the reason we could not observe alteration of neutral lipid bodies in oleic acid incubated *Plasmodium* cultures in our study.

Differential scanning colorimetry examination of phase transitions and molecular orientation in the liquid state of neutral lipids, indicate that acyl moieties positioning in glycerolipids decreases the fluidity of dispersed lipid droplets(133) which is another possible reason for lipid droplets degeneration. Lipids phase transition temperature depends on the head group, hydrocarbon chain length, and degree of unsaturation of lipids. The lipid composition of hemozoin is rich in saturated, mono stearic glycerol (MSG), and mono palmitic glycerol (MPG). Unsaturated monooleic glycerol (MOG), monolinoleic glycerol (MLG) was absent in parasite and sucrose purified hemozoin. These saturated lipids (MSG, MPG) possess a higher melting temperature than unsaturated dioleoylglycerol (DOG) and dilinoleoylglycerol (DLG). Hence the addition of a double bond containing phospholipids reduces the hydrophobic interactions and decreases the melting temperature. Hence PUFAs DHA and AA incubation may induce the *cis* double bonds in lipid droplets. This causes a kink in the carbon chain that prevents these fatty acids from packing tightly in the membrane, and increase the fluidity and dispersal of the neutral lipid bodies which can be the possible

explanation for the DHA induced NLBs degeneration in trophozoite of *Plasmodium*. Digestive vacuole permeabilization or disruption can lead to apoptosis like cell death of parasite (134, 135). Chloroquine and quinacrine induce programmed cell death like apoptosis by inducing digestive vacuole permeabilization and mitochondrial depolarization of the parasite (136). In mammalian cells depolarization of mitochondrial membrane and fragmentation of nuclear DNA are the apoptotic features. In our study we observed DHA induced the mitochondrial membrane depolarization at the concentration which DHA able to form apoptotic features pyknotic structures in *Plasmodium* infected erythrocytes and also abrogates the digestive vacuole NLBs infers similar to chloroquine, DHA may induce programmed cell death like apoptosis in *P. falciparum*.

DHA and EPA suppress pathogenicity by inducing cellular membrane disruption in *Porphyromonas gingivalis* and *Fusobacterium nucleatum pathogens* (137). DHA a potent inhibitor of enoylacyl carrier protein reductase (Fab I) of *P. falciparum* (97) and *Staphylococcus aureus* (138). Inhibition of Fab I reduce the fatty acid chain elongation and further affect the phospholipid biosynthesis machinery. Hence the presence of DHA might inhibit the enzymes in the biosynthetic pathway and alter the neutral lipid content. *Alternatively* DHA induced peroxidation and chloroquine induced ROS might degrade the NLBs at the trophozoite stage of *Plasmodium*. The inefficiency of these compounds in altering the schizont stage NLBs is not understood. It is interesting to know whether DHA and chloroquine inhibit the synthesis of NLBs or degrade these. A detailed study is required to further confirm the mechanism of action of DHA and chloroquine on NLBs alteration.

3. Robust erythrophagocytosis induced cell death and
immune modulation in Raw 264.7 macrophage cell line

3.1 Introduction

Monocytes/ macrophages are innate immune cells that protect the host by controlling the pathogen growth through phagocytosis, secreting cytokines, and presenting antigens. Macrophage activation by malaria pathogenesis results in the secretion of pro-inflammatory cytokines. These cytokines play an essential role in the sequestration of *Plasmodium* infected erythrocytes (iRBC) to the brain, lung, placenta, and other tissues by inducing the vascular endothelial cell adhesion molecules (139). Parasite infection causes surface receptor molecules' expression like intercellular adhesion molecule (ICAM) and chemokine receptors on macrophages, which further promotes macrophages' binding to endothelial cells and facilitates their infiltration into damaged tissue and causes severe malaria (140). Inflammatory response executed by macrophages is mainly pro and anti-inflammation. During the pathogenic condition, macrophages induce pro-inflammatory condition to inhibit the parasite growth. An anti-inflammatory state activated after the pathogen clearance to protect tissue damage. Alteration in inflammatory pathway regulation causes detrimental effects (141). Phagocyte - reduced macrophages secrete proinflammatory cytokines like TNF- α and IFN- γ into the serum (142). Tissue-resident CD169⁺macrophages release the IL-10 anti-inflammatory cytokines. Their absence causes severe malaria through blood-brain barrier disruption, and vascular permeabilization of the target tissues and increased deposition of hemozoin (143). During initial infection, the phagocytic activity is more, and with repeated infection, the macrophages lose its activity (144, 145). Macrophages are prone to phagocytose mature stages like trophozoite and schizont stages of infected erythrocytes (146, 147). Ring stage erythrocyte ingested macrophages could degrade the haemoglobin and repeat the phagocytic activity. Mature stage parasite engulfed macrophages failed to degrade the hemozoin and inhibit the phagocytic activity (61). Hemoglobin derived heme causes the redox imbalance and induces apoptosis and oxidative burst in robust iRBC phagocytosed

macrophages (63, 148). Macrophages are active in producing proinflammatory lipid derivatives eicosanoids, prostaglandins, and leukotrienes (149, 150). Simultaneously the resolvins and lipoxins synthesized by macrophages from the lipids induce anti-inflammatory condition and inhibit apoptosis (151). Hence it is interesting to study the role of lipids in the induction of apoptosis of iRBC engulfed macrophages.

Autophagy acts as a cytoprotective in oxidative stress, starvation, and endoplasmic stress activation (152). Autophagy inhibition induces the M1 macrophage polarization (proinflammatory) and its activation promotes M2 phenotype (anti-inflammatory) (153). Immune cell activation alters their morphology and facilitates their migration to the infected tissue and secretes the proinflammatory lipid derivatives. mTORC1 and mTORC2 regulate this metabolic process in activated immune cells (154). PI3K-mTORC1 pathway regulates the increased protein synthesis in LPS treated macrophages (155, 156). Ehrlichia gram-negative bacteria induce mTORC1 dependent M1 phenotype macrophages, which accumulate in the liver and causes fatality. In contrast nonlethal form activates and accumulates M2 phenotype (157). *P. falciparum* infection accumulates CD40+ M1 macrophages in the lung and causes pulmonary edema (158). It is interesting to study the role of *Plasmodium* infection in macrophage autophagy and polarization regulation.

Cerebral malaria is a severe form of malaria induces brain resident macrophages/microglial activation and increases the number of perivascular macrophages in infected brain tissue which further aggravate inflammation (159, 160). Aging increased lipid droplets accumulation in microglia that inhibits their phagocytic activity. Lipid droplets increase the reactive oxygen species, proinflammatory cytokines in mice, and human brain tissue (55). Lipid laden cells are differentially distributed in brain parenchyma, including lateral ventricle walls and hippocampus, which includes neurogenic, niches (161). Lateral ventricle subependymal zone rich of radial glial cells transports the new cells to the different

regions of the brain, neurons to the olfactory bulb, glial cells to the cortex and corpus callosum (162). This study elucidated the apoptosis and autophagy regulation in *Plasmodium* infected RBC (iRBC) engulfed macrophages cell death and macrophage-induced neuroinflammation in cerebral malaria.

3.2 Materials and methods

3.2.1 Infection of mice and blood recovery

BALB/c mice of 4-6 weeks age was infected with 10⁶ *P. berghei* ANKA infected RBC (iRBC). When parasitemia was reached 40-50 percentages, blood was collected through the retro-orbital method from anesthetized mice in heparinized tubes. Then blood was washed with cold PBS separated RBC by centrifuging at 1200rpm for 10 min and counted. Isolated RBC was incubated with Raw 264.7 macrophages at a different ratio. Blood from control mice was processed similarly (cRBC).

The animal experiment in this study was approved by the Institutional Animal Ethics Committee (IAEC) as per CPCSE guidelines.

3.2.2 Raw 264.7 cell culture and treatment

Raw 264.7 cells were cultured in DMEM media with 10% FBS at 37°C under 5% CO₂. Cells were seeded 24 hr before the experiment. On the day of experiment, fresh media added incubated the cells along with iRBC from the ratio of 1:10 to 1:100 and cRBC 1:100 (macrophage: iRBC). Following treatment non-phagocytosed, RBC was lysed using ammonium chloride RBC lysis buffer, washed with cold PBS, and used for further analysis.

3.2.3 CFSE staining of RBC

RBC was stained with CFSE (Cayman, US), as shown before (63). Briefly, RBC at 2×10^{-7} cells/mL was incubated in CFSE staining buffer (PBS containing 0.1% BSA and 2.5 μ M CFSE) for 10 min. The reaction was blocked by adding complete media for 10 min on ice. Later RBC was washed with RPMI media.

3.2.4 Quantification of erythrophagocytosis in Docosahexaenoic acid (DHA) treated macrophages

Raw 264.7 macrophages were treated with DHA overnight, with increasing concentration from 30 μM to 90 μM. Cells were washed with cold PBS and added fresh complete media. DHA treated macrophages were incubated with iRBC and cRBC in 1:50 (macrophage: RBC) ratio for 6 hr. After incubation non -phagocytosed RBC was lysed with ammonium chloride buffer. Internalized RBC was estimated in PBS washed macrophage using FACS BD LSRFortessaTM cell analyzer by batch analysis. For confocal image, cells were seeded on poly L lysine coated coverslips and cultured and incubated the cells with RBC as stated above. After ammonium chloride lysis of RBC, cells were imaged under confocal microscopy to estimate phagocytosed RBC by macrophages.

3.2.5 Western blot analysis

Cells were lysed on ice in buffer containing 10mM Tris pH 7.4, 0.32M sucrose, 0.25mM Na2EDTA, 1mM Na3VO4, 1mM PMSF, 20mM beta-glycerophosphate & 20mM NaF by sonication. The concentration of protein lysate was estimated by the Bradford method and proteins were subjected to SDS-PAGE with 40 µg protein used for each well. After separation, the proteins on the gel were transferred on to nitrocellulose membrane overnight. The membrane was blocked with 5% skimmed milk (Himedia, India) in TBS for 1 h.

Membrane incubated with primary antibodies anti-caspase-3, anti-cleaved caspase-3, anti-p53(sc21872 r), anti-mTORC1, anti-phospho-mTORC1, anti-phospho-p70S6K, anti-LC₃I&II, anti-β-actin at 4°C overnight. Membrane washed with TBS and TBST (TBS+0.1% Tween 20) for 3 times and probed with horseradish peroxidase (HRP) conjugated secondary antibody (Sigma Aldrich, US) for 1 h at room temperature. The membrane was washed with TBS and TBST for 5 times each 5min. Protein bands were developed using femtoLUCENTTM PLUS-HRP chemiluminescent reagent (G-Biosciences, US). The protein bands were densitometrically quantified using ImageJ software (NIH, US).

3.2.6 Immunofluorescence

Brain tissue sections were made using cryotome and placed on silane coated slides and stored at -80°C. For immunofluorescence the sections were permeabilized with 0.3% triton-X-100 in PBS for 30 min at room temperature. 5% goat serum in PBST was used as a blocking solution to block the sections for 1 h at room temperature. Sections were incubated with primary antibody anti-GFAP (CST, US) overnight at 4°C. Washed the sections with PBS for 3 times each 5 min and incubated with Alexa Fluor – 555 conjugated goat anti-mouse IgG (CST, US) for 1 h and washed the sections and mounted with anti-fade DAPI solution and imaged under confocal microscopy (Carl-Zeiss, Germany).

3.2.7 Bodipy 493/503 staining

Brain sections were permeabilized with 0.3% triton-X-100 in PBS for 30 min and incubated with Bodipy 493/503 of 1mg/ml concentration at 37°C for 15 min, washed the sections in PBS for 3 times each 5 min. Mounted the sections with anti-fade DAPI solution and imaged under confocal microscopy (Carl-Zeiss, Germany).

3.2.8 Semi-quantitative PCR

RNA was isolated from the mouse brain using TRI Reagent® (Sigma-Aldrich, US) and measured the quantity using NanoDropTM spectrophotometer. cDNA was synthesized from the 1 μg of RNA of each sample using BluePrintTM 1st strand cDNA synthesis kit 6115A (Takara) following manufacturer instructions. 1 μl of cDNA of the sample was subjected to semi-quantitative PCR using DreamTaqTMGreen PCR Master Mix K1081 (Thermo Scientific, US) as per the manufacturer's protocol. A nucleic acid sequence of primers was perilipin-1 (5'CAGAATATGCCGCCAACACC 3', 5'GGCTGACTCCTTGTCTGGTG3'), perilipin-2 (5'AAGAGAAGCATCGGCTACG3', 5' GCGATAGCCAGAGTACGTG3'), perilipin-3 (5' GCAACTGCTGAGACCATG3', 5' GGCTGCACAACAGGTTCCTC3').

3.3 Results

3.3.1 Lipid droplets biogenesis and cell adhesion molecule induction in iRBC engulfed macrophages.

To analyse the effect of *P. berghei* ANKA infected RBC (iRBC) on lipid droplet formation, we incubated the Raw 264.7 macrophages with iRBC at a different ratio of macrophage: iRBC for 48 h. We found that macrophages incubated with iRBC at a ratio of 1:50 and 1:100 induced lipid droplets compared to cRBC incubated macrophages of similar ratio and 1:10 ratio of iRBC as detected by Bodipy 493/505 staining as shown in Figure 3.1A. We also estimated the expression of lipid droplet stabilizing protein perilipin-2 expression in macrophages incubated with iRBC. Macrophages with iRBC in a ratio of 1:50 and 1:100 has shown significantly increased perilipin-2 expression (p< 0.0009 and p<0.0003 respectively) as compared to 1:100 ratio of cRBC incubated macrophages as shown in Figure 3.1B & 3.1C. Lipid droplets facilitate the expression of cell adhesion molecules on macrophages. In our study we found the increased expression of ICAM-1 cell adhesion molecules in iRBC co-

cultured macrophages while cRBC incubated macrophages failed to induce the ICAM-1 expression even at 1:50 ratio as shown in Figure 3.1D.

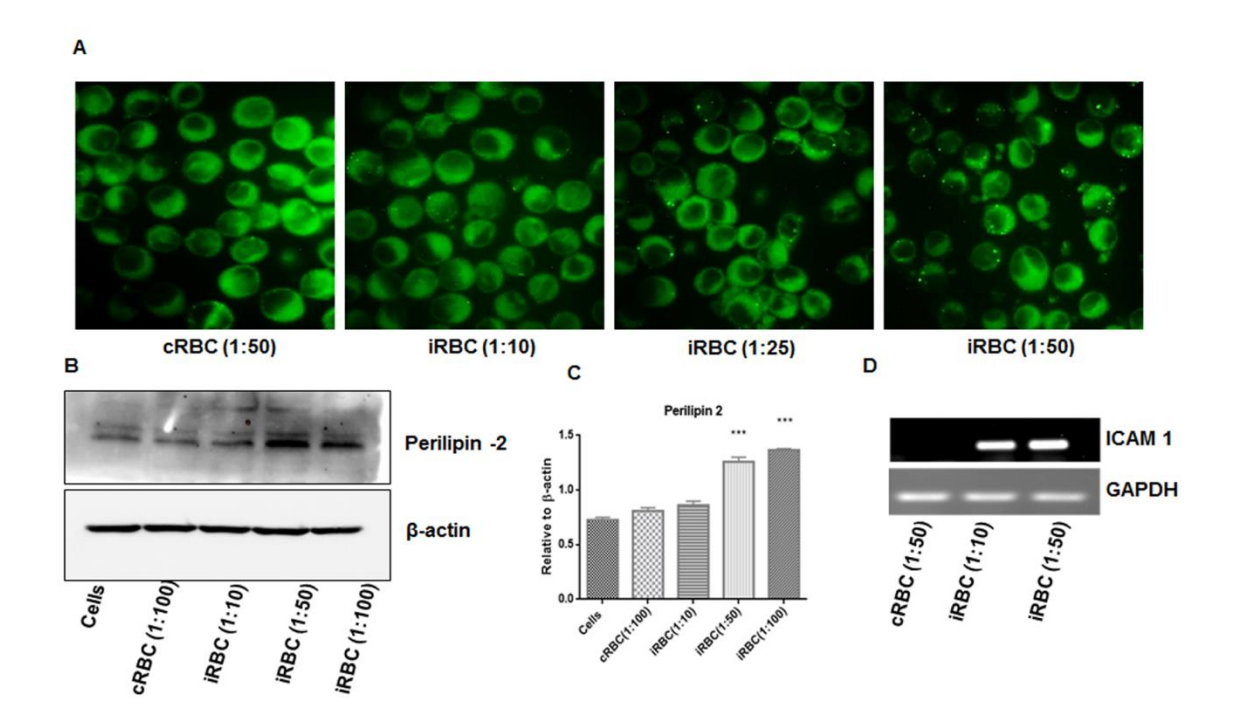


Figure 3.1 Lipid droplet accumulation and induced ICAM-1 expression in enhanced iRBC phagocytosed Raw 264.7 macrophages. (A) Confocal microscopy images of BODIPY 493/503 stained neutral lipid droplets of Raw 264.7 macrophages incubated with different ratios of cRBC and iRBC. (B) Representative immunoblot of perilipin-2 protein expression in Raw 264.7 macrophages incubated with different ratios of cRBC and iRBC. Immunoblot of β-actin confirms equal loading. (C) Graph showing a perilipin-2 level of Raw 264.7 macrophages. Statistical significance indicated by ****, p< 0.0001, *, p<0.05 compared to cRBC incubated macrophages. (D) ICAM-1 gene expression in cRBC and iRBC incubated Raw 264.7 macrophages. Housekeeping gene GAPDH (glyceraldehyde 3-phosphate dehydrogenase) is used as a loading control. cRBC (control mice blood), iRBC (*Plasmodium berghei ANKA* infected mice blood)

3.3.2 Robust erythrophagocytosis induces caspase-mediated apoptosis in Raw 264.7 macrophage cell lines

Enhanced iRBC phagocytosis induces cell death in macrophages. We observed increased propidium iodide staining in iRBC co-cultured macrophages compared to cRBC with a ratio of 1:100 for 48 h, as shown in Figure 3.2A confirms the cell death in iRBC incubated

macrophages. The immunoblot analysis further confirms that this cell death was mediated by caspase 3. Incubation of iRBC with a 1:50 and 1:100 ratio significantly increases the expression of cleaved casp3/total casp3 levels (p<0.0001) in macrophages compared to cRBC of ratio 1:100 incubated macrophages as shown in Figure 3.2B & 3.2D. The tumor suppressor gene p53 induces the activation of apoptosis. iRBC at 1:50 and 1:100 ratio showed a significant increase in the expression of p53 levels compared with iRBC of 1:10 ratio and cRBC of 1:100 as showed in Figure 3.2B & 3.2C (p=0.0002 & p=0.003).

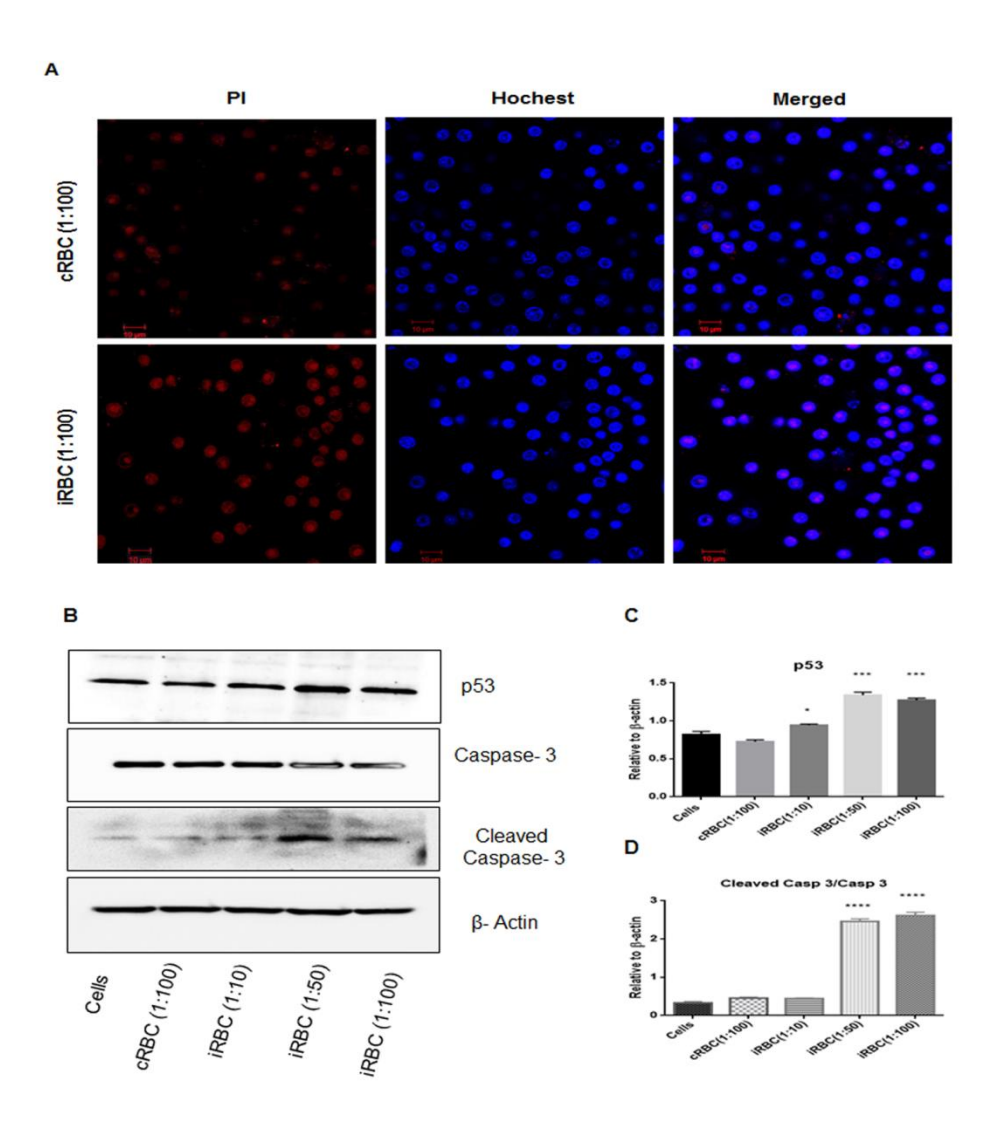


Figure 3.2 Cell death and Caspase-3, p53 expression in robust iRBC phagocytosed Raw 264.7 macrophages. (A) Confocal microscopy images of PI/Hochest stained Raw 264.7 macrophages incubated with cRBC and iRBC of 1:100 ratio for 48 h. (B) Representative immunoblot of p53, caspase-3, and cleaved caspase-3 protein of Raw 264.7 macrophages incubated with different ratios of

cRBC and iRBC. Immunoblot of β -actin confirms equal loading. (C-D) Graph showing p53, cleaved caspase3/caspase3 level of Raw 264.7 macrophages incubated with cRBC and iRBC. Statistical significance indicated by ****, p< 0.0001, compared to cRBC incubated Raw 264.7 macrophages.

3.3.3 Robust erythrophagocytosis inhibits autophagy in Raw 264.7 macrophages

Autophagy is essential for macrophage polarization. Autophagy regulation in Raw 264.7 macrophages after enhanced erythrophagocytosis was analysed by western blotting. As shown in Figure 3.3A macrophages incubated with 1:50 ratio of iRBC have exhibited a significant decrease in autophagy marker protein ratio of LC3-II to LC3-I level (p=0.03) compare with cRBC incubated macrophages. An increase in iRBC ratio (1:100) further decreases the ratio of LC3-II to LC3-I (p=0.001). While less iRBC ratio (1:10) did not affect macrophage autophagy marker LC3-II to LC3-I level similar to the cRBC (1:100) confirms robust erythrophagocytosis inhibits autophagy in Raw 264.7 macrophages. Autophagy inhibition accumulates p62 induces ROS levels and chromosomal instability, which correlates with signaling molecules of nuclear factor erythroid protein 2 (NRF 2), mTOR, and nuclear factor kappa B (NF-κB) (163). As shown in Figure 3.3A, we found a significantly increased expression of p62 levels in macrophages incubated with a 1:100 ratio of iRBC compared to a similar ratio of cRBC (1:100). While 1:10 and 1:50 ratio of iRBC did not show any alteration in p62 levels of macrophages. mTOR regulates the cell growth and autophagy through downstream ribosomal kinase s6K protein. We observed a significant increase of pmTORC1/ mTORC1 ratio in the macrophages incubated with 1:50 and 1:100 ratio of iRBC (p<0.0001) compared to 1:100 cRBC. At the same time, p70s6K exhibited the increased expression in iRBC incubated macrophages in correspondence to p-mTORC1/ mTORC1 ratio.

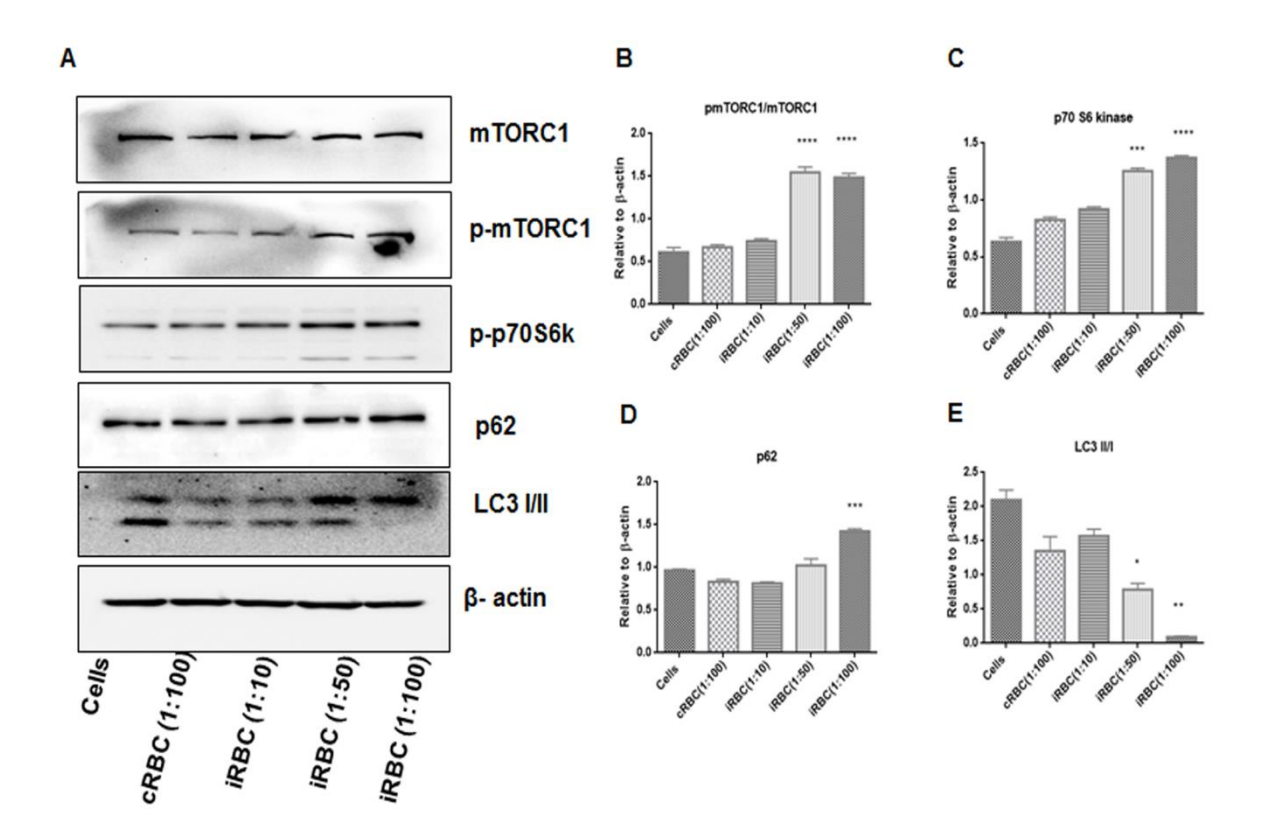


Figure 3.3 mTORC1/p70S6K mediated autophagy inhibition in robust iRBC phagocytosed Raw 264.7 macrophages. (A) Representative immunoblots of mTORC1, phosphor-mTORC1, phosphor-70S6K, p62, and LC3 I/II of Raw 264.7 macrophages incubated with different ratio of cRBC and iRBC for 48 h. Immunoblot of β-actin confirms equal loading. (B-D) Graph showing phosphor-mTORC1/mTORC1, phospho-70S6K, phosphor-62, LC3II/I levels of Raw 264.7 macrophages incubated with cRBC and iRBC. Statistical significance was indicated by ****, p< 0.0001, *,p<0.05 compared to cRBC incubated Raw 264.7 macrophages.

3.3.4 Enhanced erythrophagocytosis phagocytosis activates Raw 264.7 macrophage M1 polarization

Autophagy inhibition activates the NF-kB mediated pro-inflammatory condition in the macrophages of the M1 phenotype. As shown in Figure 3.4, higher ratio of 1:50 and 1:100 iRBC incubated macrophages shown M1 phenotype with increased expression of proinflammatory cytokine genes like IL-1 β and TNF- α compared to cRBC (1:100) incubated macrophages in semi-quantitative PCR analysis. While an anti-inflammatory gene TGF- β didn't show alteration in macrophages incubated with iRBC and cRBC.

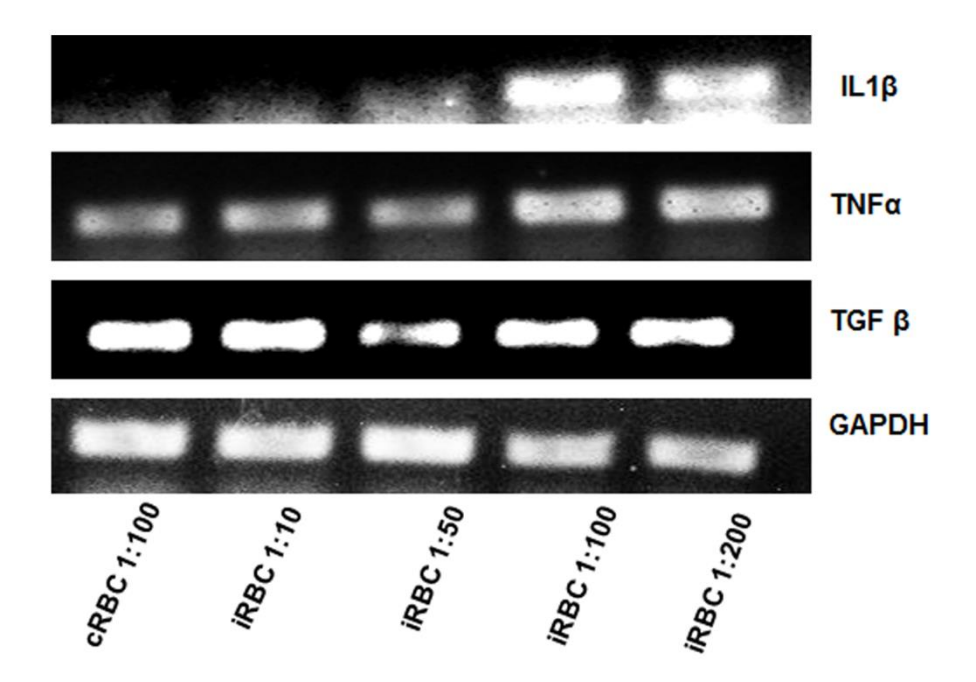


Figure 3.4 Robust iRBC incubation induces proinflammatory cytokine gene expression in Raw 264.7 macrophages. Gene expression of IL-1 β , TNF- α , TGF- β cytokines in cRBC and iRBC of different ratio incubated Raw 264.7 macrophages. Housekeeping gene GAPDH (glyceraldehyde 3-phosphate dehydrogenase) is used as a loading control. cRBC (control mice blood), iRBC (*Plasmodium berghei ANKA* infected mice blood).

3.3.5 Cerebral malaria induces infiltration of circulatory leukocytes into the brain tissue

Autophagy inhibition and increased expression of p62 induces the cell adhesion and migratory effect of high glucose incubated macrophage cell lines (164). As the iRBC phagocytosis inhibits autophagy and induces the expression of p62 in Raw 264.7 macrophages. We investigated the leukocyte infiltration in cerebral malaria severe form malaria by FACS analysis. Brain immune cells were isolated from c57BL/6 mice at days 1, 3, 5, and 7 of post-infection with *P. berghei* ANKA and stained with PercP-CD45, which stains circulatory macrophages and neutrophils and APC-CD11b for brain resident macrophages/microglia and did FACS analysis. As shown in Figure 3.5 we observed the circulatory leukocytes in days 5 and 7 of post-infection in isolated mice brain with cerebral symptoms. Whereas before the cerebral malaria symptoms i.e., at day 1 and 3 post-infection,

we didn't observe the circulatory leukocytes in an infected brain similar to the control mice brain.

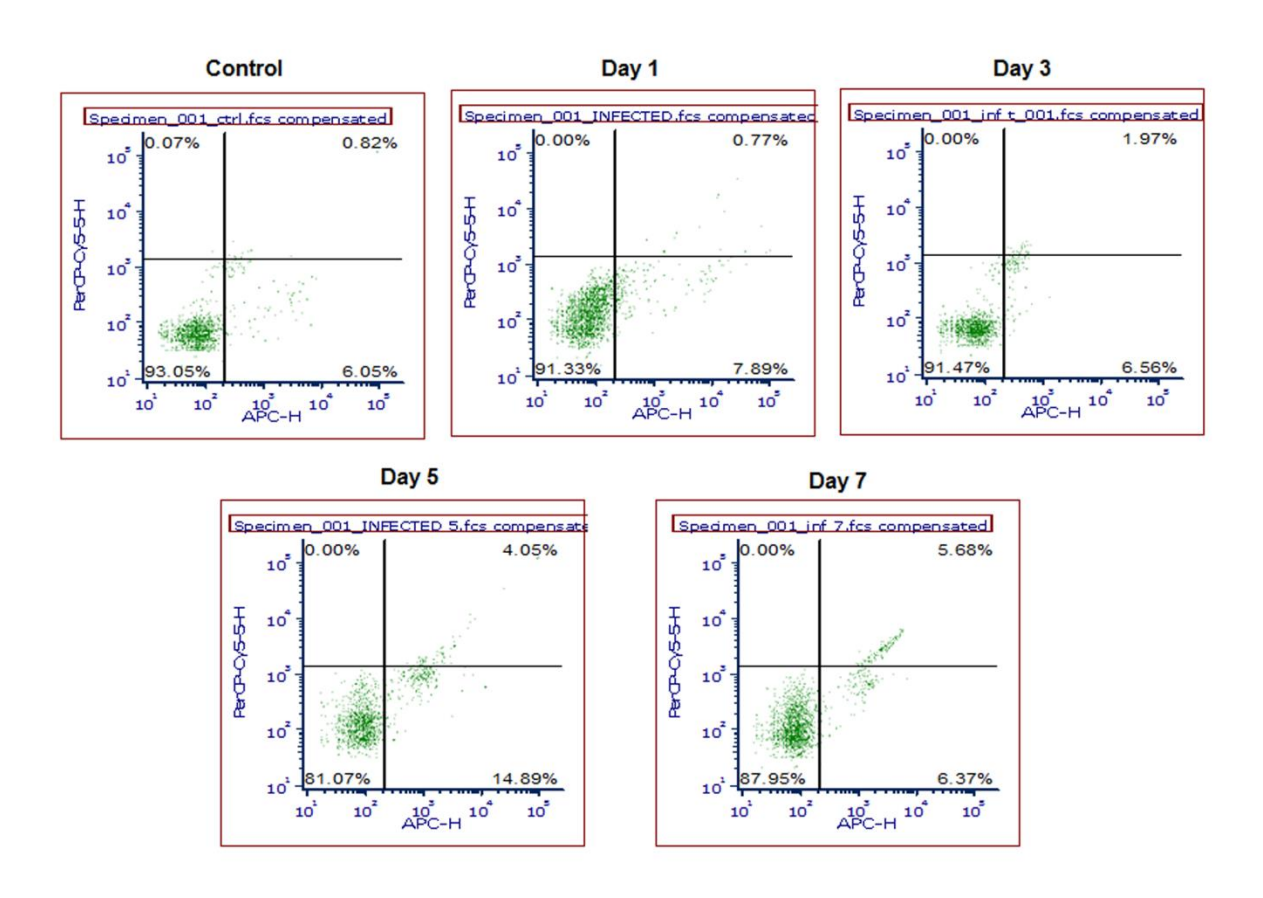


Figure 3.5 FACS analysis of peripheral leukocyte infiltration into *P. berghei ANKA* **infected mice brain tissue.** The figure represents the dot plot image of immune cells of P. berghei ANKA infected mice brain at day 1, 3, 5, and 7 of post-infection. Peripheral leukocytes were stained with PerCP-CD45 and brain resident macrophages/microglia stained with APC-CD11b. Increased percentage of the immune cell population of CD45+-CD11b+ represents the infiltration of peripheral leukocytes into mice brain tissue at day 5 and 7 of post-infection.

3.3.6 Docosahexaenoic acid (DHA) enhances erythrophagocytic activity of Raw 264.7 macrophage cell lines.

P. berghei ANKA infected RBC (iRBC) phagocytosis induces macrophages' proinflammatory condition and inhibits M2 phenotype macrophage polarization. Hence we treated the macrophages with DHA, an anti-inflammatory molecule, overnight and incubated with

carboxyfluorescein succinimidyl ester (CFSE) stained iRBC and cRBC of 1:100 ratio for 24 h. Cells were imaged under confocal microscopy. As shown in Figure 3.6A, 100 µM DHA treated macrophages has shown increased green fluorescence represents the CFSE stained iRBC compared to untreated iRBC incubated macrophages. While the cRBC incubated macrophages couldn't phagocytose, we didn't find the green fluorescence in cRBC incubated macrophages. Simultaneously, as shown in Figure 3.6B, FACS analysis further confirmed that increasing DHA concentration also enhances the phagocytic activity of macrophages. 90 µM DHA treated macrophages has shown double the times of phagocytic activity compared to untreated macrophages.

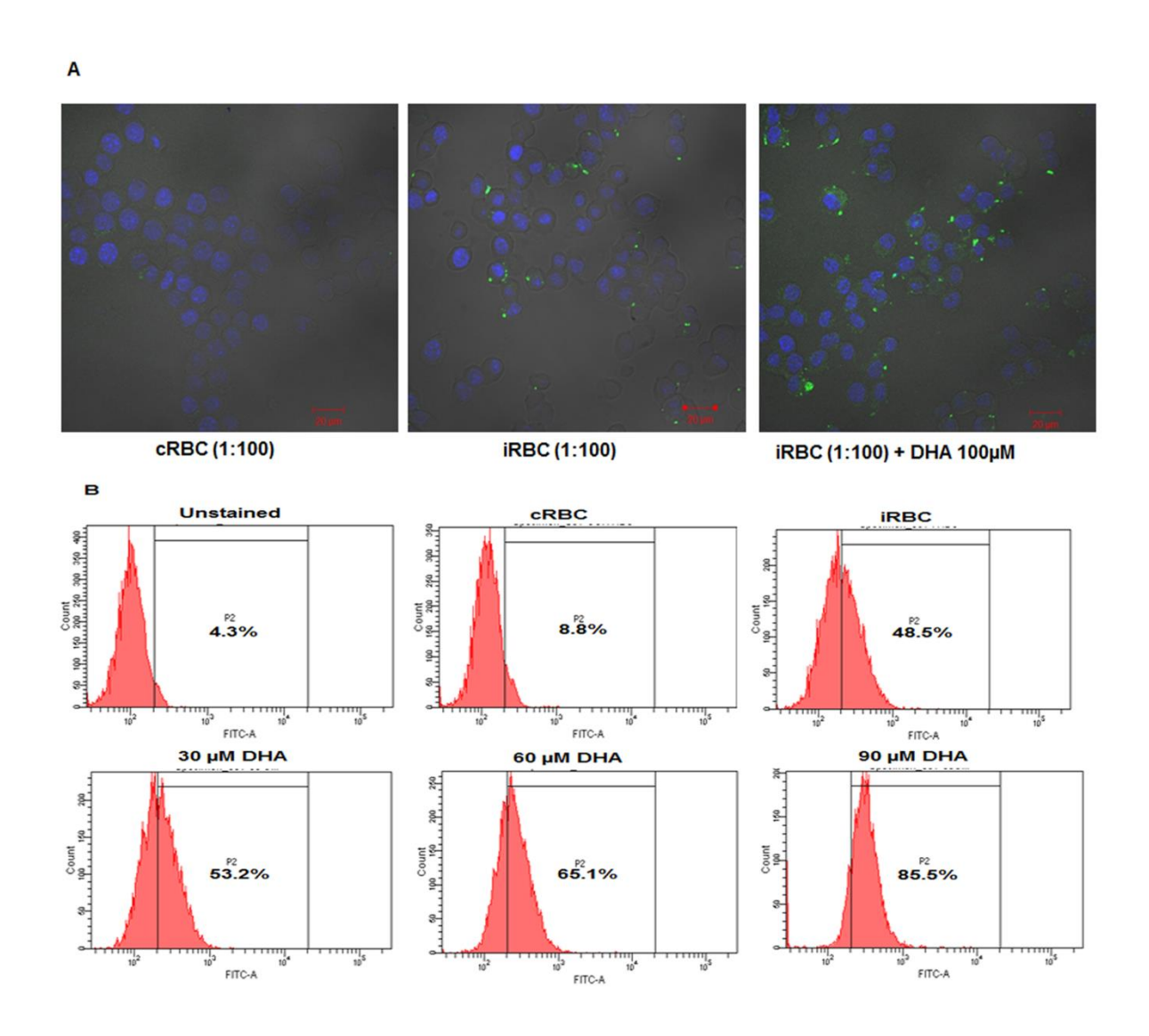


Figure 3.6 Docosahexaenoic acid (DHA) induced iRBC phagocytosis in Raw 264.7 macrophages.

(A) Confocal microscopy images of control and 100 μ M DHA treated Raw 264.7 macrophages incubated with CFSE stained cRBC, iRBC (1:100 ratio of macrophage: RBC) for 6 h. (B) FACS batch analysis of histograms represents the percentage of RBC engulfed by control and DHA of 30, 60 and 90 μ M DHA treated Raw 264.7 macrophages upon incubation with cRBC and iRBC of ratio 1:100 for 6 h. Green (CFSE stained RBC), Blue- DAPI (stains macrophage nucleus).

3.3.7 Lipid droplet induction in cerebral malaria infected brain

As the infiltrated leukocytes induce the brain's inflammatory condition, we analysed the lipid droplets in cerebral malaria in infected brain sections by staining with Bodipy 493/503. As shown in Figure 3.7B, we observed lipid droplets at the ependymal cell layer of the mice brain's subventricular zone of lateral ventricles. Perilipin protein stabilizes the lipid droplets structure. As shown in Figure 3.7A, we found increased expression of perilipin-3 gene expression in cerebral malaria-infected mice brain compared to the control mice brain. At the same time we couldn't observe alteration of perilipin-1 and perilipin-2 gene expression in cerebral malaria-infected mice brain compared to control mice brain.

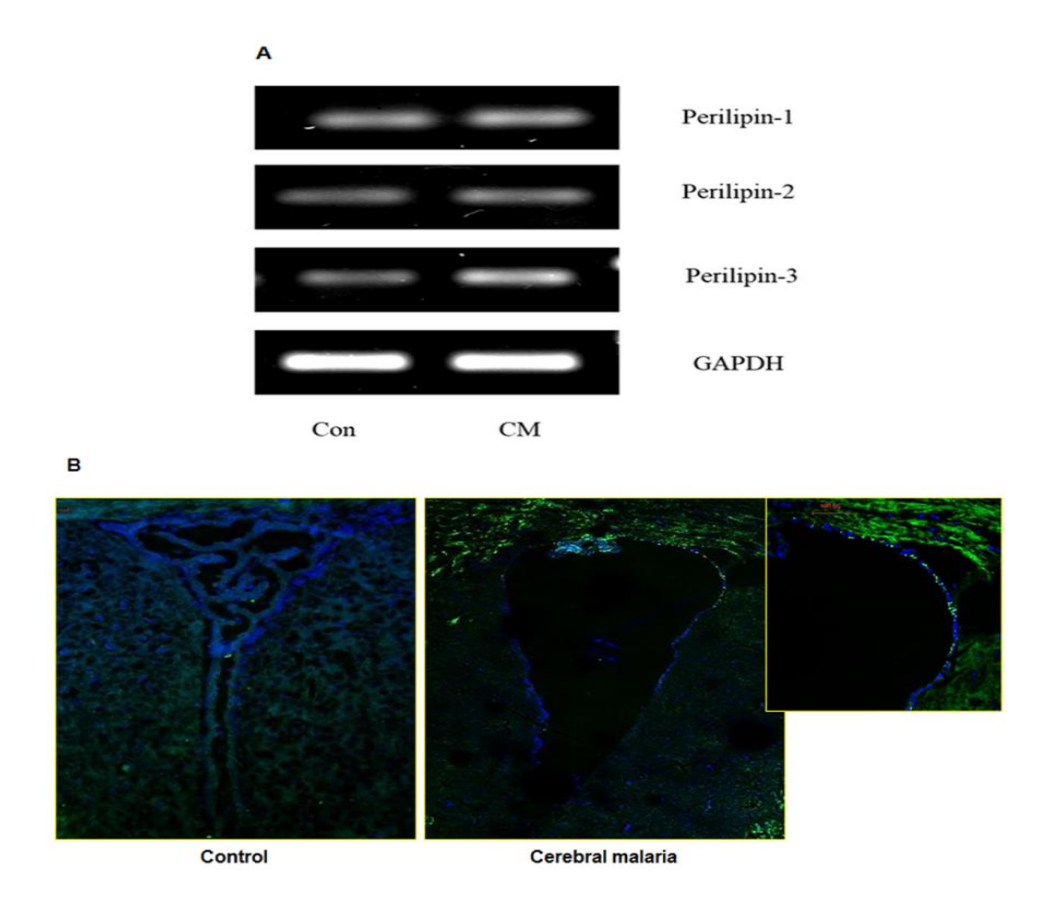


Figure 3.7 Cerebral malaria induced lipid droplets accumulation in brain tissue. (A) Gene expression of lipid droplet stabilizing gene perilipin isoforms perilipin-1, perilipin-2, and perilipin-3 in control and cerebral malaria infected brain tissue. (B) Confocal microscopy image of Bodipy 493/503 stained brain sections of control and cerebral malaria mice brain. The image represents the lipid droplet accumulation in cerebral malaria-infected mice brain lateral ventricle ependymal cell layer. Green-BODIPY stained lipid droplets, Blue-DAPI (stains nucleus of brain cells).

3.3.8 Lateral ventricle enlargement and choroid plexus degeneration in the cerebral malaria mice brain

Choroid plexus is composed of epithelial cells situated in the brain's lateral ventricles and functions as a vascular blood-cerebrospinal fluid barrier (BCSFB). These epithelial cells are continuous with ependymal cells and constitute the layer for Lateral ventricles, separate brain

parenchyma from the CSF. BCSFB permeabilization facilitates the infiltration of stromal immune cells and toxic substances into the CSF and causes tissue damage. Figure 3.8A, indicates the enlargement of the lateral ventricle size in the CM brain compared to the control brain. In choroid plexus, the gap junctions are filled with astrocytes. As shown in Figure 3.8B, the Glial fibrillary acidic protein (GFAP) stained control brain section represents the definite structure of choroid plexus in lateral ventricle, while in CM infected brain section showed deformed choroid plexus. At the same time, we observed increased staining of GFAP in the SVZ of the CM infected brain but not in the control brain sections.

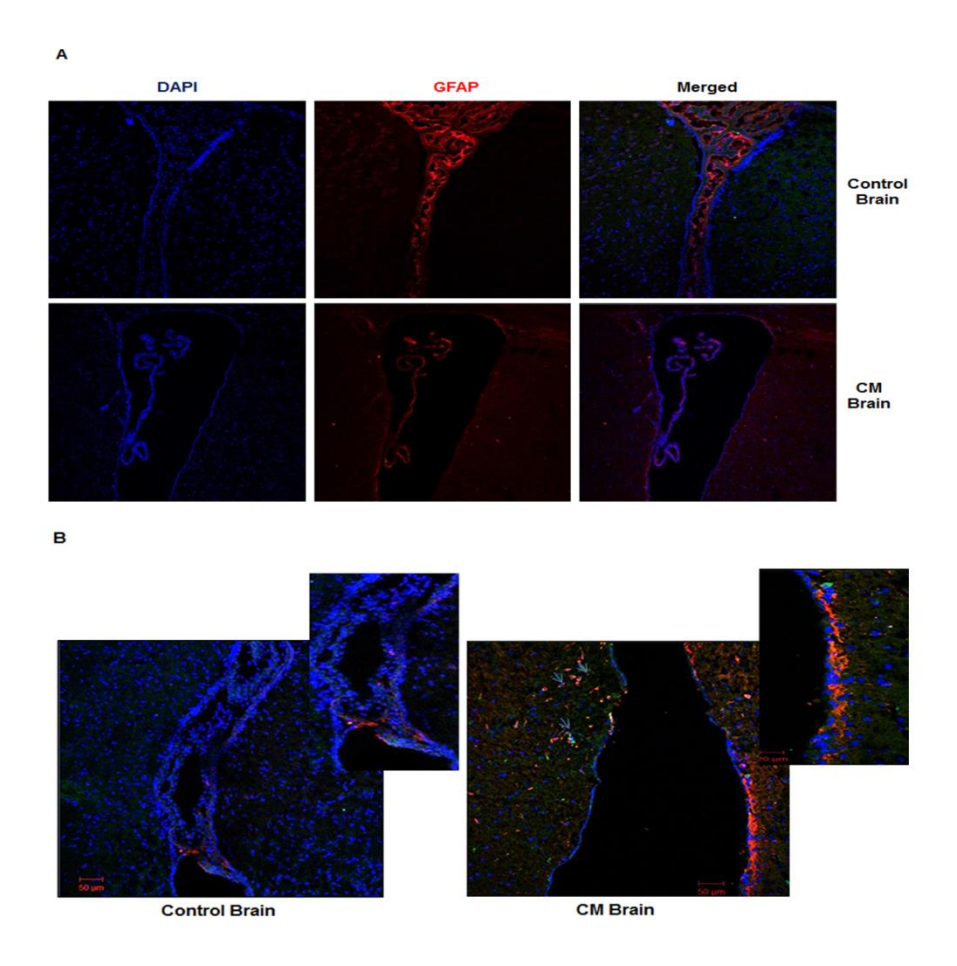


Figure 3.8 Cerebral malaria infection induced the choroid plexus structure deformation and active astrocytosis at subventricular zone of lateral ventricle. (A) Confocal microscopy images of GFAP an astrocyte marker stained control and cerebral malaria mice brain sections. (B) Confocal microscopy image of GFAP staining represents the active astrocytosis (arrow mark) in cerebral

malaria mice brain sections and the absence of active astrocytosis in control mice brain. Red- GFAP (astrocyte marker), Blue- DAPI (stains nucleus of brain cells).

3.4 Discussion

The human immune system mainly consists of the innate and adaptive immune system. Neutrophils, macrophages, and dendritic cells play an essential role in the innate immune system. We studied the correlation between phagocytosis and apoptosis of macrophages due to Plasmodium-infected RBC (iRBC) uptake by macrophages. When we incubated with an increasing ratio of iRBC, macrophages' apoptosis was increased compared to cRBC incubation. Robust erythrophagocytosis induced the apoptosis of macrophages was mediated by hemin induced redox imbalance, which support our finding of macrophage cell death at a high ratio of iRBC incubation (63). The other pathogens like mycobacteria, legionella, shigella, and salmonella utilize host macrophages for their intracellular growth; also induce apoptosis in macrophages upon phagocytosis (165, 166). Simultaneously, some extracellular bacteria like staphylococci, streptococci, and Escherichia coli were also induced apoptosis in macrophages after phagocytosis (167, 168). To further study the molecular mechanism which mediates this apoptosis, we have checked the expression of caspase-3. The increased expression of cleaved cap3/casp3 ratio in iRBC incubated macrophages confirmed that the apoptosis was caspase-mediated. With increasing iRBC ratio further increases, the cleaved cap3/casp3 ratio level and low iRBC ratio (1:10) didn't show any alteration in cleaved cap3/casp3 ratio level when compared to cRBC (1:100) incubated macrophages infers that enhanced erythrophagocytosis induces the apoptosis of macrophages. Further, we observed increased p53 expression levels in iRBC incubated macrophages indicated the p53 apoptotic induced gene activated caspase-3.

Autophagy inhibits apoptosis mediated cell death by scavenging the damaged organelles, nutrient recycling, and removing protein aggregates. Simultaneously, in some

cases, autophagy activation induces phosphatidylserine exposure and apoptotic body formation and causes cell death. Many proteins play an important role in cross-talk between autophagy and apoptosis in macrophages (169). Hence we analysed the autophagy regulation in iRBC incubated macrophages. We observed decreased expression of an autophagy marker LC3-II/LC3-I ratio level in iRBC incubated macrophages in correspondence to their increased iRBC ratio confirms the autophagy inhibition in enhanced iRBC phagocytosed macrophages. The p62 interacts with autophagic substrates and transports them to autophagosomes for degradation. Same time p62 will undergo degradation. Autophagy inhibition accumulates autophagic substrate p62 may induce caspase -3 and caspase -8 mediated apoptosis (170, 171). Our study showed increased p62 expression levels in enhanced iRBC phagocytosed macrophages corresponding to increase cleaved casp3/casp3 ratio level infers the possible role of cross-talk between autophagy and apoptosis in iRBC engulfed macrophages. The mammalian target of rapamycin (mTOR) signaling pathway regulates translation, cytokine responses, antigen presentation, macrophage polarization, and cell migration. Cancer therapy, targeting the mTOR pathway, function as immunosuppressive and anti-proliferative. Constitutive activation of mTOR is detrimental, as it promotes the reactive oxygen species generation with enhanced mitochondrial biogenesis (172). Our study observed activation of mTOR by increased expression of pmTOR/mTOR ratio level and increased expression of the p70s6K ribosomal downstream protein of mTOR pathway in iRBC incubated macrophages confirms the mTOR/s6K pathway mediated autophagy inhibition in enhanced iRBC incubated macrophages.

Ehrlichia bacteria polarize macrophages into the M1 phenotype which induce proinflammatory conditions through mTORC1 dependent manner. External stimulation modulates intracellular signals like NFkB and mTOR regulates the macrophage polarization. Autophagy inhibition enforces M2 polarized macrophages to M1 macrophages by activating

the NFkB signaling (173). In our study, we found increased pro-inflammatory cytokines IL-1β and TNF-α level in macrophages incubated with a high ratio of iRBC (1:100 and 1:200) compared to fewer number (1:10 and1:50) and cRBC (1:200) incubated macrophages. At the same time we couldn't observe any alteration in M2 macrophages secreted anti-inflammatory cytokine TGF-β level indicates that robust iRBC phagocytosis induces M1 polarization in macrophages. As autophagy activation plays an important role in the induction of macrophage M2 polarization, our findings infer that autophagy inhibition in enhanced iRBC phagocytosis might induce macrophages' M1 polarization. Macrophage autophagy inhibition and increased p62 level induce their infiltration into the kidney during diabetic nephropathy (164). Autophagy activator rapamycin-treated cancer cells shown less migration activity confirms the role of autophagy in cell migration (174).

We estimated the infiltration of vascular leukocytes into brain parenchyma in cerebral malaria pathogenesis. *P. berghei* ANKA infected C57BL/6 mice induce cerebral malaria symptoms on 7-10 days of post-infection with 25-30 percentage of parasitemia. We found CD45+ peripheral leukocytes in day 5 and 7 of post-infection mice brain compared to day 1, 3, and control mice brain, indicating that phagocytosis of iRBC might induce the macrophage migration causes cerebral malaria pathology by infiltrating into brain tissue. Immunomodulatory drug FTY 720 prevents the recruitment and infiltration of macrophages. It protects mice from cerebral malaria death further supports the immunomodulation in iRBC phagocytosed macrophages and their infiltration in our study (175).

Treatment of macrophages with IFN- γ , a major inflammatory cytokine secreted in bacterial infection, induces TAG containing lipid droplets (176). LPS activation increases the lipid droplets in macrophages by a mechanism of increased CD36 expression increases the fatty acid uptake and accumulates those in TAG (177). Our study found increased lipid droplet numbers with increasing iRBC ratio incubation with Raw 264.7 macrophages, where

we found active proinflammatory conditions. In Chagas disease, the macrophages recruited to the heart were shown to increase lipid droplets (178) supports the lipid droplet that might play a role in macrophage migration. Our study observed increased intercellular adhesion molecule expression -1 (ICAM-1) on iRBC incubated macrophages compared to cRBC incubated macrophages. It supports the ability of iRBC phagocytosed macrophages migration by binding through cell adhesion molecule expressed on the membrane. TLR-2 mediates the induced lipid droplets in *Chlamydia pneumoniae* infected macrophages that further adhere to the vascular endothelial cells and cause atherosclerosis to support the lipid droplet mediated macrophage cell adhesion (179).

Plasmodium berghei infected mice exhibited lipid droplets accumulation in targeted organs like kidney and liver (180, 181). We observed the infected macrophages infiltration into the brain in cerebral malaria. We are interested in analysing the lipid droplets accumulation in cerebral malaria brain section by Bodipy staining. We observed lipid droplet accumulation in the lateral ventricle ependymal cell layer of CM infected mice brain. Further study is required to know which brain cells specifically have this lipid droplet accumulation. Simultaneously, we observed the deformation of choroid plexus morphology by GFAP staining in cerebral malaria infected brain sections compared to the control mice brain. Epithelial cells of choroid plexus form the BCSFB and protect toxins' infiltration into CSF from the blood capillaries. The lateral ventricle ependymal cells are continuous with choroid plexus epithelial cells and separate the brain parenchyma from CSF. Our study indicates that the choroid plexus deformation and lipid droplets induction on ependymal cells of lateral ventricles may induce the permeability of lateral ventricles which allows the transport of toxins into the brain parenchyma and aggravates cerebral malaria symptoms. Immunofluorescence of cerebral malaria infected brain sections with GFAP exhibited intense staining of astrocytes near the subventricular zone (SVZ) and along with the ependymal cell,

layer represents reactive astrocytosis. The experimental mouse stroke induces the ependymal cell, and SVZ GFAP expression indicates that neurodegenerative disease activates SVZ astrocytosis for neurogenesis (182). Further study is required to analyze the function of SVZ activated astrocytes in cerebral malaria.

4A. Anti-parasitic activity of penicinoline alkaloids and
their mechanism of action against Plasmodium falciparum

4A.1 Introduction

Nature is a rich source of biologically potent bioactive substances which are structurally unique. Natural products contain complex ring systems and certain hetero atoms which may be responsible for their pharmacological activity. Alkaloids are a class of naturally occurring compounds that contain at least one nitrogen. They have a wide range of pharmacological activities including anti-malarial example is quinine, the first anti-malarial drug. It is extracted from the bark of Cinchona tree. In a quest to discover a substitute of quinine, chloroquine was synthesized which belongs to a class of amino quinolines. Quinolones are structurally derived from the quinoline a heterobicyclic aromatic compound and possess broad-spectrum antibiotics that act against different bacteria. Quinolones contains a bicyclic core structure with 4-oxo-1,4-dihydroquinoline skeleton (183). Nalidixic acid was the initial quinolone discovered as a by-product while synthesizing the anti-malarial quinine compound and used against urinary tract infection (UTI) caused by gram negative bacterium (184, 185). Quinolones also functions as anti-cancer (186), anti-viral (187) and, as anti-oxidants (188). Casimiroa edulis seeds isolated casimiroine exhibits anti-cancer activity (189). 4-quinolone alkaloids isolated from plants and microbes show antibacterial activity against Helicobacter pylori (190-192). Some of the scaffolds displayed anti-malarial activity (193). Quinolones mainly target the gyrase a type II topoisomerase of the parasite, and inhibits the DNA synthesis (194). Endochin acts against the cytochrome bc1 complex of the avian malaria parasite. Quinolones are found in many natural resources such as plants, animals, and microbes. Plant-derived quinolones contain 2(1H)-quinolone and 4(1H)-quinolone derived from 2-hydroxyquinoline and 4-hydroxyquinoline, respectively to form the alkaloid core structure (195). 4(1H)-quinolones are explored on the multiple developmental stages of parasite life cycle (196-198). Current drug therapy for malaria as recommended by WHO uses artemisinin in combination with other antimalarial drugs. Emerging resistance of parasite to currently available drugs necessitates the development of new compounds. However, no antimalarial activity of penicinoline alkaloids have been reported so far in literature. This coupled with our past experience in screening of bioactive compounds prompted us to probe the efficacy of alkaloids for their antimalarial efficacy.

4A.2 Materials and Methods

4A.2.1 Parasite culture

P. falciparum 3D7 cultures were maintained by the bell jar candle method at 37 ℃ in RPMI 1640 medium supplemented with 0.5% Albumax I (Invitrogen) and 0.1M hypoxanthine containing 5% red blood cells (RBC)

4A.2.2 Compounds preparation

Compounds was dissolved in 100% dimethyl sulfoxide (DMSO) for the drug assays, two fold serial drug dilutions were made in medium and added to 96-well culture plates at 100 μ l per well. Synchronized mature Trophozoite stage Parasites was diluted to a 2 × stock consisting of 0.6% to 0.9% parasite and 2% haematocrit in medium, and 100 μ L are added per well already containing 100 μ L of medium with or without compound present at different concentrations. Plates was then maintained by the bell jar candle method at 37°C for 48 h and the parasitemia was measured after 48 h by using Giemsa stain method and by flow cytometry

4A.2.3 Giemsa staining

After 48 h of incubation, a thin blood smear slide was prepared, air dried, methanol fixed, and stained in Giemsa solution (1:5 ratio) for 20 min. After staining, slides was washed in tap water and air dried. The Giemsa stained slides was examined for counting the number of parasites in random adjacent microscopic fields, equivalent to about 5,000 erythrocytes at 100 × magnification.

4A.2.4 Flow cytometry

After 48 h of incubation culture was transferred into tubes containing 100 μ l of PBS-EtBr at 10 μ g/mL and Incubated in darkness for 45 mins, centrifuged the tubes at 1200 rpm, 1 minute to pellet cells, and removed supernatant, washed the pellet in PBS, resuspend the parasites into 300 μ L of PBS and transferred samples to FACs tubes to measure parasitemia on flow cytometer (199).

4A.2.5 Cytotoxicity assays (MTT)

Cytotoxicity of compounds was determined by using 3-(4, 5- dimethylthiazol-2- yl)-2,5-diphenyltetrazolium bromide (MTT). Cells was seeded at 1x10~4 in each well of 96-well plates. After 24hr cells were treated with different concentrations of compounds (0.48uM to 500uM) in two fold serial dilution or vehicle (0.25% DMSO) for 24 h. After 24 h of treatment, $200\mu l$ of medium containing MT (0.5mg/ml) was added to each well of 96 well plates and incubated for 4 h in CO2 chamber at 37° C. Reduced formazan crystals were dissolved in $100\mu l$ of DMSO and absorbance was measured at 570 nm on a multi plate reader (Teccan infinite-200). All treatments were performed in triplicate and repeated thrice; results were expressed as mean \pm SEM (200).

4A.2.6 β-hematin polymerization assay

Compound were serially diluted in water (20 μ L) and solutions were added to the 96 well microtiter plate in the order of NP-40 stock solution (5 μ L), acetone (7 μ L), and heme suspension (25 μ L). The NP-40 stock solution (348 μ M) was prepared in water. A 25 mM stock solution of hematin was prepared by dissolving hemin chloride in DMSO followed by one minute of sonication. The heme solution was then filtered through a 0.22 μ m PVDF membrane filter unit. From this solution, the heme suspension (228 μ M) was added to a 2 M acetate buffer at pH 4.9 and vortexed for 5 s. The plate was then incubated for six hours in a

shaking water bath at 45 rpm and 37 °C. Following incubation, the microtiter plate was removed from the water bath and the assay was analysed using the pyridine-ferrochrome method. Following the addition of 15 μL of acetone to each well of the plate, 8 μL of a pyridine solution was added (50% pyridine, 20% acetone, water and 200 mM HEPES, pH 7.4) so that the final concentration of pyridine was 5% (v/v). Following 30 min of shaking to facilitate the solubilisation of free heme, the absorbance of the resulting complex was measured at 405 nm using spectrofluorometer plate reader (Teccan infinite F-200, Switzerland).

4A.2.7 Stage- specific growth assessment

Synchronized *P. falciparum* 3d7 culture was aliquoted into ring, trophozoite and schizont stages and treated with the compounds transiently and observed the growth morphology as described in chapter 1 materials & methods section.

4A.3 Results

4A.3.1 P. falciparum growth inhibition effect of penicinoline alkaloids

The antimalarial property of penicinoline alkaloids, such as penicinoline E, marinamide and methyl marinamide were evaluated *in vitro* against the drug-sensitive *Plasmodium falciparum* 3D7. Microscopic evaluation of parasitemia was studied by Giemsa stain method²¹ and percentage inhibition of parasitemia in relation to control was calculated. Drug response graph of percent parasitemia inhibition was plotted for all three alkaloids to determine IC₅₀ value as shown in Figure 4A.1B, 4A.2B, 4A.3B. Penicinoline E and methyl marinamide had an IC₅₀ of 1.5 μM while marinamide had IC₅₀ of 25μM against chloroquine sensitive strain (pf3d7) and 4.68μM, 2.34μM and 25μM respectively against chloroquine resistant strain (pfDd2) of *Plasmodium falciparum*. Inhibition of parasite growth by alkaloids was further confirmed by flow cytometry using EtBr, Where EtBr binds to the parasite nucleic acid of

infected erythrocytes and emits fluorescence enabling quantification (red dots) and uninfected erythrocytes due to lack of nucleus do not fluoresce (black dots) as shown in Figure 4A.1C, 4A.2C, 4A.3C. With increasing concentration of penicinoline E, methyl marinamide and marinamide, parasitized erythrocytes decreased.

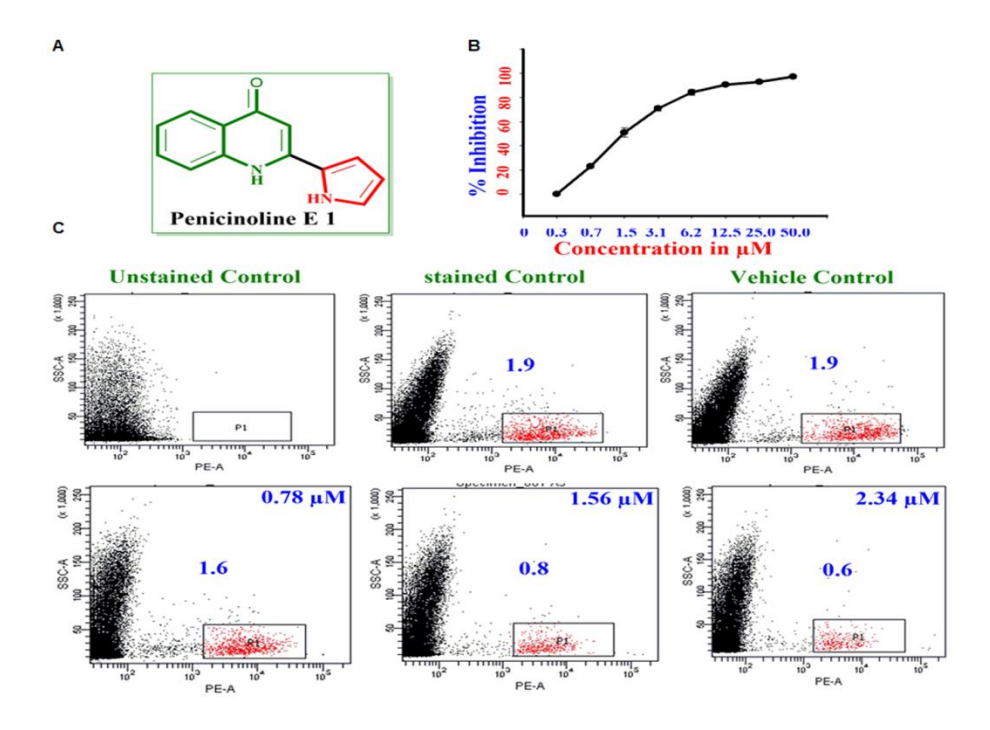


Figure 4A.1 Penicinoline E inhibits the *P. falciparum* **growth.** (A) Structure of Penicinoline E showing its functional groups. (B) Inhibition of *P. falciparum* 3D7 by penicinoline E. Synchronized trophozoite stage parasites were incubated with increasing doses of penicinoline E for 48 h. Parasitemia levels were determined by microscopy using Giemsa stain, and percent inhibition was calculated. Mean and standard errors from three experiments were plotted. (C) Parasitemia was determined by FACS using EtBr-based fluorescence measurement, where red dots represent *Plasmodium falciparum* infected erythrocytes and black dots are uninfected erythrocytes.

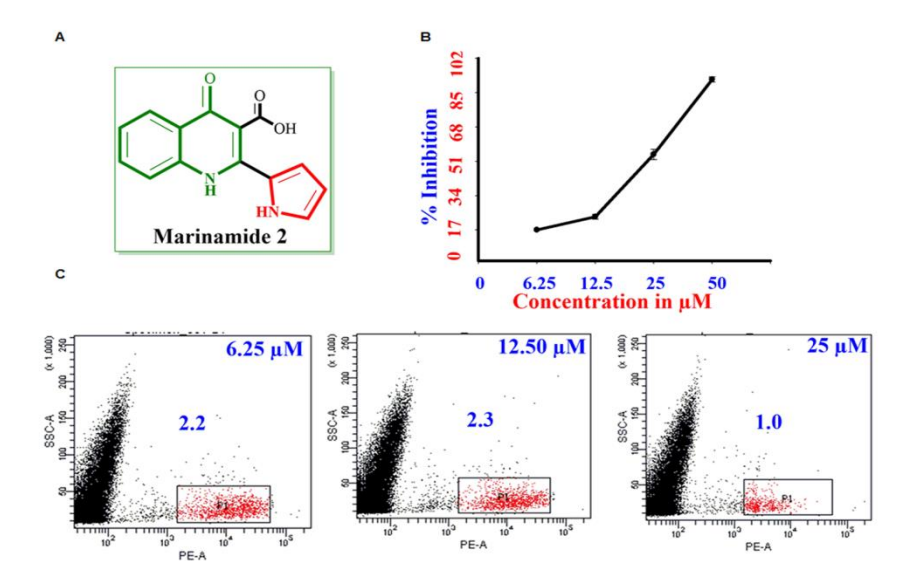


Figure 4A.2 Marinamide inhibits the *P. falciparum* **growth** (A) Structure of marinamide showing its functional groups. (B) Inhibition of *P. falciparum* 3D7 by Marinamide. Synchronized Trophozoite stage-specific parasites were incubated with increasing doses of Marinamide for 48 h. Parasitemia levels were determined by microscopy using Giemsa stain, and percent inhibition was calculated. Mean and standard errors from three experiments were plotted. (C) Parasitemia was determined by FACS using EtBr-based fluorescence measurement, where red dots represent *P. falciparum* infected erythrocytes and black dots are uninfected erythrocytes.

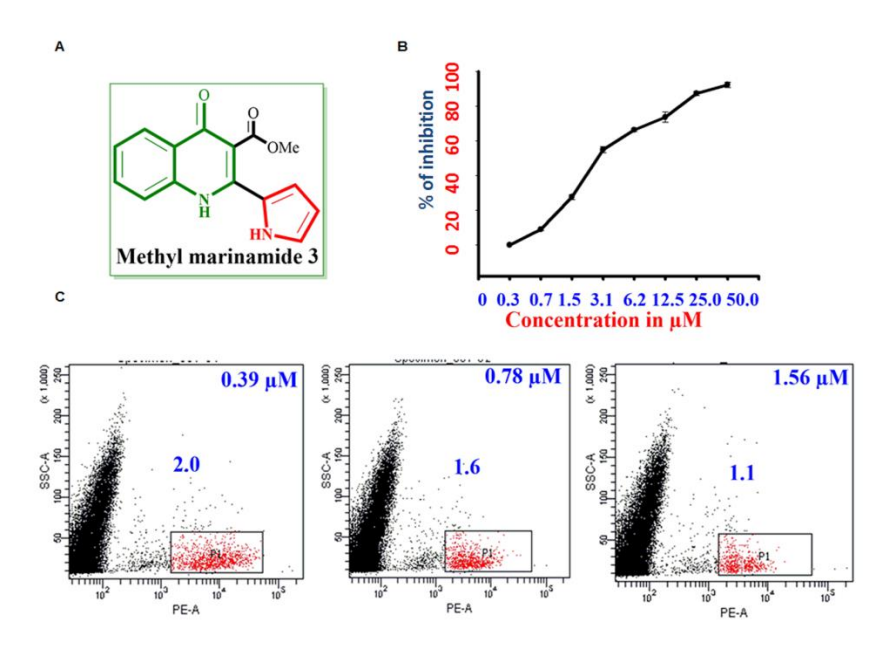


Figure 4A.3 Methyl marinamide inhibits the *P. falciparum* **growth.** (A) Structure of methyl marinamide showing its functional groups. (B) Inhibition of *P. falciparum* 3D7 by Methyl marinamide. Synchronized trophozoite stage-specific parasites were incubated with increasing doses of Methyl marinamide **3** for 48h. Parasitemia levels were determined by microscopy using giemsa stain, and percent inhibition was calculated. Mean and standard errors from three experiments were

plotted against the concertation. (C) Parasitemia was determined by FACS using EtBr-based fluorescence measurement, where red dots represent *Plasmodium falciparum* infected erythrocytes and black dots are uninfected erythrocytes.

4A.3.2 Cytotoxicity of penicinoline alkaloids against Raw 264.7 macrophages

To compare the selectivity of the alkaloid compounds for malaria parasites versus normal cells, cytotoxicity tests were carried out using mice macrophages RAW 264.7 cells. MTT assay was used as a colorimetric assay for cellular growth and survival. Penicinoline E and methyl marinamide had a CC_{50} of $500\mu M$ and $250~\mu M$ respectively as shown in Figure 4A.4A & 4A.4C, whereas marinamide hasn't shown any toxicity as shown in Figure 4A.4B towards the mice cell line.

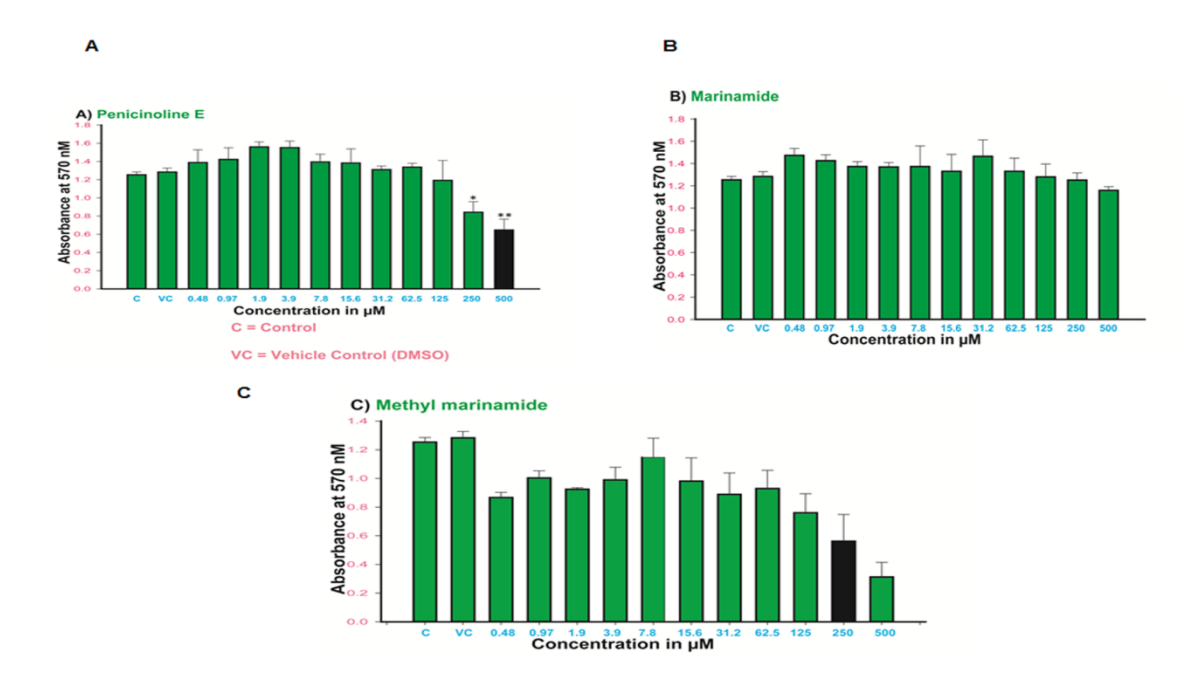


Figure 4A.4 Cytotoxicity assay for the compounds against RAW 264.7 macrophages. Cells were incubated with increasing doses of compounds for 24h. A, B and C represents the IC_{50} of compounds penicinoline, marinamide and methyl marinamide respectively measured by using MTT (0.5mg/ml) reagent, absorbance was measured at 570 nm on a multi plate reader (Teccan infinite-200). All treatments were performed in triplicate and repeated thrice; results were expressed as mean \pm SEM.

4A.3.3 β-hematin synthesis inhibition of penicinoline alkaloids.

Hemozoin assay was done to determine the effect of alkaloids on hemozoin formation which is unique to *Plasmodium*. Hemozoin crystal is formed by biomineralization of

ferriprotoporphyrin IX (heme) the free toxic byproduct of erythrocyte haemoglobin degradation by *Plasmodium* parasite. The neutral lipid particles of parasite digestive vacuole plays important role in the formation of this crystal. To mimic these conditions and to study the potentiality of alkaloid compounds to inhibit hemozoin formation, lipophilic detergent NP-40 was used to mediate the formation of β-hematin, the synthetic analog of hemozoin. In principle NP-40 incubated with synthetic hemin at 37 °C facilitates the synthesis of hemozoin crystal, the free hemin reacts with pyridine and forms brown color that can be quantified using spectrophotometer at 405 nm wavelength. As evident from Figure 4A.5 increasing the concentration of alkaloids increases the free hemin in reaction mixture which fails to convert into hemozoin thereby increasing the optical density values. In this experiment penicinoline E and methyl marinamide have shown IC₅₀ of hemozoin synthesis at 62.5 μ M which is similar to the chloroquine a positive control of inhibitor for hemozoin synthesis whereas marinamide has shown IC₅₀ of hemozoin synthesis at 250 μ M.

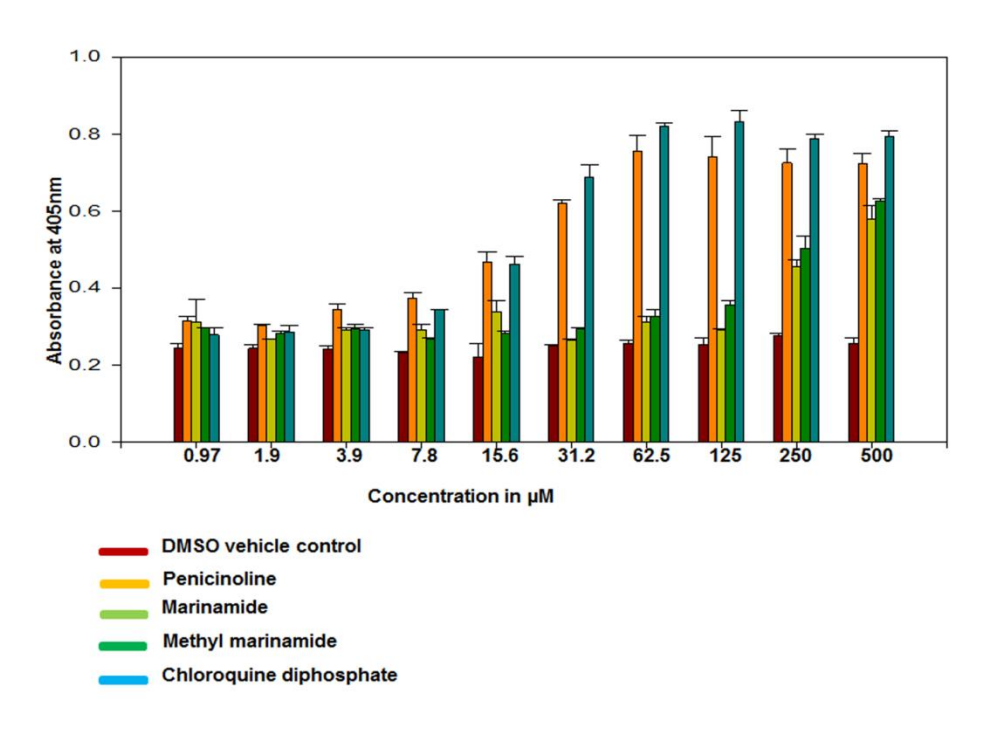


Figure 4A.5 β-hematin polymerization inhibition effect of penicinoline alkaloids. NP-40 polymerizes free synthetic hemin into β -hematin. Increasing the concentration of compound inhibits the polymerization reaction. The brown color formed by the reaction of free hemin in reaction mixture

with pyridin measured at 405nm using a multi plate reader (Teccan infinite-200). Mean and standard errors from three experiments were plotted against the concertation.

4A.3.4 P. falciparum stage specific growth inhibition of penicinoline alkaloids.

Tightly synchronized parasite culture was aliquoted into ring, trophozoite and schizont stages. Each stage was specifically and transiently treated with IC90 concentration of penicinoline alkaloid compounds for 12h. After the treatment culture was washed and supplemented with complete media and parasitemia was estimated for every 12 h up to 60 h of post infection. As shown in Figure 4A.6, 4A.7, and 4A.8 trophozoite stage parasite culture treated with penicinoline alkaloid compounds didn't infect fresh erythrocytes and showed the trophozoite stage morphology similar to the unremoved culture, whereas the ring stage and schizont stage treated cultures were infected fresh erythrocytes and exhibited ring stage morphology at 48 h of post infection similar to the untreated culture. At 60 h of post infection the marinamide and methyl marinamide treated trophozoite stage culture could recover the growth and infected fresh RBC showed ring stage morphology with 12 h delay in growth compared to the untreated parasite culture, whereas the penicinoline E treated trophozoite stage culture couldn't recover and remained in the trophozoite stage similar to the unremoved culture.

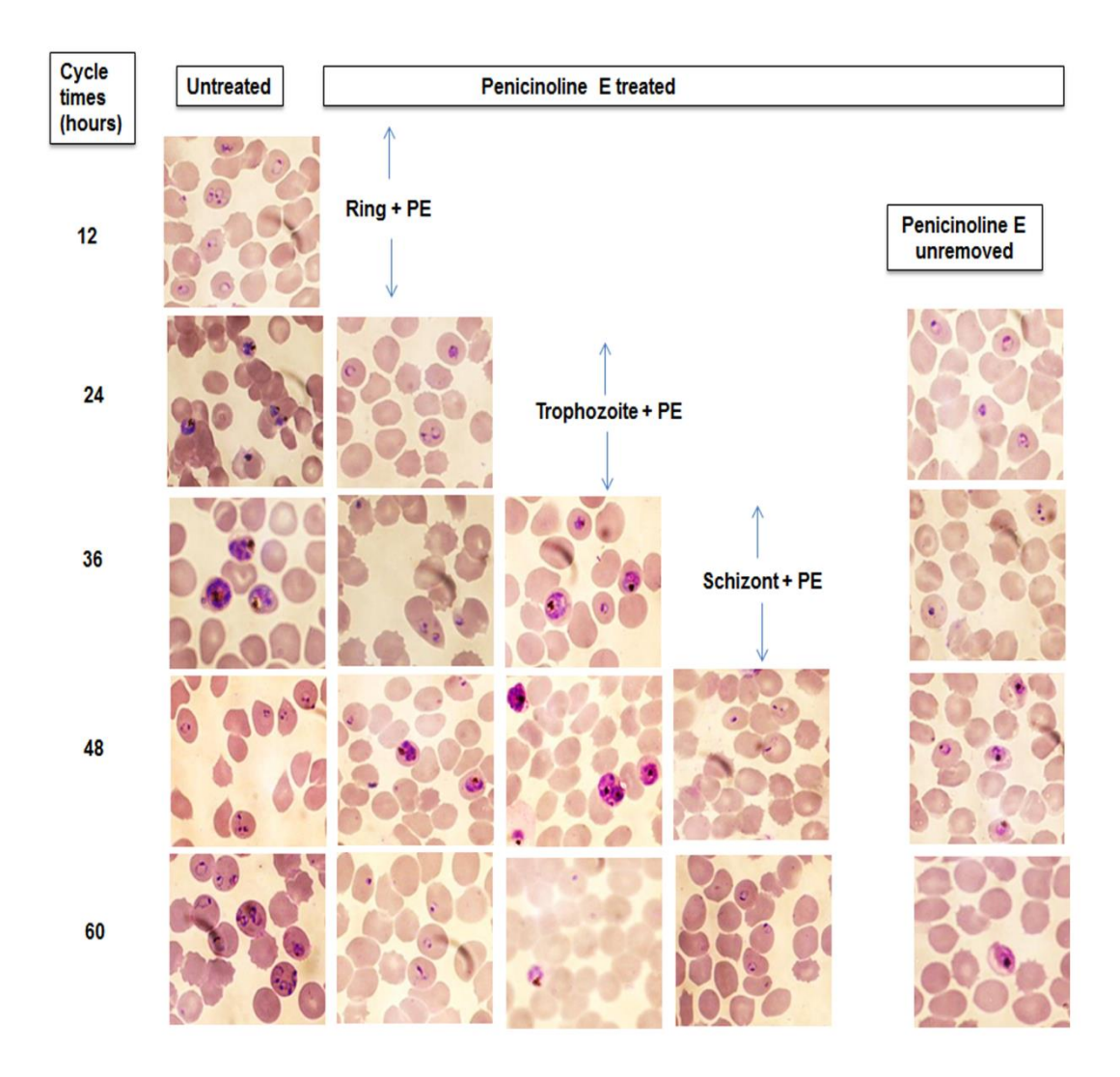


Figure 4A.6 Effect of transient treatment of penicinoline E at various plasmodial stages. Giemsa stained images represent the morphology of the parasite treated with penicinoline E compound at various stages corresponding to ring (Ring + PE), trophozoite (Trophozoite + PE) and schizont (Schizont + PE) stages for 12 hr. after that compound is washed off and the growth of parasite was monitored up to 60 h of post infection for every 12 h.

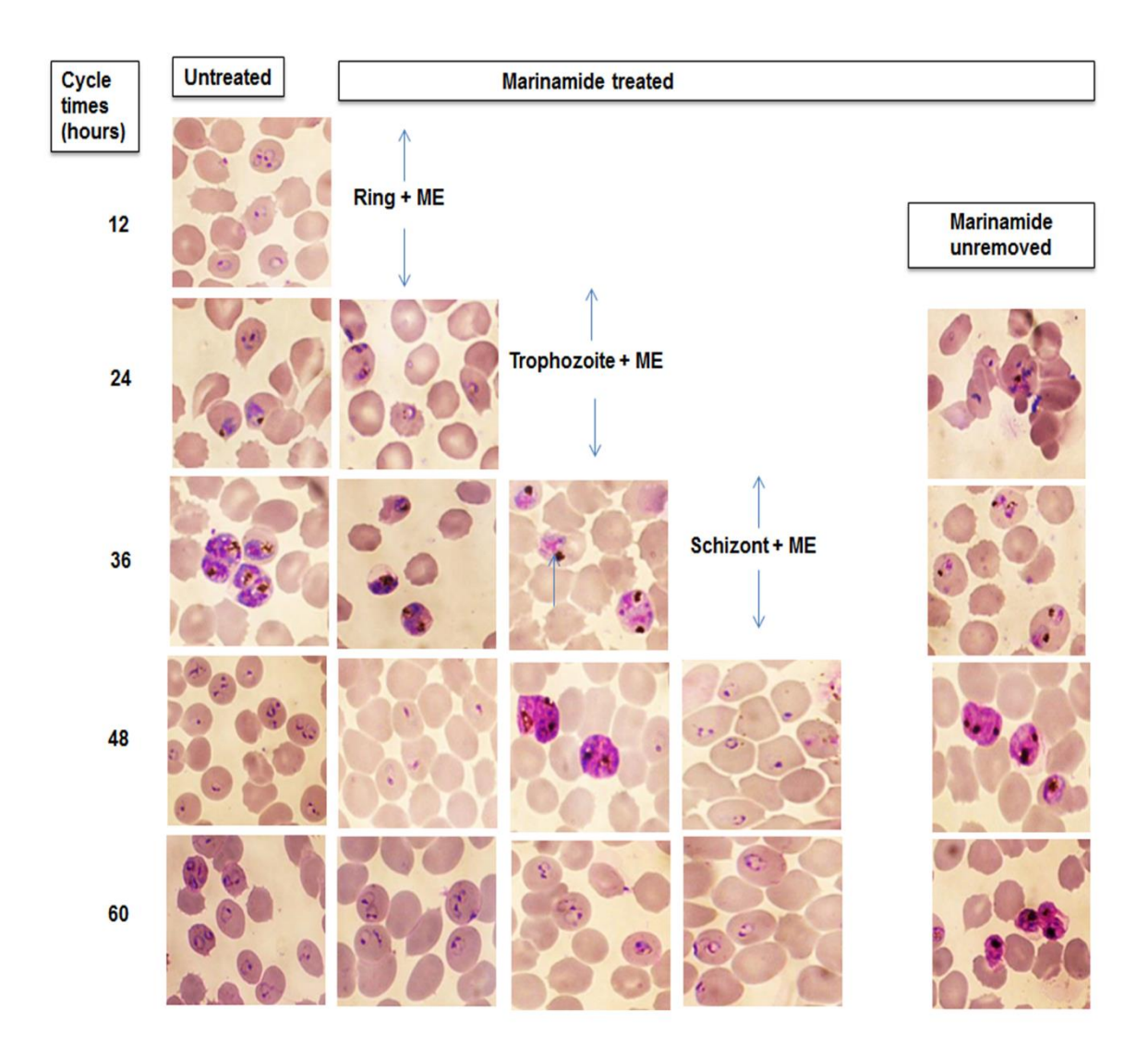


Figure 4A.7 Effect of transient treatment of marinamide at various plasmodial stages. Giemsa stained images represent the morphology of the parasite treated with marinamide compound at various stages corresponding to ring (Ring + ME), trophozoite (Trophozoite + ME) and schizont (Schizont + ME) stages for 12 hr. after that compound is washed off and the growth of parasite was monitored up to 60 h of post infection for every 12 h.

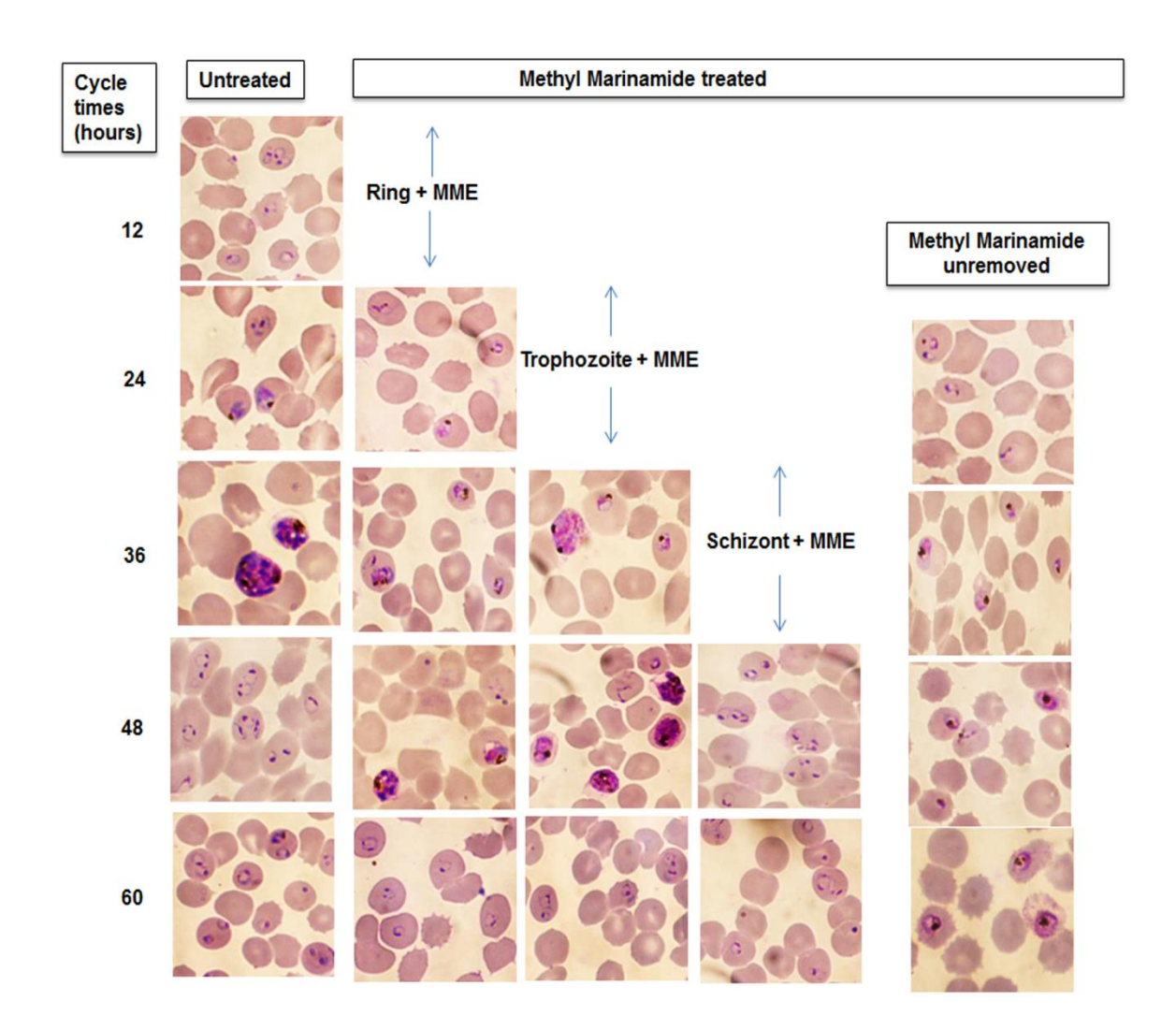


Figure 4A.8 Effect of transient treatment of methyl marinamide at various plasmodial stages. Giemsa stained images represent the morphology of the parasite treated with methyl marinamide compound at various stages corresponding to ring (Ring + MME), trophozoite (Trophozoite + MME) and schizont (Schizont + MME) stages for 12 hr. after that compound is washed off and the growth of parasite was monitored up to 60 h of post infection for every 12 h.

4A.4 Discussion

We have estimated the antiplasmodial activity of penicinoline E, marinamide and methyl marinamide which are total synthesized by Suzuki-Miyaura coupling followed by dearomatization with overall yield of 70-97%. Compared with marinamide, penicinoline E and methyl marinamide were potent against P. falciparum 3d7 with an IC50 value of 1.56 µM. Chloroquine belongs to the quinolone family inhibits the growth by inhibiting the hemozoin synthesis of *Plasmodium* parasite (201). We found penicinoline E and methyl marinamide potently inhibited the NP-40 induced β-hematin synthesis with an IC50 of 62.5 µM similar to the chloroquine further supports their antiparasitic activity. Hemozoin synthesis occur maximum at trophozoite stage of *Plasmodium* parasite. When we transiently treated the Plasmodium falciparum at ring, trophozoite and schizont stages with penicinoline alkaloids, penicinoline E inhibited the trophozoite stage treated parasite growth irreversibly supports the hemozoin synthesis inhibition activity of penicinoline E. Methyl marinamide treatment delayed the trophozoite stage treated parasite growth compared to untreated parasite culture. The ring and schizont stage parasite culture treated with penicinoline alkaloids didn't show any alteration compared to untreated culture indicates the specific action of penicinoline alkaloids against trophozoite stage of *P. falciparum*.

4B.	Thiazolyl	derivativ	ves as a cl	lass of an	timalaria	l agents

4B.1 Introduction

Thiazole scaffolds are found in many natural products (202) and possess diverse medicinal and pharmaceutical applications such as antitubercular (203, 204), anticonvulsant (205), anticancer (206), antiviral (207), antimicrobial (208), antimalarial (209) and anti-inflammatory activity (210). Coumarin is a vital pharmacophore having many applications in the fields of medicinal chemistry as well as pharmaceuticals like antifungal (211), anti-HIV agents (212), anti-Alzheimers (213) and also acts as a luminescent material (214). When the coumarin ring is attached with the thiazole ring, it exhibits improved biological activities like being an anti-inflammatory and anti-analgesic agent (215). On the other hand, thiadiazines are also versatile, biologically important heterocyclic molecules (216) with proven applications as an antidepressant (217), antihypertensive (218), and antiproliferative agents (219). Furthermore, thiazoles attached to coumarins, thiadiazine, and thiosemicarbazones are documented to exhibit an enhanced spectrum of biological activities (220, 221). Here we analysed the coumarinyl hydrazino thiazole and coumarinyl hydrazino thiadiazine moieties antiplasmodial activity and their mechanism of action against *P. falciparum*.

4B.2 Materials and Methods

4B.2.1 SYBR green fluorescence-based antiplasmodial assay

Antiplasmodial activity was estimated using SYBR green fluorescence compound as stated in chapter-1 material & methods section.

4B.2.2 Cytotoxicity assay (MTT)

The toxicity of the compounds against normal cells was estimated using the J774.2 macrophage cell line as described in chapter-4A material & methods section.

4B.2.3 Stage-specific growth assessment

Synchronized *P. falciparum* 3d7 culture was aliquoted into ring, trophozoite and, schizont stages and treated with the compounds transiently and observed the growth morphology as described in chapter-2, materials & methods section.

4B.2.4 Lactate dehydrogenase (LDH) assay

LDH assay was conducted to measure the cytotoxicity of compounds 4h, 4i, 4k, and 4l against synchronized P. falciparum 3D7 culture in vitro. The culture was adjusted to 1–1.5% parasitemia and 2% hematocrit in a 96-well plate containing serially diluted compounds and grown for 48 hr. Later, the percentage of cytotoxicity was estimated using a Cayman's LDH cytotoxicity assay kit. The LDH released from the P. falciparum due the action compounds reduces NAD+ to NADH and H+ by oxidation of lactate to pyruvate. Using NADH and H+, diaphorase reduced a tetrazolium salt (INT) to 7colored formazan, which has a maximum absorbance at 490–520 nM.

4B.3 Results

4B.3.1 *In vitro* antimalarial activity and cytotoxicity of compounds

The antimalarial properties of all derivatives were evaluated in vitro against the chloroquine (CQ) resistant (Dd2) and CQ-sensitive (3D7) strains of *P. falciparum* parasite. Thirteen compounds exhibited half-maximal inhibitory concentration (IC50) values below 6.30 μ M against both sensitive and resistant 3D7 and Dd2 strains. All IC50 values against CQ-sensitive and -resistant strains were tabulated in Table 3. Compound 6g showed an IC50 value of 12.5 \pm 0.12 μ M and the remaining nine compounds showed no activity (>24 μ M) in the 3D7 strain. Four compounds 4h, 4i, 4k, 4l showed reasonable activity with an IC50 value of 3.2, 2.7, 2.7, and 2.8 μ M against the CQ-sensitive strain of *P. falciparum*. These

compounds also showed inhibition of the CQ-resistant strain with an IC50 value of 3.25, 3.25, 3.13, and 3.5 µM (Table 4). Furthermore, lactate dehydrogenase (LDH) assay was conducted to measure the cytotoxicity of 4h, 4i, 4k, and 4l against synchronized P. falciparum 3D7 culture in vitro. These four compounds showed IC50 at 3.12 µM concentration against P. falciparum 3D7 culture as showed in table 2. Only three compounds from this series (6b, 6c, and 6e) showed activity around 6.15-6.25 µM against the CQsensitive strain of P. falciparum. Hence, in both series, the active compounds were 4h, 4i, 4k, and 4l. The IC50 of chloroquine against 3D7 is 26 ± 2.5 nM and that of Dd2 is 184 ± 10.6 nM whereas the antimalarial activity of these four compounds cannot be compared to that of chloroquine, the functional group modifications at thiazole or coumarin moiety have tremendous prospects in further development and this work is in progress in this laboratory. To check the toxicity of the compounds against normal cell cytotoxicity, tests were carried out against mice macrophage J774.2 cells using the 3-(4,5-dimethylthiazol-2-yl)-2,5diphenyltetrazolium bromide (MTT) colorimetric method. Compounds 4i and 4k had a cytotoxic concentration 50 (CC50) of 500 μM, whereas 4h and 4l showed a CC50 of 250 μM, respectively as shown in Table 4.

S.NO	Compound	IC50(μM)	IC50(μM)
	Name	3d7 strain	Dd2 strain
1	4a	6.37±0.87	6.73±0.21
2	4b	5.35±0.37	6.25±0.15
3	4c	5.71±0.39	5.85±0.83
4	4d	5.35±0.37	6.25±0.41
5	4e	>50	nd*
6	4f	4.16±0.83	5.22±0.35
7	4g	4.66 ± 0.83	5.12±0.20
8	4h	3.20±0.43	3.25±0.88
9	4i	2.70±0.20	3.25±0.31
10	4j	5.37±0.37	6.12±0.20

11	4k	2.70±0.22	3.13±0.42
12	41	2.85±0.20	3.52±0.31
13	6a	25.00±0.18	nd
14	6b	6.15±0.28	7.32 ± 0.43
15	6c	6.15±0.10	6.53±0.22
16	6d	26.00±0.44	nd
17	6e	6.25±0.78	nd
18	6f	25.8±0.26	nd
19	6g	12.50±0.12	nd
20	6h	26.20±0.40	nd
21	6i	25.20±0.24	nd
22	6j	24.00±0.13	nd

Table 3 Compound structures (4a–l, 6a–k) and half-maximal inhibitory concentration (IC50) values with 3D7 strain and Dd2 strain

Note: IC50 of chloroquine against 3D7 is 26 ± 2.5 nM and Dd2 is 184 ± 10.6 nM. Abbreviation: nd, not determined.

	IC ₅₀ (μM) ^a		CC ₅₀ (μM) ^b	
Compound	pf3D7	pfDd2	J774.2	
4h	3.208±0.43	3.25±0.88	250	
4i	2.706±0.20	3.251±0.42	500	
4k	2.708±0.20	3.138±0.42	500	
41	2.85±0.20	3.521±0.31	250	

Table 4 Antimalarial activities of active compounds against blood-stage parasites and in vitro cytotoxicity

Abbreviations: CC50, cytotoxic concentration 50; IC50, half-maximal inhibitory concentration.

^aBlood-stage antiplasmodial activity was determined against the CQ sensitive strain 3D7 and CQ-resistant strain Dd2 of P. falciparum.

^bCytotoxicity was determined against a mouse macrophage (J774.2) cell line; data are expressed as the CC50, which is the concentration required to reduce cell viability by 50%.

4B.3.2 *P. falciparum* stage specific growth inhibition

To check the growth inhibition activity of compounds 4h, 4i, 4k and 4l against *P. falciparum*, the parasite culture was treated with an IC90 concentration at their corresponding stages, that is, ring (R), trophozoite (T), and schizont (S) stages for 12 hr. The compound was removed after 12 hr by several washes and supplemented with complete Roswell Park Memorial Institute (RPMI) media for further growth of the parasite. The parasitemia was estimated from Giemsa stained smears. Figure 4B.3A shows that there is no increase of parasitemia at 48 hr in the ring stage treated culture (R + 4l) similar to unremoved culture (UR + 4l) when compared to control. The survived parasites of ring stage treated and unremoved cultures were further grown and infected fresh red blood cell (RBC) forming rings at 48 hr after removal of the compound as shown in Figure 4B.3B, but we found they could not grow further, and the morphology remained at the ring stage even after 60 and 72 hr when compared with the control. The control attained the trophozoite stage at a similar cycle time. Trophozoite (T + 4l) and schizont (S + 4l) stage treated parasites have more parasitemia than the ring stage treated culture and their growth morphology is similar to control at 60 and 72 hr. The compounds 4h and 4k have shown ring stage growth inhibition of the parasite in unremoved culture as shown in Figure 4B.1 and 4B.2 but they did not show growth inhibition in transiently treated cultures at the specific stage of the parasite with IC90 concentration. These results show that the compound 4l is more active in inhibiting the growth of the ring stage of the *P. falciparum* 3D7.

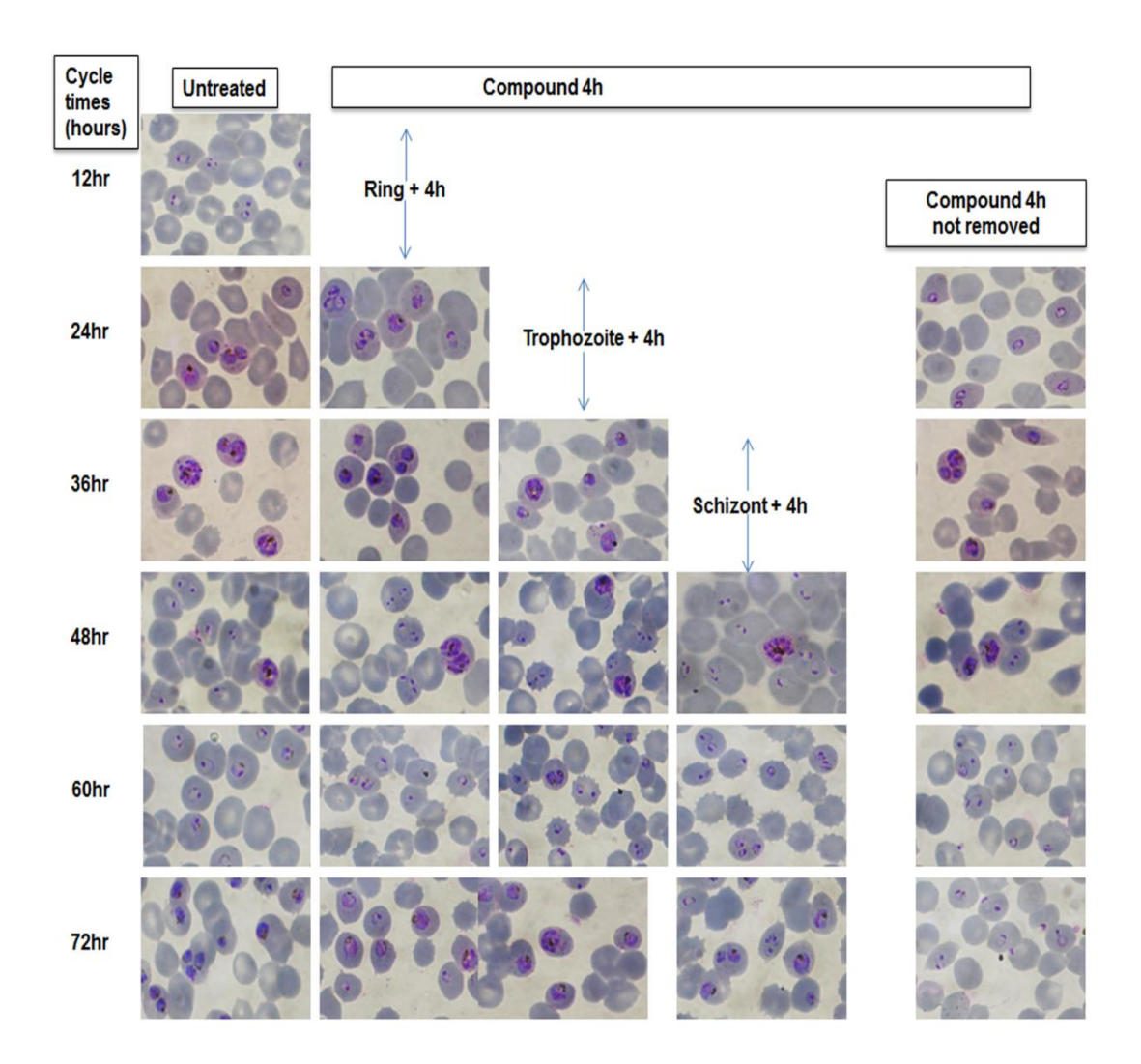


Figure 4B.1 Effect of compound 4h transient treatment at various plasmodial stages. Giemsa stained images represent the morphology of the parasite treated with compound 4h compound at various stages corresponding to ring (Ring + 4h), trophozoite (Trophozoite + 4h) and schizont (Schizont + 4h) stages for 12 hr. after that compound is washed off and the growth of parasite was monitored up to 72 h of post infection for every 12 h.

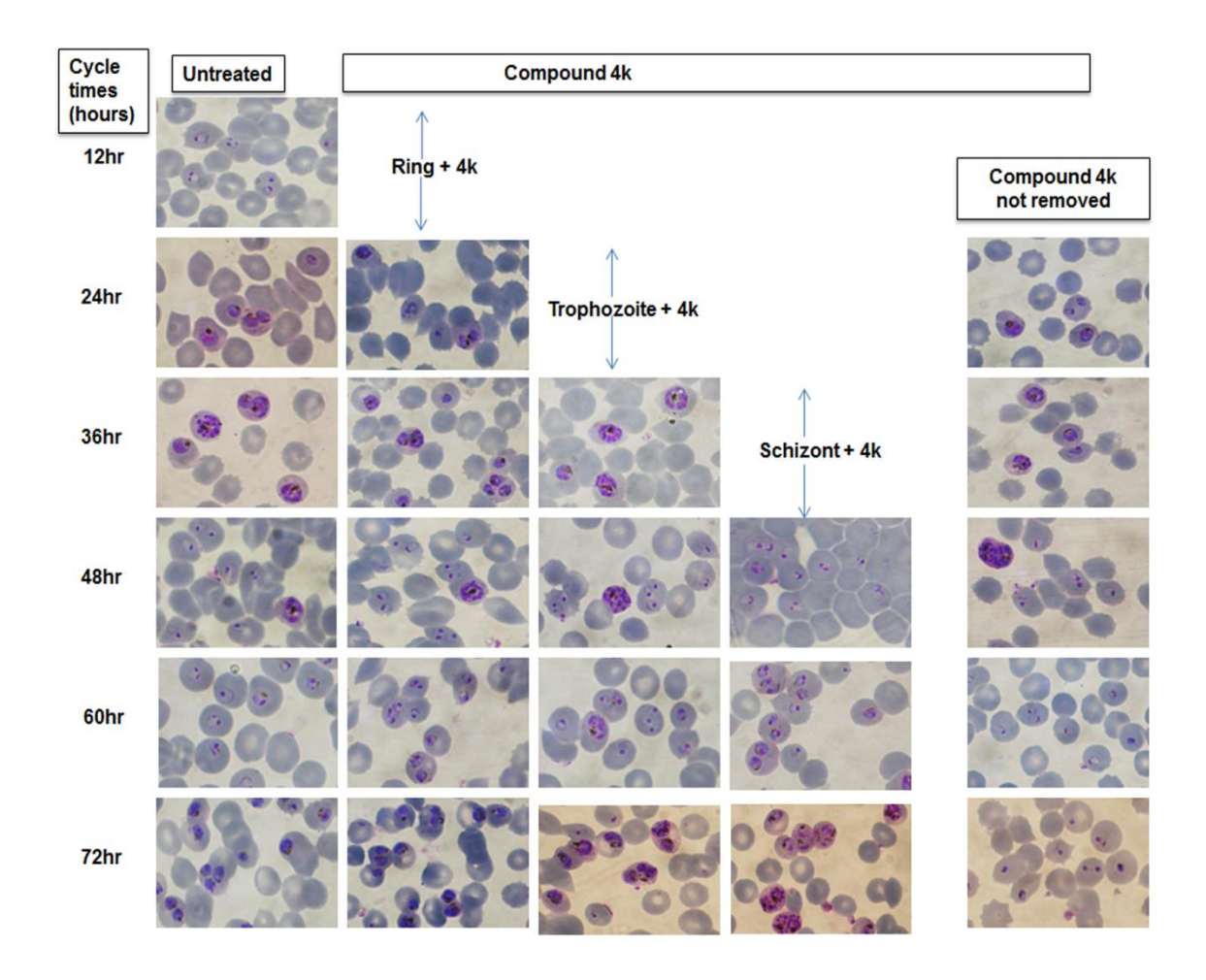


Figure 4B.2 Effect of compound 4k transient treatment at various plasmodial stages. Giemsa stained images represent the morphology of the parasite treated with compound 4k compound at various stages corresponding to ring (Ring + 4k), trophozoite (Trophozoite + 4k) and schizont (Schizont + 4k) stages for 12 hr. after that compound is washed off and the growth of parasite was monitored up to 72 h of post infection for every 12 h.

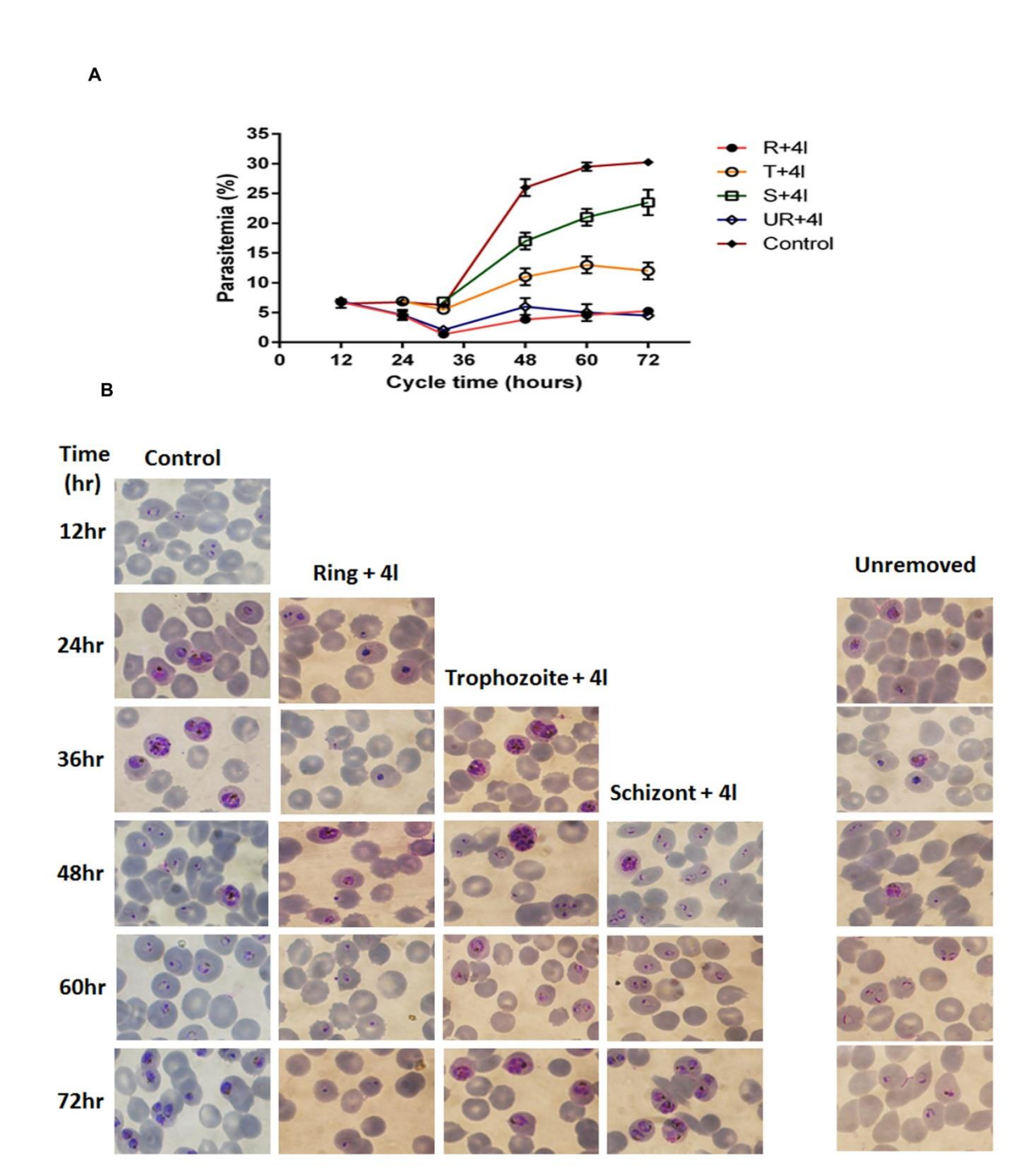


Figure 4B.3 Effect of compound 4l transient treatment at various plasmodial stages. (A) Growth of parasitemia after treatment with compound 4l at various *Plasmodium* falciparum 3D7 growth stages; 12 hr post-infection cultures were treated with compound 4l at various stages corresponding to ring (R + 4l), trophozoite (T + 4l) and schizont (S + 4l) stages. After that, the compound was removed and the parasitemia was monitored for up to 72 hr post-infection. Results are represented as the mean of three individual experiments \pm standard error. (B) Giemsa stained images represent the morphology of the parasite at the corresponding stages. Representation used is R + 4l (closed circles), T + 4l (open circles), S + 4l (open square), unremoved 4l (open diamond), control (closed diamond).

4B.4 Discussion

Combinatorial drug synthesis is a major interest in medicinal chemistry to discover new drugs. Hence we analyzed the coumarin and thiazole ring combined synthetic compounds anti- malaria activity. We found coumarinyl hydrazino thiazole showed potent antiplasmodial activity compared to coumarinyl hydrazino thiadiazine moieties. In general, the thiazolyl hydrazonothiazolamine series having halogenated and electron-rich coumarin substituents showed good activity compared with simple phenyl substituted thiazolyl hydrazonothiazolamines. Interestingly coumarinyl hydrazino thiazole compounds are active after 48 h incubation and inhibiting the second cycle growth of *P. falciparum*. Tetracyclins are effective after 96 h of incubation indicates their slow-acting nature. Doxycycline treated parasites are failed to synthesize merozoites at the end of the second cycle, further supports the coumarinyl hydrazino thiazole 4l compound action against parasite ring stage growth inhibition in the second cycle (222). In contrast, 4h and 4k compounds couldn't inhibit the parasite growth in partially treated stage-specific cultures, but in unremoved parasite culture, they did inhibit the ring stage growth in a second cycle similar to the compound.

5. References

- 1. Miller RL, Ikram S, Armelagos GJ, Walker R, Harer WB, Shiff CJ, et al. Diagnosis of Plasmodium falciparum infections in mummies using the rapid manual ParaSight-F test. Transactions of the Royal Society of Tropical Medicine and Hygiene. 1994;88(1):31-2.
- 2. Carter R, Mendis KN. Evolutionary and historical aspects of the burden of malaria. Clinical microbiology reviews. 2002;15(4):564-94.
- 3. Flint J, Harding RM, Boyce AJ, Clegg JB. The population genetics of the haemoglobinopathies. Bailliere's clinical haematology. 1993;6(1):215-62.
- 4. Reiter P. From Shakespeare to Defoe: malaria in England in the Little Ice Age. Emerging infectious diseases. 2000;6(1):1-11.
- 5. Cox FE. History of the discovery of the malaria parasites and their vectors. Parasites & vectors. 2010;3(1):5.
- 6. Gething PW, Patil AP, Smith DL, Guerra CA, Elyazar IR, Johnston GL, et al. A new world malaria map: Plasmodium falciparum endemicity in 2010. Malaria journal. 2011;10:378.
- 7. Mironova V, Shartova N, Beljaev A, Varentsov M, Grishchenko M. Effects of Climate Change and Heterogeneity of Local Climates small o, Cyrillicn the Development of Malaria Parasite (Plasmodium vivax) in Moscow Megacity Region. International journal of environmental research and public health. 2019;16(5).
- 8. White NJ, Warrell DA, Chanthavanich P, Looareesuwan S, Warrell MJ, Krishna S, et al. Severe hypoglycemia and hyperinsulinemia in falciparum malaria. The New England journal of medicine. 1983;309(2):61-6.
- 9. Taylor TE, Molyneux ME, Wirima JJ, Fletcher KA, Morris K. Blood glucose levels in Malawian children before and during the administration of intravenous quinine for severe falciparum malaria. The New England journal of medicine. 1988;319(16):1040-7.
- 10. Kitchen LW, Vaughn DW, Skillman DR. Role of US military research programs in the development of US Food and Drug Administration--approved antimalarial drugs. Clinical infectious diseases: an official publication of the Infectious Diseases Society of America. 2006;43(1):67-71.
- 11. Harinasuta T, Suntharasamai P, Viravan C. Chloroquine-resistant falciparum malaria in Thailand. Lancet. 1965;2(7414):657-60.
- 12. White NJ, Hien TT, Nosten FH. A Brief History of Qinghaosu. Trends in parasitology. 2015;31(12):607-10.
- 13. Fuller AC, Harhay MO. Population Growth, Climate Change and Water Scarcity in the Southwestern United States. American journal of environmental sciences. 2010;6(3):249-52.
- 14. Tavares J, Formaglio P, Thiberge S, Mordelet E, Van Rooijen N, Medvinsky A, et al. Role of host cell traversal by the malaria sporozoite during liver infection. The Journal of experimental medicine. 2013;210(5):905-15.
- 15. Baer K, Roosevelt M, Clarkson AB, Jr., van Rooijen N, Schnieder T, Frevert U. Kupffer cells are obligatory for Plasmodium yoelii sporozoite infection of the liver. Cellular microbiology. 2007;9(2):397-412.
- 16. Frevert U, Engelmann S, Zougbede S, Stange J, Ng B, Matuschewski K, et al. Intravital observation of Plasmodium berghei sporozoite infection of the liver. PLoS biology. 2005;3(6):e192.
- 17. Sanders PR, Gilson PR, Cantin GT, Greenbaum DC, Nebl T, Carucci DJ, et al. Distinct protein classes including novel merozoite surface antigens in Raft-like membranes of Plasmodium falciparum. The Journal of biological chemistry. 2005;280(48):40169-76.
- 18. Bannister LH, Dluzewski AR. The ultrastructure of red cell invasion in malaria infections: a review. Blood cells. 1990;16(2-3):257-92; discussion 93-7.
- 19. Adams JH, Hudson DE, Torii M, Ward GE, Wellems TE, Aikawa M, et al. The Duffy receptor family of Plasmodium knowlesi is located within the micronemes of invasive malaria merozoites. Cell. 1990;63(1):141-53.
- 20. Ward GE, Miller LH, Dvorak JA. The origin of parasitophorous vacuole membrane lipids in malaria-infected erythrocytes. Journal of cell science. 1993;106 (Pt 1):237-48.

- 21. Pouvelle B, Gormley JA, Taraschi TF. Characterization of trafficking pathways and membrane genesis in malaria-infected erythrocytes. Mol Biochem Parasitol. 1994;66(1):83-96.
- 22. Atkinson CT, Aikawa M, Perry G, Fujino T, Bennett V, Davidson EA, et al. Ultrastructural localization of erythrocyte cytoskeletal and integral membrane proteins in Plasmodium falciparum-infected erythrocytes. European journal of cell biology. 1988;45(2):192-9.
- 23. Sherling ES, Perrin AJ, Knuepfer E, Russell MRG, Collinson LM, Miller LH, et al. The Plasmodium falciparum rhoptry bulb protein RAMA plays an essential role in rhoptry neck morphogenesis and host red blood cell invasion. PLoS pathogens. 2019;15(9):e1008049.
- 24. Marti M, Good RT, Rug M, Knuepfer E, Cowman AF. Targeting malaria virulence and remodeling proteins to the host erythrocyte. Science. 2004;306(5703):1930-3.
- 25. Abu Bakar N, Klonis N, Hanssen E, Chan C, Tilley L. Digestive-vacuole genesis and endocytic processes in the early intraerythrocytic stages of Plasmodium falciparum. Journal of cell science. 2010;123(Pt 3):441-50.
- 26. Goldberg DE, Slater AF, Beavis R, Chait B, Cerami A, Henderson GB. Hemoglobin degradation in the human malaria pathogen Plasmodium falciparum: a catabolic pathway initiated by a specific aspartic protease. The Journal of experimental medicine. 1991;173(4):961-9.
- 27. Hoang AN, Sandlin RD, Omar A, Egan TJ, Wright DW. The neutral lipid composition present in the digestive vacuole of Plasmodium falciparum concentrates heme and mediates beta-hematin formation with an unusually low activation energy. Biochemistry. 2010;49(47):10107-16.
- 28. Pandey AV, Babbarwal VK, Okoyeh JN, Joshi RM, Puri SK, Singh RL, et al. Hemozoin formation in malaria: a two-step process involving histidine-rich proteins and lipids. Biochemical and biophysical research communications. 2003;308(4):736-43.
- 29. Vial HJ, Eldin P, Tielens AG, van Hellemond JJ. Phospholipids in parasitic protozoa. Mol Biochem Parasitol. 2003;126(2):143-54.
- 30. van Dooren GG, Marti M, Tonkin CJ, Stimmler LM, Cowman AF, McFadden GI. Development of the endoplasmic reticulum, mitochondrion and apicoplast during the asexual life cycle of Plasmodium falciparum. Molecular microbiology. 2005;57(2):405-19.
- 31. Clark IA, Budd AC, Alleva LM, Cowden WB. Human malarial disease: a consequence of inflammatory cytokine release. Malaria journal. 2006;5:85.
- 32. Schumann RR. Malarial fever: hemozoin is involved but Toll-free. Proceedings of the National Academy of Sciences of the United States of America. 2007;104(6):1743-4.
- 33. Skorokhod OA, Alessio M, Mordmuller B, Arese P, Schwarzer E. Hemozoin (malarial pigment) inhibits differentiation and maturation of human monocyte-derived dendritic cells: a peroxisome proliferator-activated receptor-gamma-mediated effect. J Immunol. 2004;173(6):4066-74.
- 34. Lamikanra AA, Brown D, Potocnik A, Casals-Pascual C, Langhorne J, Roberts DJ. Malarial anemia: of mice and men. Blood. 2007;110(1):18-28.
- 35. Waitumbi JN, Opollo MO, Muga RO, Misore AO, Stoute JA. Red cell surface changes and erythrophagocytosis in children with severe plasmodium falciparum anemia. Blood. 2000;95(4):1481-6.
- 36. Stoute JA, Odindo AO, Owuor BO, Mibei EK, Opollo MO, Waitumbi JN. Loss of red blood cell-complement regulatory proteins and increased levels of circulating immune complexes are associated with severe malarial anemia. J Infect Dis. 2003;187(3):522-5.
- 37. Sterkers Y, Scheidig C, da Rocha M, Lepolard C, Gysin J, Scherf A. Members of the low-molecular-mass rhoptry protein complex of Plasmodium falciparum bind to the surface of normal erythrocytes. J Infect Dis. 2007;196(4):617-21.
- 38. Newbold C, Craig A, Kyes S, Rowe A, Fernandez-Reyes D, Fagan T. Cytoadherence, pathogenesis and the infected red cell surface in Plasmodium falciparum. Int J Parasitol. 1999:29(6):927-37
- 39. Toure FS, Ouwe-Missi-Oukem-Boyer O, Bisvigou U, Moussa O, Rogier C, Pino P, et al. Apoptosis: a potential triggering mechanism of neurological manifestation in Plasmodium falciparum malaria. Parasite Immunol. 2008;30(1):47-51.

- 40. Clark IA, Rockett KA, Cowden WB. Possible central role of nitric oxide in conditions clinically similar to cerebral malaria. Lancet. 1992;340(8824):894-6.
- 41. Griffith JW, Sokol CL, Luster AD. Chemokines and chemokine receptors: positioning cells for host defense and immunity. Annual review of immunology. 2014;32:659-702.
- 42. Swanson PA, 2nd, Hart GT, Russo MV, Nayak D, Yazew T, Pena M, et al. CD8+ T Cells Induce Fatal Brainstem Pathology during Cerebral Malaria via Luminal Antigen-Specific Engagement of Brain Vasculature. PLoS pathogens. 2016;12(12):e1006022.
- 43. Rivera Fernandez N, Colin Barenque L, Romero Silva SE, Salas Garrido G, Jimenez Rosey SG, Zepeda Rodriguez A, et al. Ependymal damage in a Plasmodium yoelii yoelii lethal murine malaria model. Histology and histopathology. 2015;30(2):245-53.
- 44. English M, Sauerwein R, Waruiru C, Mosobo M, Obiero J, Lowe B, et al. Acidosis in severe childhood malaria. QJM. 1997;90(4):263-70.
- 45. Day NP, Phu NH, Mai NT, Chau TT, Loc PP, Chuong LV, et al. The pathophysiologic and prognostic significance of acidosis in severe adult malaria. Crit Care Med. 2000;28(6):1833-40.
- 46. Maitland K, Newton CR. Acidosis of severe falciparum malaria: heading for a shock? Trends in parasitology. 2005;21(1):11-6.
- 47. Poovassery J, Moore JM. Murine malaria infection induces fetal loss associated with accumulation of Plasmodium chabaudi AS-infected erythrocytes in the placenta. Infection and immunity. 2006;74(5):2839-48.
- 48. Desai M, ter Kuile FO, Nosten F, McGready R, Asamoa K, Brabin B, et al. Epidemiology and burden of malaria in pregnancy. The Lancet Infectious diseases. 2007;7(2):93-104.
- 49. Rogerson SJ, Mwapasa V, Meshnick SR. Malaria in pregnancy: linking immunity and pathogenesis to prevention. Am J Trop Med Hyg. 2007;77(6 Suppl):14-22.
- 50. Buffet PA, Gamain B, Scheidig C, Baruch D, Smith JD, Hernandez-Rivas R, et al. Plasmodium falciparum domain mediating adhesion to chondroitin sulfate A: a receptor for human placental infection. Proceedings of the National Academy of Sciences of the United States of America. 1999;96(22):12743-8.
- 51. Gamain B, Smith JD, Miller LH, Baruch DI. Modifications in the CD36 binding domain of the Plasmodium falciparum variant antigen are responsible for the inability of chondroitin sulfate A adherent parasites to bind CD36. Blood. 2001;97(10):3268-74.
- 52. Kusuhara H, Sugiyama Y. Efflux transport systems for organic anions and cations at the blood-CSF barrier. Adv Drug Deliv Rev. 2004;56(12):1741-63.
- 53. Curtis MA, Faull RL, Eriksson PS. The effect of neurodegenerative diseases on the subventricular zone. Nat Rev Neurosci. 2007;8(9):712-23.
- 54. Walther TC, Chung J, Farese RV, Jr. Lipid Droplet Biogenesis. Annu Rev Cell Dev Biol. 2017;33:491-510.
- 55. Marschallinger J, Iram T, Zardeneta M, Lee SE, Lehallier B, Haney MS, et al. Lipid-droplet-accumulating microglia represent a dysfunctional and proinflammatory state in the aging brain. Nat Neurosci. 2020;23(2):194-208.
- 56. Hamilton LK, Dufresne M, Joppe SE, Petryszyn S, Aumont A, Calon F, et al. Aberrant Lipid Metabolism in the Forebrain Niche Suppresses Adult Neural Stem Cell Proliferation in an Animal Model of Alzheimer's Disease. Cell Stem Cell. 2015;17(4):397-411.
- 57. Labbe K, Saleh M. Cell death in the host response to infection. Cell Death Differ. 2008;15(9):1339-49.
- 58. Steers N, Schwenk R, Bacon DJ, Berenzon D, Williams J, Krzych U. The immune status of Kupffer cells profoundly influences their responses to infectious Plasmodium berghei sporozoites. Eur J Immunol. 2005;35(8):2335-46.
- 59. Belachew EB. Immune Response and Evasion Mechanisms of Plasmodium falciparum Parasites. J Immunol Res. 2018;2018:6529681.

- 60. Schwarzer E, Alessio M, Ulliers D, Arese P. Phagocytosis of the malarial pigment, hemozoin, impairs expression of major histocompatibility complex class II antigen, CD54, and CD11c in human monocytes. Infection and immunity. 1998;66(4):1601-6.
- 61. Schwarzer E, Turrini F, Ulliers D, Giribaldi G, Ginsburg H, Arese P. Impairment of macrophage functions after ingestion of Plasmodium falciparum-infected erythrocytes or isolated malarial pigment. The Journal of experimental medicine. 1992;176(4):1033-41.
- 62. Youssef LA, Rebbaa A, Pampou S, Weisberg SP, Stockwell BR, Hod EA, et al. Increased erythrophagocytosis induces ferroptosis in red pulp macrophages in a mouse model of transfusion. Blood. 2018;131(23):2581-93.
- 63. Cambos M, Scorza T. Robust erythrophagocytosis leads to macrophage apoptosis via a hemin-mediated redox imbalance: role in hemolytic disorders. Journal of leukocyte biology. 2011;89(1):159-71.
- 64. Deshmukh R, Trivedi V. Phagocytic uptake of oxidized heme polymer is highly cytotoxic to macrophages. PLoS One. 2014;9(7):e103706.
- 65. Hengartner MO. The biochemistry of apoptosis. Nature. 2000;407(6805):770-6.
- 66. Lavrik I, Golks A, Krammer PH. Death receptor signaling. Journal of cell science. 2005;118(Pt 2):265-7.
- 67. Kroemer G, Galluzzi L, Brenner C. Mitochondrial membrane permeabilization in cell death. Physiol Rev. 2007;87(1):99-163.
- 68. Gozuacik D, Kimchi A. Autophagy and cell death. Curr Top Dev Biol. 2007;78:217-45.
- 69. Kuma A, Mizushima N. Physiological role of autophagy as an intracellular recycling system: with an emphasis on nutrient metabolism. Semin Cell Dev Biol. 2010;21(7):683-90.
- 70. Yang Z, Klionsky DJ. Mammalian autophagy: core molecular machinery and signaling regulation. Curr Opin Cell Biol. 2010;22(2):124-31.
- 71. Kuma A, Mizushima N, Ishihara N, Ohsumi Y. Formation of the approximately 350-kDa Apg12-Apg5.Apg16 multimeric complex, mediated by Apg16 oligomerization, is essential for autophagy in yeast. The Journal of biological chemistry. 2002;277(21):18619-25.
- 72. Noboru Mizushima YO, Tamotsu Yoshimori. Autophagosome Formation in Mammalian Cells. cell structure and function. 2002;27(6):421-9.
- 73. Castedo M, Ferri KF, Kroemer G. Mammalian target of rapamycin (mTOR): pro- and antiapoptotic. Cell Death Differ. 2002;9(2):99-100.
- 74. Mammucari C, Milan G, Romanello V, Masiero E, Rudolf R, Del Piccolo P, et al. FoxO3 controls autophagy in skeletal muscle in vivo. Cell Metab. 2007;6(6):458-71.
- 75. Boya P, Gonzalez-Polo RA, Casares N, Perfettini JL, Dessen P, Larochette N, et al. Inhibition of macroautophagy triggers apoptosis. Mol Cell Biol. 2005;25(3):1025-40.
- 76. Oberstein A, Jeffrey PD, Shi Y. Crystal structure of the Bcl-XL-Beclin 1 peptide complex: Beclin 1 is a novel BH3-only protein. The Journal of biological chemistry. 2007;282(17):13123-32.
- 77. Yousefi S, Perozzo R, Schmid I, Ziemiecki A, Schaffner T, Scapozza L, et al. Calpain-mediated cleavage of Atg5 switches autophagy to apoptosis. Nature cell biology. 2006;8(10):1124-32.
- 78. Zhang YM, Rock CO. Membrane lipid homeostasis in bacteria. Nature reviews Microbiology. 2008;6(3):222-33.
- 79. Waller RF, Keeling PJ, Donald RG, Striepen B, Handman E, Lang-Unnasch N, et al. Nuclear-encoded proteins target to the plastid in Toxoplasma gondii and Plasmodium falciparum. Proceedings of the National Academy of Sciences of the United States of America. 1998;95(21):12352-7.
- 80. Hsiao LL, Howard RJ, Aikawa M, Taraschi TF. Modification of host cell membrane lipid composition by the intra-erythrocytic human malaria parasite Plasmodium falciparum. The Biochemical journal. 1991;274 (Pt 1):121-32.
- 81. Kumaratilake LM, Robinson BS, Ferrante A, Poulos A. Antimalarial properties of n-3 and n-6 polyunsaturated fatty acids: in vitro effects on Plasmodium falciparum and in vivo effects on P. berghei. The Journal of clinical investigation. 1992;89(3):961-7.

- 82. Krugliak M, Deharo E, Shalmiev G, Sauvain M, Moretti C, Ginsburg H. Antimalarial effects of C18 fatty acids on Plasmodium falciparum in culture and on Plasmodium vinckei petteri and Plasmodium yoelii nigeriensis in vivo. Experimental parasitology. 1995;81(1):97-105.
- 83. Suksamrarn A, Buaprom M, Udtip S, Nuntawong N, Haritakun R, Kanokmedhakul S. Antimycobacterial and antiplasmodial unsaturated carboxylic acid from the twigs of Scleropyrum wallichianum. Chemical & pharmaceutical bulletin. 2005;53(10):1327-9.
- 84. Tasdemir D, Topaloglu B, Perozzo R, Brun R, O'Neill R, Carballeira NM, et al. Marine natural products from the Turkish sponge Agelas oroides that inhibit the enoyl reductases from Plasmodium falciparum, Mycobacterium tuberculosis and Escherichia coli. Bioorganic & medicinal chemistry. 2007;15(21):6834-45.
- 85. Kabara JJ, Swieczkowski DM, Conley AJ, Truant JP. Fatty acids and derivatives as antimicrobial agents. Antimicrobial agents and chemotherapy. 1972;2(1):23-8.
- 86. Saito H, Tomioka H, Yoneyama T. Growth of group IV mycobacteria on medium containing various saturated and unsaturated fatty acids. Antimicrobial agents and chemotherapy. 1984;26(2):164-9.
- 87. Seidel V, Taylor PW. In vitro activity of extracts and constituents of Pelagonium against rapidly growing mycobacteria. International journal of antimicrobial agents. 2004;23(6):613-9.
- 88. Carballeira NM, Montano N, Amador LA, Rodriguez AD, Golovko MY, Golovko SA, et al. Novel Very Long-Chain alpha-Methoxylated Delta5,9 Fatty Acids from the Sponge Asteropus niger Are Effective Inhibitors of Topoisomerases IB. Lipids. 2016;51(2):245-56.
- 89. Tasdemir D, Sanabria D, Lauinger IL, Tarun A, Herman R, Perozzo R, et al. 2-Hexadecynoic acid inhibits plasmodial FAS-II enzymes and arrests erythrocytic and liver stage Plasmodium infections. Bioorganic & medicinal chemistry. 2010;18(21):7475-85.
- 90. Wood R, Lee T. Metabolism of 2-hexadecynoate and inhibition of fatty acid elongation. The Journal of biological chemistry. 1981;256(23):12379-86.
- 91. Ginsburg H. Some reflections concerning host erythrocyte-malarial parasite interrelationships. Blood cells. 1990;16(2-3):225-35.
- 92. Wongsrichanalai C, Pickard AL, Wernsdorfer WH, Meshnick SR. Epidemiology of drugresistant malaria. The Lancet Infectious diseases. 2002;2(4):209-18.
- 93. de Dios AC, Casabianca LB, Kosar A, Roepe PD. Structure of the amodiaquine-FPIX mu oxo dimer solution complex at atomic resolution. Inorganic chemistry. 2004;43(25):8078-84.
- 94. Ignatushchenko MV, Winter RW, Bachinger HP, Hinrichs DJ, Riscoe MK. Xanthones as antimalarial agents; studies of a possible mode of action. FEBS letters. 1997;409(1):67-73.
- 95. Hartwig CL, Rosenthal AS, D'Angelo J, Griffin CE, Posner GH, Cooper RA. Accumulation of artemisinin trioxane derivatives within neutral lipids of Plasmodium falciparum malaria parasites is endoperoxide-dependent. Biochemical pharmacology. 2009;77(3):322-36.
- 96. Pisciotta JM, Coppens I, Tripathi AK, Scholl PF, Shuman J, Bajad S, et al. The role of neutral lipid nanospheres in Plasmodium falciparum haem crystallization. The Biochemical journal. 2007;402(1):197-204.
- 97. Carballeira NM. New advances in fatty acids as antimalarial, antimycobacterial and antifungal agents. Progress in lipid research. 2008;47(1):50-61.
- 98. Piola P, Fogg C, Bajunirwe F, Biraro S, Grandesso F, Ruzagira E, et al. Supervised versus unsupervised intake of six-dose artemether-lumefantrine for treatment of acute, uncomplicated Plasmodium falciparum malaria in Mbarara, Uganda: a randomised trial. Lancet. 2005;365(9469):1467-73.
- 99. Rieckmann KH, Campbell GH, Sax LJ, Mrema JE. Drug sensitivity of plasmodium falciparum. An in-vitro microtechnique. Lancet. 1978;1(8054):22-3.
- 100. Smilkstein M, Sriwilaijaroen N, Kelly JX, Wilairat P, Riscoe M. Simple and inexpensive fluorescence-based technique for high-throughput antimalarial drug screening. Antimicrobial agents and chemotherapy. 2004;48(5):1803-6.

- 101. Moneriz C, Marin-Garcia P, Garcia-Granados A, Bautista JM, Diez A, Puyet A. Parasitostatic effect of maslinic acid. I. Growth arrest of Plasmodium falciparum intraerythrocytic stages. Malaria journal. 2011;10:82.
- 102. Carter MD, Phelan VV, Sandlin RD, Bachmann BO, Wright DW. Lipophilic mediated assays for beta-hematin inhibitors. Combinatorial chemistry & high throughput screening. 2010;13(3):285-92.
- 103. Kalkanidis M, Klonis N, Tschan S, Deady LW, Tilley L. Synergistic interaction of a chloroquine metabolite with chloroquine against drug-resistant malaria parasites. Biochemical pharmacology. 2004;67(7):1347-53.
- 104. Yi J, Thomas LM, Richter-Addo GB. Structure of human R-state aquomethemoglobin at 2.0 A resolution. Acta crystallographica Section F, Structural biology and crystallization communications. 2011;67(Pt 6):647-51.
- 105. Wu G, Robertson DH, Brooks CL, 3rd, Vieth M. Detailed analysis of grid-based molecular docking: A case study of CDOCKER-A CHARMm-based MD docking algorithm. Journal of computational chemistry. 2003;24(13):1549-62.
- 106. Gehlhaar DK, Verkhivker GM, Rejto PA, Sherman CJ, Fogel DB, Fogel LJ, et al. Molecular recognition of the inhibitor AG-1343 by HIV-1 protease: conformationally flexible docking by evolutionary programming. Chemistry & biology. 1995;2(5):317-24.
- 107. Jain AN. Scoring noncovalent protein-ligand interactions: a continuous differentiable function tuned to compute binding affinities. Journal of computer-aided molecular design. 1996;10(5):427-40.
- 108. Muegge I, Martin YC. A general and fast scoring function for protein-ligand interactions: a simplified potential approach. Journal of medicinal chemistry. 1999;42(5):791-804.
- 109. Muegge I. PMF scoring revisited. Journal of medicinal chemistry. 2006;49(20):5895-902.
- 110. Allison AC, Eugui EM. The role of cell-mediated immune responses in resistance to malaria, with special reference to oxidant stress. Annual review of immunology. 1983;1:361-92.
- 111. Dockrell HM, Playfair JH. Killing of Plasmodium yoelii by enzyme-induced products of the oxidative burst. Infection and immunity. 1984;43(2):451-6.
- 112. Rockett KA, Awburn MM, Cowden WB, Clark IA. Killing of Plasmodium falciparum in vitro by nitric oxide derivatives. Infection and immunity. 1991;59(9):3280-3.
- 113. Ferrante A, Rzepczyk CM, Allison AC. Polyamine oxidase mediates intra-erythrocytic death of Plasmodium falciparum. Transactions of the Royal Society of Tropical Medicine and Hygiene. 1983;77(6):789-91.
- 114. Simoes AP, van den Berg JJ, Roelofsen B, Op den Kamp JA. Lipid peroxidation in Plasmodium falciparum-parasitized human erythrocytes. Archives of biochemistry and biophysics. 1992;298(2):651-7.
- 115. Fabbri C, de Cassia Mascarenhas-Netto R, Lalwani P, Melo GC, Magalhaes BM, Alexandre MA, et al. Lipid peroxidation and antioxidant enzymes activity in Plasmodium vivax malaria patients evolving with cholestatic jaundice. Malaria journal. 2013;12:315.
- 116. Schwarzer E, Kuhn H, Valente E, Arese P. Malaria-parasitized erythrocytes and hemozoin nonenzymatically generate large amounts of hydroxy fatty acids that inhibit monocyte functions. Blood. 2003;101(2):722-8.
- 117. Sigala PA, Crowley JR, Hsieh S, Henderson JP, Goldberg DE. Direct tests of enzymatic heme degradation by the malaria parasite Plasmodium falciparum. The Journal of biological chemistry. 2012;287(45):37793-807.
- 118. Fitch CD, Cai GZ, Chen YF, Shoemaker JD. Involvement of lipids in ferriprotoporphyrin IX polymerization in malaria. Biochimica et biophysica acta. 1999;1454(1):31-7.
- 119. Bendrat K, Berger BJ, Cerami A. Haem polymerization in malaria. Nature. 1995;378(6553):138-9.
- 120. Sullivan DJ, Jr., Matile H, Ridley RG, Goldberg DE. A common mechanism for blockade of heme polymerization by antimalarial quinolines. The Journal of biological chemistry. 1998;273(47):31103-7.

- 121. Pandey AV, Tekwani BL. Depolymerization of malarial hemozoin: a novel reaction initiated by blood schizontocidal antimalarials. FEBS letters. 1997;402(2-3):236-40.
- 122. Clark AL, Matera KM. Effect of unsaturation in fatty acids on the binding and oxidation by myeloperoxidase: ramifications for the initiation of atherosclerosis. Bioorganic & medicinal chemistry letters. 2010;20(19):5643-8.
- 123. Bonamore A, Farina A, Gattoni M, Schinina ME, Bellelli A, Boffi A. Interaction with membrane lipids and heme ligand binding properties of Escherichia coli flavohemoglobin. Biochemistry. 2003;42(19):5792-801.
- 124. Slater AF, Cerami A. Inhibition by chloroquine of a novel haem polymerase enzyme activity in malaria trophozoites. Nature. 1992;355(6356):167-9.
- 125. Sullivan DJ, Jr., Gluzman IY, Goldberg DE. Plasmodium hemozoin formation mediated by histidine-rich proteins. Science. 1996;271(5246):219-22.
- 126. Jani D, Nagarkatti R, Beatty W, Angel R, Slebodnick C, Andersen J, et al. HDP-a novel heme detoxification protein from the malaria parasite. PLoS pathogens. 2008;4(4):e1000053.
- 127. Noland GS, Briones N, Sullivan DJ, Jr. The shape and size of hemozoin crystals distinguishes diverse Plasmodium species. Mol Biochem Parasitol. 2003;130(2):91-9.
- 128. Palacpac NM, Hiramine Y, Seto S, Hiramatsu R, Horii T, Mitamura T. Evidence that Plasmodium falciparum diacylglycerol acyltransferase is essential for intraerythrocytic proliferation. Biochemical and biophysical research communications. 2004;321(4):1062-8.
- 129. Mitamura T, Palacpac NM. Lipid metabolism in Plasmodium falciparum-infected erythrocytes: possible new targets for malaria chemotherapy. Microbes and infection. 2003;5(6):545-52.
- 130. Vielemeyer O, McIntosh MT, Joiner KA, Coppens I. Neutral lipid synthesis and storage in the intraerythrocytic stages of Plasmodium falciparum. Mol Biochem Parasitol. 2004;135(2):197-209.
- 131. Palacpac NM, Hiramine Y, Mi-ichi F, Torii M, Kita K, Hiramatsu R, et al. Developmental-stage-specific triacylglycerol biosynthesis, degradation and trafficking as lipid bodies in Plasmodium falciparum-infected erythrocytes. Journal of cell science. 2004;117(Pt 8):1469-80.
- 132. Nolan SJ, Romano JD, Kline JT, Coppens I. Novel Approaches To Kill Toxoplasma gondii by Exploiting the Uncontrolled Uptake of Unsaturated Fatty Acids and Vulnerability to Lipid Storage Inhibition of the Parasite. Antimicrobial agents and chemotherapy. 2018;62(10).
- 133. Berlin E, Sainz E. Acyl chain interactions and the modulation of phase changes in glycerolipids. Biochimica et biophysica acta. 1986;855(1):1-7.
- 134. Ch'ng JH, Kotturi SR, Chong AG, Lear MJ, Tan KS. A programmed cell death pathway in the malaria parasite Plasmodium falciparum has general features of mammalian apoptosis but is mediated by clan CA cysteine proteases. Cell death & disease. 2010;1:e26.
- 135. Ch'ng JH, Liew K, Goh AS, Sidhartha E, Tan KS. Drug-induced permeabilization of parasite's digestive vacuole is a key trigger of programmed cell death in Plasmodium falciparum. Cell death & disease. 2011;2:e216.
- 136. Lee YQ, Goh AS, Ch'ng JH, Nosten FH, Preiser PR, Pervaiz S, et al. A high-content phenotypic screen reveals the disruptive potency of quinacrine and 3',4'-dichlorobenzamil on the digestive vacuole of Plasmodium falciparum. Antimicrobial agents and chemotherapy. 2014;58(1):550-8.
- 137. Sun M, Zhou Z, Dong J, Zhang J, Xia Y, Shu R. Antibacterial and antibiofilm activities of docosahexaenoic acid (DHA) and eicosapentaenoic acid (EPA) against periodontopathic bacteria. Microbial pathogenesis. 2016;99:196-203.
- 138. Zheng CJ, Yoo JS, Lee TG, Cho HY, Kim YH, Kim WG. Fatty acid synthesis is a target for antibacterial activity of unsaturated fatty acids. FEBS letters. 2005;579(23):5157-62.
- 139. Ortega-Pajares A, Rogerson SJ. The Rough Guide to Monocytes in Malaria Infection. Frontiers in immunology. 2018;9:2888.
- 140. Jenkins NE, Chakravorty SJ, Urban BC, Kai OK, Marsh K, Craig AG. The effect of Plasmodium falciparum infection on expression of monocyte surface molecules. Transactions of the Royal Society of Tropical Medicine and Hygiene. 2006;100(11):1007-12.

- 141. Nathan C. Points of control in inflammation. Nature. 2002;420(6917):846-52.
- 142. Terkawi MA, Nishimura M, Furuoka H, Nishikawa Y. Depletion of Phagocytic Cells during Nonlethal Plasmodium yoelii Infection Causes Severe Malaria Characterized by Acute Renal Failure in Mice. Infection and immunity. 2016;84(3):845-55.
- 143. Gupta P, Lai SM, Sheng J, Tetlak P, Balachander A, Claser C, et al. Tissue-Resident CD169(+) Macrophages Form a Crucial Front Line against Plasmodium Infection. Cell Rep. 2016;16(6):1749-61.
- 144. Brown AE, Webster HK, Teja-Isavadharm P, Keeratithakul D. Macrophage activation in falciparum malaria as measured by neopterin and interferon-gamma. Clinical and experimental immunology. 1990;82(1):97-101.
- 145. Ho M, White NJ, Looareesuwan S, Wattanagoon Y, Lee SH, Walport MJ, et al. Splenic Fc receptor function in host defense and anemia in acute Plasmodium falciparum malaria. J Infect Dis. 1990;161(3):555-61.
- 146. Shear HL, Nussenzweig RS, Bianco C. Immune phagocytosis in murine malaria. The Journal of experimental medicine. 1979;149(6):1288-98.
- 147. Celada A, Cruchaud A, Perrin LH. Opsonic activity of human immune serum on in vitro phagocytosis of Plasmodium falciparum infected red blood cells by monocytes. Clinical and experimental immunology. 1982;47(3):635-44.
- 148. Wu X, Gowda NM, Gowda DC. Phagosomal Acidification Prevents Macrophage Inflammatory Cytokine Production to Malaria, and Dendritic Cells Are the Major Source at the Early Stages of Infection: IMPLICATION FOR MALARIA PROTECTIVE IMMUNITY DEVELOPMENT. The Journal of biological chemistry. 2015;290(38):23135-47.
- 149. Bae YS, Oh H, Rhee SG, Yoo YD. Regulation of reactive oxygen species generation in cell signaling. Mol Cells. 2011;32(6):491-509.
- 150. Hortelano S, Castrillo A, Alvarez AM, Bosca L. Contribution of cyclopentenone prostaglandins to the resolution of inflammation through the potentiation of apoptosis in activated macrophages. J Immunol. 2000;165(11):6525-31.
- 151. Prieto P, Cuenca J, Traves PG, Fernandez-Velasco M, Martin-Sanz P, Bosca L. Lipoxin A4 impairment of apoptotic signaling in macrophages: implication of the PI3K/Akt and the ERK/Nrf-2 defense pathways. Cell Death Differ. 2010;17(7):1179-88.
- 152. Mizushima N, Komatsu M. Autophagy: renovation of cells and tissues. Cell. 2011;147(4):728-41.
- 153. Harris J, Lang T, Thomas JPW, Sukkar MB, Nabar NR, Kehrl JH. Autophagy and inflammasomes. Mol Immunol. 2017;86:10-5.
- 154. Weichhart T, Hengstschlager M, Linke M. Regulation of innate immune cell function by mTOR. Nat Rev Immunol. 2015;15(10):599-614.
- 155. Ivanov SS, Roy CR. Pathogen signatures activate a ubiquitination pathway that modulates the function of the metabolic checkpoint kinase mTOR. Nat Immunol. 2013;14(12):1219-28.
- 156. Lelouard H, Schmidt EK, Camosseto V, Clavarino G, Ceppi M, Hsu HT, et al. Regulation of translation is required for dendritic cell function and survival during activation. J Cell Biol. 2007;179(7):1427-39.
- 157. Haloul M, Oliveira ERA, Kader M, Wells JZ, Tominello TR, El Andaloussi A, et al. mTORC1-mediated polarization of M1 macrophages and their accumulation in the liver correlate with immunopathology in fatal ehrlichiosis. Sci Rep. 2019;9(1):14050.
- 158. Klinkhamhom A, Glaharn S, Srisook C, Ampawong S, Krudsood S, Ward SA, et al. M1 macrophage features in severe Plasmodium falciparum malaria patients with pulmonary oedema. Malaria journal. 2020;19(1):182.
- 159. Pais TF, Chatterjee S. Brain macrophage activation in murine cerebral malaria precedes accumulation of leukocytes and CD8+ T cell proliferation. J Neuroimmunol. 2005;163(1-2):73-83.
- 160. Wilson KD, Stutz SJ, Ochoa LF, Valbuena GA, Cravens PD, Dineley KT, et al. Behavioural and neurological symptoms accompanied by cellular neuroinflammation in IL-10-deficient mice infected with Plasmodium chabaudi. Malaria journal. 2016;15(1):428.

- 161. Shimabukuro MK, Langhi LG, Cordeiro I, Brito JM, Batista CM, Mattson MP, et al. Lipid-laden cells differentially distributed in the aging brain are functionally active and correspond to distinct phenotypes. Sci Rep. 2016;6:23795.
- 162. Kazanis I. The subependymal zone neurogenic niche: a beating heart in the centre of the brain: how plastic is adult neurogenesis? Opportunities for therapy and questions to be addressed. Brain. 2009;132(Pt 11):2909-21.
- 163. Moscat J, Diaz-Meco MT. p62: a versatile multitasker takes on cancer. Trends Biochem Sci. 2012;37(6):230-6.
- 164. Jiang Y, Zhao Y, Zhu X, Liu Y, Wu B, Guo Y, et al. Effects of autophagy on macrophage adhesion and migration in diabetic nephropathy. Ren Fail. 2019;41(1):682-90.
- 165. Kornfeld H, Mancino G, Colizzi V. The role of macrophage cell death in tuberculosis. Cell Death Differ. 1999;6(1):71-8.
- 166. Navarre WW, Zychlinsky A. Pathogen-induced apoptosis of macrophages: a common end for different pathogenic strategies. Cellular microbiology. 2000;2(4):265-73.
- 167. Baran J, Guzik K, Hryniewicz W, Ernst M, Flad HD, Pryjma J. Apoptosis of monocytes and prolonged survival of granulocytes as a result of phagocytosis of bacteria. Infection and immunity. 1996;64(10):4242-8.
- 168. Ali F, Lee ME, Iannelli F, Pozzi G, Mitchell TJ, Read RC, et al. Streptococcus pneumoniae-associated human macrophage apoptosis after bacterial internalization via complement and Fcgamma receptors correlates with intracellular bacterial load. J Infect Dis. 2003;188(8):1119-31.
- 169. Eisenberg-Lerner A, Bialik S, Simon HU, Kimchi A. Life and death partners: apoptosis, autophagy and the cross-talk between them. Cell Death Differ. 2009;16(7):966-75.
- 170. Zhang C, Feng X, He L, Zhang Y, Shao L. The interrupted effect of autophagic flux and lysosomal function induced by graphene oxide in p62-dependent apoptosis of F98 cells. J Nanobiotechnology. 2020;18(1):52.
- 171. Huang S, Okamoto K, Yu C, Sinicrope FA. p62/sequestosome-1 up-regulation promotes ABT-263-induced caspase-8 aggregation/activation on the autophagosome. The Journal of biological chemistry. 2013;288(47):33654-66.
- 172. Chen C, Liu Y, Liu R, Ikenoue T, Guan KL, Liu Y, et al. TSC-mTOR maintains quiescence and function of hematopoietic stem cells by repressing mitochondrial biogenesis and reactive oxygen species. The Journal of experimental medicine. 2008;205(10):2397-408.
- 173. Chang CP, Su YC, Lee PH, Lei HY. Targeting NFKB by autophagy to polarize hepatoma-associated macrophage differentiation. Autophagy. 2013;9(4):619-21.
- 174. Tuloup-Minguez V, Hamai A, Greffard A, Nicolas V, Codogno P, Botti J. Autophagy modulates cell migration and beta1 integrin membrane recycling. Cell Cycle. 2013;12(20):3317-28.
- 175. Nacer A, Movila A, Sohet F, Girgis NM, Gundra UM, Loke P, et al. Experimental cerebral malaria pathogenesis--hemodynamics at the blood brain barrier. PLoS pathogens. 2014;10(12):e1004528.
- 176. Rosas-Ballina M, Guan XL, Schmidt A, Bumann D. Classical Activation of Macrophages Leads to Lipid Droplet Formation Without de novo Fatty Acid Synthesis. Frontiers in immunology. 2020;11:131.
- 177. Feingold KR, Shigenaga JK, Kazemi MR, McDonald CM, Patzek SM, Cross AS, et al. Mechanisms of triglyceride accumulation in activated macrophages. Journal of leukocyte biology. 2012;92(4):829-39.
- 178. Melo RC, D'Avila H, Fabrino DL, Almeida PE, Bozza PT. Macrophage lipid body induction by Chagas disease in vivo: putative intracellular domains for eicosanoid formation during infection. Tissue & cell. 2003;35(1):59-67.
- 179. Cao F, Castrillo A, Tontonoz P, Re F, Byrne GI. Chlamydia pneumoniae--induced macrophage foam cell formation is mediated by Toll-like receptor 2. Infection and immunity. 2007;75(2):753-9.

- 180. Rodriguez-Acosta A, Finol HJ, Pulido-Mendez M, Marquez A, Andrade G, Gonzalez N, et al. Liver ultrastructural pathology in mice infected with Plasmodium berghei. Journal of submicroscopic cytology and pathology. 1998;30(2):299-307.
- 181. Pulido-Mendez M, Finol HJ, Giron ME, Aguilar I. Ultrastructural pathological changes in mice kidney caused by Plasmodium berghei infection. Journal of submicroscopic cytology and pathology. 2006;38(2-3):143-8.
- 182. Young CC, van der Harg JM, Lewis NJ, Brooks KJ, Buchan AM, Szele FG. Ependymal ciliary dysfunction and reactive astrocytosis in a reorganized subventricular zone after stroke. Cereb Cortex. 2013;23(3):647-59.
- 183. Bisacchi GS. Origins of the Quinolone Class of Antibacterials: An Expanded "Discovery Story". Journal of medicinal chemistry. 2015;58(12):4874-82.
- 184. Lesher GY, Froelich EJ, Gruett MD, Bailey JH, Brundage RP. 1,8-Naphthyridine Derivatives. A New Class of Chemotherapeutic Agents. J Med Pharm Chem. 1962;91:1063-5.
- 185. Emmerson AM, Jones AM. The quinolones: decades of development and use. J Antimicrob Chemother. 2003;51 Suppl 1:13-20.
- 186. Rajabalian S, Foroumadi A, Shafiee A, Emami S. Functionalized N(2-oxyiminoethyl) piperazinyl quinolones as new cytotoxic agents. J Pharm Pharm Sci. 2007;10(2):153-8.
- 187. Tabarrini O, Massari S, Daelemans D, Stevens M, Manfroni G, Sabatini S, et al. Structure-activity relationship study on anti-HIV 6-desfluoroquinolones. Journal of medicinal chemistry. 2008;51(17):5454-8.
- 188. Greeff J, Joubert J, Malan SF, van Dyk S. Antioxidant properties of 4-quinolones and structurally related flavones. Bioorganic & medicinal chemistry. 2012;20(2):809-18.
- 189. J Agric Food Chem.
- 190. Rho TC, Bae EA, Kim DH, Oh WK, Kim BY, Ahn JS, et al. Anti-Helicobacter pylori activity of quinolone alkaloids from Evodiae fructus. Biol Pharm Bull. 1999;22(10):1141-3.
- 191. The Synthesis of Quinolone Natural Products from Pseudonocardia sp. .
- 192. Hamasaki N, Ishii E, Tominaga K, Tezuka Y, Nagaoka T, Kadota S, et al. Highly selective antibacterial activity of novel alkyl quinolone alkaloids from a Chinese herbal medicine, Gosyuyu (Wu-Chu-Yu), against Helicobacter pylori in vitro. Microbiol Immunol. 2000;44(1):9-15.
- 193. Winter RW, Kelly JX, Smilkstein MJ, Dodean R, Hinrichs D, Riscoe MK. Antimalarial quinolones: synthesis, potency, and mechanistic studies. Experimental parasitology. 2008;118(4):487-97.
- 194. Tang Girdwood SC, Nenortas E, Shapiro TA. Targeting the gyrase of Plasmodium falciparum with topoisomerase poisons. Biochemical pharmacology. 2015;95(4):227-37.
- 195. Heeb S, Fletcher MP, Chhabra SR, Diggle SP, Williams P, Camara M. Quinolones: from antibiotics to autoinducers. FEMS Microbiol Rev. 2011;35(2):247-74.
- 196. Nilsen A, LaCrue AN, White KL, Forquer IP, Cross RM, Marfurt J, et al. Quinolone-3-diarylethers: a new class of antimalarial drug. Sci Transl Med. 2013;5(177):177ra37.
- 197. Nilsen A, Miley GP, Forquer IP, Mather MW, Katneni K, Li Y, et al. Discovery, synthesis, and optimization of antimalarial 4(1H)-quinolone-3-diarylethers. Journal of medicinal chemistry. 2014;57(9):3818-34.
- 198. Winter R, Kelly JX, Smilkstein MJ, Hinrichs D, Koop DR, Riscoe MK. Optimization of endochin-like quinolones for antimalarial activity. Experimental parasitology. 2011;127(2):545-51.
- 199. Grimberg BT. Methodology and application of flow cytometry for investigation of human malaria parasites. J Immunol Methods. 2011;367(1-2):1-16.
- 200. Ferrari M, Fornasiero MC, Isetta AM. MTT colorimetric assay for testing macrophage cytotoxic activity in vitro. J Immunol Methods. 1990;131(2):165-72.
- 201. Chong CR, Sullivan DJ, Jr. Inhibition of heme crystal growth by antimalarials and other compounds: implications for drug discovery. Biochemical pharmacology. 2003;66(11):2201-12.
- 202. Kazmaier U, Persch A. A straightforward approach towards 5-substituted thiazolylpeptides via the thio-Ugi-reaction. Organic & biomolecular chemistry. 2010;8(23):5442-7.

- 203. Jeankumar VU, Renuka J, Santosh P, Soni V, Sridevi JP, Suryadevara P, et al. Thiazole-aminopiperidine hybrid analogues: design and synthesis of novel Mycobacterium tuberculosis GyrB inhibitors. Eur J Med Chem. 2013;70:143-53.
- 204. Makam P, Kankanala R, Prakash A, Kannan T. 2-(2-Hydrazinyl)thiazole derivatives: design, synthesis and in vitro antimycobacterial studies. Eur J Med Chem. 2013;69:564-76.
- 205. Ghogare JG, Bhandari SV, Bothara KG, Madgulkar AR, Parashar GA, Sonawane BG, et al. Design, synthesis and pharmacological screening of potential anticonvulsant agents using hybrid approach. Eur J Med Chem. 2010;45(3):857-63.
- 206. Demirayak IKS. Synthesis and Anticancer Activities of Some Thiazole Derivatives, Phosphorus, Sulfur, and Silicon and the Related Elements. 2009;184(9):2197-207.
- 207. Dawood KM, Eldebss TM, El-Zahabi HS, Yousef MH. Synthesis and antiviral activity of some new bis-1,3-thiazole derivatives. Eur J Med Chem. 2015;102:266-76.
- 208. Bondock S, Naser T, Ammar YA. Synthesis of some new 2-(3-pyridyl)-4,5-disubstituted thiazoles as potent antimicrobial agents. Eur J Med Chem. 2013;62:270-9.
- 209. Bueno JM, Carda M, Crespo B, Cunat AC, de Cozar C, Leon ML, et al. Design, synthesis and antimalarial evaluation of novel thiazole derivatives. Bioorganic & medicinal chemistry letters. 2016;26(16):3938-44.
- 210. Helal MH, Salem MA, El-Gaby MS, Aljahdali M. Synthesis and biological evaluation of some novel thiazole compounds as potential anti-inflammatory agents. Eur J Med Chem. 2013;65:517-26.
- 211. Sardari S, Mori Y, Horita K, Micetich RG, Nishibe S, Daneshtalab M. Synthesis and antifungal activity of coumarins and angular furanocoumarins. Bioorganic & medicinal chemistry. 1999;7(9):1933-40.
- 212. Zhou P, Takaishi Y, Duan H, Chen B, Honda G, Itoh M, et al. Coumarins and bicoumarin from Ferula sumbul: anti-HIV activity and inhibition of cytokine release. Phytochemistry. 2000;53(6):689-97.
- 213. Anand P, Singh B, Singh N. A review on coumarins as acetylcholinesterase inhibitors for Alzheimer's disease. Bioorganic & medicinal chemistry. 2012;20(3):1175-80.
- 214. Bullock SJ, Felton CE, Fennessy RV, Harding LP, Andrews M, Pope SJ, et al. Coumarin-based luminescent ligand that forms helicates with dicationic metal ions. Dalton Trans. 2009(47):10570-3.
- 215. Ibrar A, Tehseen Y, Khan I, Hameed A, Saeed A, Furtmann N, et al. Coumarin-thiazole and -oxadiazole derivatives: Synthesis, bioactivity and docking studies for aldose/aldehyde reductase inhibitors. Bioorg Chem. 2016;68:177-86.
- 216. G.Riveraa R. A versatile approach to hybrid thiadiazine-based molecules by the Ugi four-component reaction. Tetrahedron Letters. 2017;58(18):1784-7.
- 217. Sarapultsev AP, Chupakhin ON, Sarapultsev PA, Sidorova LP, Tseitler TA. Pharmacologic Evaluation of Antidepressant Activity and Synthesis of 2-Morpholino-5-phenyl-6H-1,3,4-thiadiazine Hydrobromide. Pharmaceuticals (Basel). 2016;9(2).
- 218. Wang D, Liu W, Yi F, Zhao Y, Chen J. Palladium-catalyzed direct C-H arylation of 3-aryl-2H-benzo[1,2,4]thiadiazine 1,1-dioxides: an efficient strategy to the synthesis of benzothiadiazine-1,1-dioxide derivatives. Organic & biomolecular chemistry. 2016;14(6):1921-4.
- 219. Guerra A, Gonzalez-Naranjo P, Campillo NE, Varela J, Lavaggi ML, Merlino A, et al. Novel Imidazo[4,5-c][1,2,6]thiadiazine 2,2-dioxides as antiproliferative trypanosoma cruzi drugs: Computational screening from neural network, synthesis and in vivo biological properties. Eur J Med Chem. 2017;136:223-34.
- 220. Ayati A, Emami S, Asadipour A, Shafiee A, Foroumadi A. Recent applications of 1,3-thiazole core structure in the identification of new lead compounds and drug discovery. Eur J Med Chem. 2015;97:699-718.
- 221. Moldovan CM, Oniga O, Parvu A, Tiperciuc B, Verite P, Pirnau A, et al. Synthesis and anti-inflammatory evaluation of some new acyl-hydrazones bearing 2-aryl-thiazole. Eur J Med Chem. 2011;46(2):526-34.

222. Dahl EL, Shock JL, Shenai BR, Gut J, DeRisi JL, Rosenthal PJ. Tetracyclines specifically target the apicoplast of the malaria parasite Plasmodium falciparum. Antimicrobial agents and chemotherapy. 2006;50(9):3124-31.

Anti-plasmodial activity of fatty acids and macrophage immune modulation during robust erythrophagocytosis

by Naidu Babu Ommi

Submission date: 19-Oct-2020 12:44PM (UTC+0530)

Submission ID: 1419593385

File name: Plagiarism_check_file.docx (426.15K)

Word count: 16846 Character count: 99908

Anti-plasmodial activity of fatty acids and macrophage immune modulation during robust erythrophagocytosis

mod	dulation du	ring robust erythro	ophagocytosis	
ORIGIN	IALITY REPORT			
SIMILA	7% ARITY INDEX	6% INTERNET SOURCES	15% PUBLICATIONS	1% STUDENT PAPERS
PRIMA	RY SOURCES			
1	Mudiraj, Vedula. hydrazoi hydrazoi	Sujatha, Naidu Ba Phanithi Prakash "Synthesis of thia nothiazolamines a nothiazolamines a rial agents", Arch	n Babu, Rajeso azolyl and 1,3,4-thiad as a class of	war Rao diazinyl
2	Mudiraj, Prakash Synthesi Marinam	Naveen, Naidu Ba Thippana Mallika Babu, Rajagopa is of Penicinoline hide and their Ant rySelect, 2017	arjuna, Phanith I Nagarajan. " E, Marinamid	ni Total e, Methyl
3	etd.librai	ry.vanderbilt.edu		1%

Thittayil Suresh Apoorv, Chintanuri Karthik,

Phanithi Prakash Babu. "AMP-activated protein

kinase (AMPK) is decreased in the mouse brain

et al. "Lipid-laden cells differentially distributed in the aging brain are functionally active and correspond to distinct phenotypes", Scientific Reports, 2016

Publication

39	hal.archives-ouvertes.fr Internet Source	<1%
40	Hiroyuki Kusuhara, Yuichi Sugiyama. "Efflux transport systems for drugs at the blood-brain barrier and blood-cerebrospinal fluid barrier (Part 2)", Drug Discovery Today, 2001 Publication	<1%
41	cmr.asm.org Internet Source	<1%
42	Rebecca H. Pouwer, Sophie M. Deydier, Phuc Van Le, Brett D. Schwartz et al. "Total Synthesis of Thiaplakortone A: Derivatives as Metabolically Stable Leads for the Treatment of Malaria", ACS Medicinal Chemistry Letters, 2014 Publication	<1%
43	ir.lib.hiroshima-u.ac.jp Internet Source	<1%
44	www.spandidos-publications.com Internet Source	<1%

Exclude quotes On Exclude matches < 14 words

Exclude bibliography On

FULL PAPER





Synthesis of thiazolyl hydrazonothiazolamines and 1,3,4-thiadiazinyl hydrazonothiazolamines as a class of antimalarial agents

Kodam Sujatha¹ | Naidu Babu Ommi² | Anwita Mudiraj² | Phanithi Prakash Babu² | Rajeswar Rao Vedula¹

¹Department of Chemistry, National Institute of Technology, Warangal, Telangana, India

Correspondence

Phanithi Prakash Babu, Department of Biotechnology and Bioinformatics, School of Life Sciences, University of Hyderabad, Hyderabad, Telangana 500046 India Email: prakash@uohyd.ac.in

Rajeswar Rao Vedula, Department of Chemistry, National Institute of Technology, Warangal, Telangana 506004, India. Email: rajeswarnitw@gmail.com

Abstract

Novel thiazolyl hydrazonothiazolamines and 1,3,4-thiadiazinyl hydrazonothiazolamines were synthesized by a facile one-pot multicomponent approach by the reaction of 2-amino-4-methyl-5-acetylthiazole, thiosemicarbazide or thiocarbohydrazide and phenacyl bromides or 3-(2-bromoacetyl)-2H-chromen-2-ones in acetic acid with good to excellent yields. These new compounds were screened in vitro for their antimalarial activity; among them, four compounds, 4h, 4i, 4k, 4l, showed moderate activity with half-maximal inhibitory concentration (IC₅₀) values of 3.2, 2.7, 2.7, and 2.8 and 3.2, 3.2, 3.1, and 3.5 μM against chloroquine-sensitive and -resistant strains of Plasmodium falciparum, respectively. Compound 4I inhibited the ring stage growth of P. falciparum 3D7 at an IC₉₀ concentration of 12.5 µM in a stage-specific assay method, where the culture is incubated with specific stages of P. falciparum for 12 hr, and no activity was found against the trophozoite and schizont stages, confirming that 41 may have potent action against the ring stage of P. falciparum.

KEYWORDS

2-amino-4-methyl-5-acetylthiazole, antimalarial activity, bithiazoles, multicomponent reactions, thiazolothiadiazines

1 | INTRODUCTION

Malaria is a parasitic disease transmitted to humans by the female Anopheles mosquito and continues to remain a lethal infectious disease. According to WHO 2017 report, [1] an estimated 216 million cases of malaria occurred worldwide in 2016, and India accounts for 6% of it. Plasmodium falciparum, the most virulent species of this parasite has developed resistance to most available antimalarial drugs. This has been a constant challenge to malaria control initiatives necessitating the search for novel and structurally diverse antimalarial drugs as a viable strategy to combat this issue.

Multicomponent reactions (MCRs) are modern methods for the synthesis of drug molecules.^[2] The advantages of MCRs are convergent, one pot and sequential assembling of starting materials to get the final product in a short time. MCRs play a vital role in modern organic synthesis. MCRs are good synthetic approaches for functionalized heterocyclic compounds without any side products.^[3,4]

Thiazole scaffolds (Figure 1) are found in many natural products^[5] and possess diverse medicinal and pharmaceutical applications such as antitubercular, [6,7] anticonvulsant, [8] anticancer, [9] antiviral, [10] antimicrobial, antimalarial and anti-inflammatory activity. [13]

Coumarin is an important pharmacophore having many applications in the fields of medicinal chemistry as well as pharmaceuticals like antifungal, [14] anti-HIV agents, [15] anti-Alzheimers [16] and also acts as a luminescent material. [17] When the coumarin ring is attached with the thiazole ring, it exhibits improved biological activities like being an anti-inflammatory and anti-analgesic agent. [18] On the other hand, thiadiazines are also versatile biologically important heterocyclic molecules^[19] with proven applications as antidepressant,^[20] antihypertensive^[21] and antiproliferative agents.^[22]

²Department of Biotechnology and Bioinformatics, School of Life Sciences, University of Hyderabad, Hyderabad, Telangana, India





■ Organic & Supramolecular Chemistry

Total Synthesis of Penicinoline E, Marinamide, Methyl Marinamide and their Antimalarial Activity

Badher Naveen, [a] Naidu Babu Ommi, [b] Anwita Mudiraj, [b] Thippana Mallikarjuna, [b] Phanithi Prakash Babu,*[b] and Rajagopal Nagarajan*[a]

Syntheses of unusual pyrrole alkaloids Penicinoline E, Marinamide and Methyl marinamide were successfully achieved in two steps from easily accessible starting materials with excellent overall yields 70–97%. The Suzuki-Miyaura coupling followed by dearomatization represents the key step in the synthesis of title compounds. The structure of Penicinoline E was unequivocally confirmed by single X-ray analysis. The antiplasmodial activity of alkaloids was evaluated and shown a

good antimalarial activity against human malaria parasite *Plasmodium falciparum* in vitro. Against chloroquine sensitive (pf3d7), both Penicinoline E and Methyl marinamide displayed IC₅₀ value of 1.56 μ M and Marinamide displayed IC₅₀ value of 25 μ M respectively. In addition, against chloroquine resistant strain (pfDd2) of plasmodium falciparum they have also shown 4.68 μ M, 2.34 μ M and 25 μ M respectively.

The quinolones are biologically important scaffolds due to their wide spectrum of properties. In general, quinolones are classified into two categories. One is, 2(1H)-quinolone, and the other is 4(1H)-quinolone which can be obtained from 2-hydroxy and 4-hydroxy quinolones respectively. In 1962, George Lesher et.al. isolated a compound called Nalidixic acid 4 for the first time as a minor impurity during the synthesis of antimalarial agent chloroquine. Nalidixic acid 4 (Figure 1) has a

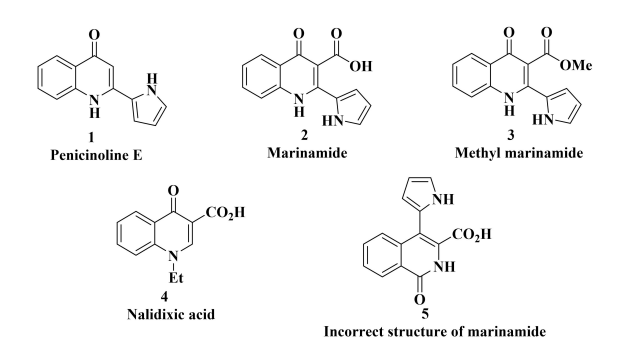


Figure 1. Structures of Penicinoline alkaloids 1-3 and chemical structures of 4 and 5.

quite interesting bioactive property and used for the treatment of urinary infections in human almost a decade, which proves the importance of quinolones. [2] Subsequently, quinolones have been found in many natural sources such as plants, animals, microbial^[3] and used as antiviral, antiurinary, antiinflammatory, antimicrobial, antimalarial and antibacterial drugs (more than 100 antibacterial agents). Furthermore, quinolones have also been used as a Multi drug resistance (MDR) drugs.^[4] Due to their fascinating bioactivities turned to be one of the main focus of chemists and biochemists. Moreover, it has been explored that 4(1H)-quinolones is being explored on the multiple developmental stages of parasite life cycle. [5],[6],[5-7] Malaria is one of the life-threatening complications mainly affecting the developing and developed countries. In 2015, approximately 214 million new cases of malaria were reported while 438,000 people died of this disease worldwide.[8] The most prevalent and lethal form of malaria is caused by Plasmodium falciparum and the rapid spread of drug-resistant plasmodium contributes to the deteriorating malaria situation^[9-11]. To combat drug resistance WHO recommends artemisinin-based combination therapy and hence the need to develop new drug combinations is an ongoing effort. Antimalarial activity of Penicinoline alkaloids has not been reported so far in the literatures.

In 2006, Yongcheng Lin *et al*, isolated marinamide alkaloid **2** and proposed the incorrect structure of the pyrrolylquinolinone **5.**^[12]

Subsequently, in 2010, She, Lin and co-workers isolated again marinamide alkaloid **2** from mangrove endophytic fungus.^[13] Finally, in 2011, König *et al* rearranged the structure of marinamide alkaloid **2** by using crystal proof structure of methyl marinamide **3.**^[14] Recently, Li and co-workers isolated and confirmed Penicinoline E **1** along with known compounds marinamide **2** and methyl marinamide **3** from marine-derived fungus *Penicillium sp.ghq208* as a yellow powder.^[15] Till date, to the best of our knowledge, no total synthesis and antimalarial

3256

 [[]a] B. Naveen, Prof.Dr. R. Nagarajan
 School of Chemistry, University of Hyderabad, Hyderabad – 500046, India.
 E-mail: nagaindole@gmail.com

[[]b] N. B. Ommi, A. Mudiraj, T. Mallikarjuna, Prof.Dr. P. P. Babu Department of Biotechnology & Bioinformatics, School of Life Sciences, University of Hyderabad, Hyderabad – 500046, India. E-mail: prakash@uohyd.ac.in

Supporting information for this article is available on the WWW under http://dx.doi.org/10.1002/slct.201700242